Probing MPS1 function in mitosis

Tale Sliedrecht

Printed by Proefschriftmaken.nl - Uitgeverij BOXPress

The research described in this thesis and printing was financially supported by the NPC and Stichting Gilles Hondius Foundation

Probing MPS1 function in mitosis

Het ontrafelen van de functie van MPS1 in mitose

(met een samenvatting in het Nederlands)

Proefschrift

ter verkrijging van de graad van doctor aan de Universiteit Utrecht op gezag van de rector magnificus, prof.dr. G.J. van der Zwaan, ingevolge het besluit van het college voor promoties in het openbaar te verdedigen op dinsdag 3 december 2013 des ochtends te 10.30 uur

door

Tale Sliedrecht

geboren op 8 september 1980 te Deventer

Promoter: Prof. dr. G.J.P.L. Kops

Content

Abbreviations

APC/C	Anaphase Promoting Complex/Cyclosome
as	Analog sensitive
BUB	Budding Uninhibited by Benzimidazole
CCAN	Constitutive Centromere-Associated Network
CDC20	Cell Division Cycle 20
CDK	Cyclin Dependent Kinase
CENP	CENtromere Protein
CIN	Chromosomal INstability
D-BOX	Destruction-box
DNA	Deoxiribonucleic acid
G-phase	Gap-phase
H(2A/3)	Histone
KEN-box	Lys-Glu-Asn-box
KMN	KNL1/MIS12/NDC80 complex
M-phase	Mitosis-phase
MAD	Mitotic Arrest Deficient
MCC	Mitotic Checkpoint Complex
MELT	Met-Glu-Leu-Thr
MPS1	Mono Polar Spindle 1
PLK	Polo Like Kinase
PP1/2A	Protein Phosphatase
Rev	Reversine
RZZ	Rod/Zwilch/ZW10 complex
SAC	Spindle Assembly Checkpoint
S-phase	Synthesis-phase

Chapter 1

General introduction

The cell cycle

Cell reproduction is fundamental to the development and function of all life. When unicellular organisms undertake cell division, the process produces an entire, new organism. Multicellular organisms depend on cell division for growth and regeneration of damaged tissue. The highly ordered series of complex events of cell reproduction is referred to as 'the cell cycle'. The cell cycle coordinates the duplication of the genome and subsequent distribution of each replicate genome into a new daughter cell. The eukaryotic cell cycle is divided into discreet phases (Figure 1). During the first gap-phase, or G1, a cell grows and prepares for DNA replication. The start of replication marks the beginning of S (for synthesis) phase that results in duplication of the chromosomes. During this phase, cohesin ring complexes, deposited along the duplicated chromosomes mediate tight linkage between duplicated chromosomes (now referred to as sister chromatids). As the cell cycle progresses the cell is provided with additional time in the second gap phase (G2) to grow and prepare for the 'grand finale' of the cell cycle: mitosis, or M-phase. Mitosis ensures equal distribution of the sister chromatids into two newly formed daughter cells. Successful completion of the cell cycle depends on the strict regulation of the cell cycle control system, which governs progression at the correct time and in the correct order.

Cyclin dependent kinases and checkpoints.

The cell cycle is propelled by changes in activity of a particular type of protein kinase, Cyclin dependent kinases or CDKs. Although concentrations of the CDK proteins are constant throughout the cell-cycle, their activity is controlled by oscillating levels of their regulatory subunits known as Cyclins [1,2]. These oscillations are determined by synthesis and proteolysis of Cyclins. Specific Cyclins associate with and activate specific CDKs. As such, oscillations in the level of specific Cyclins allows temporally controlled activation of specific CDKs and hence ordered progression through the various phases of the cell cycle. For example, mitosis in likely all eukaryotes is triggered by the Cyclin B-CDK1 complex. Synthesis of Cyclin B occurs throughout S- and G2 phases and once it reaches a particular threshold it will have provided sufficient CDK1 activity to initiate a rapid feedback loop that causes peak activity of CDK1 and subsequent entry into mitosis. Cyclin B-CDK1 activation results in the phosphorylation of a wide range of substrates, thereby promoting nuclear envelope breakdown (NEBD) and a multitude of other mitotic processes [3]. Conversely, the moment cells are ready to segregate their chromosomes, CDK1 needs to be inactivated, which occurs by rapid, proteasome-dependent degradation of Cyclin B.

The cell cycle can be modulated by strategically placed checkpoints that impinge on the Cyclin-CDK system. Cell cycle checkpoints monitor if a process has been successfully completed before entry into the next phase is allowed. Several checkpoints are known, of which the best studied ones monitor S-phase entry, M-phase entry and M-phase exit. 'Start' or the G1/S-checkpoint represents an irreversible commitment to cell cycle entry. Cell cycle entry is only permitted when conditions are ideal for cell proliferation. After DNA replication, entry into mitosis is allowed by the G2 checkpoint, which prevents cells from initiating mitosis if their DNA is damaged or part of it is unreplicated. And finally, the Spindle Assembly Checkpoint (SAC) ensures correct distribution of sister chromatids to the two to-be-formed daughter cells. Mitosis and the SAC are central in the research described here.

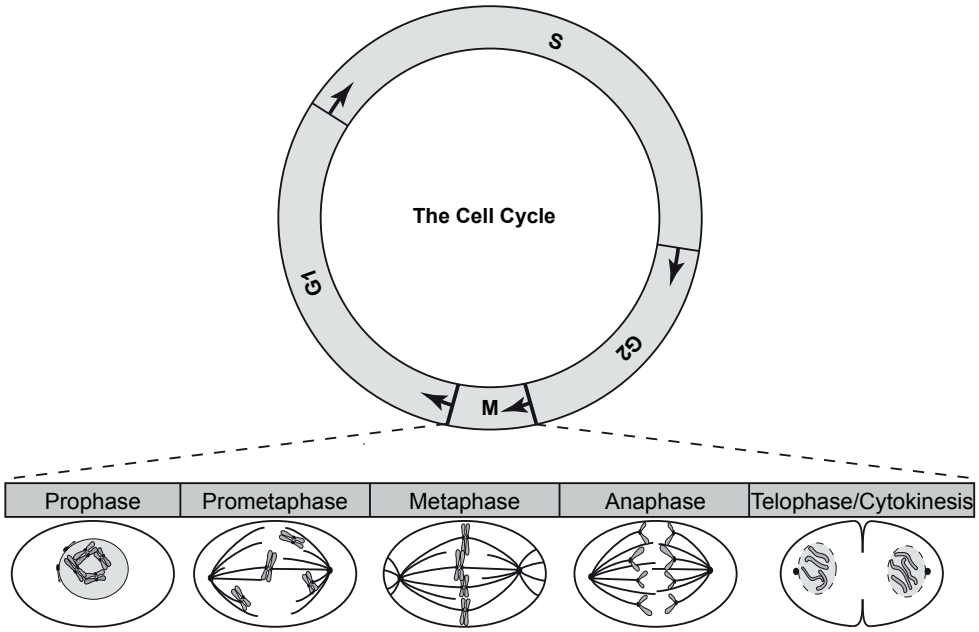

Figure 1. The cell cycle and mitosis

Schematic representation of the different stages of the cell cycle including the different stages of mitosis: After chromosomes have condensed in prophase, the nuclear envelope breaks down and spindle microtubules capture the chromosomes in prometaphase. Metaphase is achieved when all chromosomes are correctly attached in a bioriented fashion. After the physical separation of sister chromatids in anaphase, cell division is finished by telophase and cytokinesis.

Mitosis

In mitosis the duplicated, paired chromosomes are equally distributed into two newly formed daughter cells. Entry into mitosis is accompanied by dramatic cellular rearrangements like chromosome condensation, nuclear envelope breakdown and formation of a dynamic, bipolar, microtubule-based spindle. Mitosis is defined by distinct phases. The first phase, prophase, is marked by the rapid activation of Cyclin B1 - CDK1. Sister chromatids are tightly condensed in rod-like structures and centrosomes move apart to opposite sides of the nucleus (Figure 1). Nuclear envelope break down marks the start of the next phase, prometaphase. Centrosomal microtubules rapidly assemble and disassemble in search of defined sites named kinetochores, on sister chromatids (Figure 1). More details on this subject can be found in the section 'Kinetochores' below. Once attached and oriented with each sister to an opposite centrosome (referred to as 'biorientation'), the pair of sister chromatids congress to the spindle center. When all sister chromatid pairs are correctly bioriented and have aligned on the cell equator, the cell has achieved metaphase (Figure 1). The abrupt separation of sister chromatids to opposite sides marks the metaphase-to-anaphase transition (Figure 1). This separation is caused by removal of the cohesion ring complexes that were holding the sisters together, and is accompanied by the degradation of Cyclin B, which will eventually ensure exit from the mitotic state and entry into a new round of cell division. Mitosis ends with two final stages. In telophase the nuclear envelope is re-

formed around the separated sister chromatids. Actual division of the cell mass into two new daughter cells is achieved during cytokinesis (Figure 1) (reviewed in [4]).

Kinetochore

Accurate chromosome segregation requires each sister chromatid to interact with spindle microtubules. This interaction is mediated by a macromolecular protein assembly called the kinetochore. Kinetochores assemble on the centromere, a region of heterochromatin at the central constriction of the sister chromatids. Human centromeric regions are marked by the presence of 171-bp repetitive sequences named alpha-satellites, which are packaged by specialized nucleosomes containing a centromere specific histone H3 variant, CENP-A (Centromere associated protein-A) [5]. CENP-A defines the site of kinetochore formation [6,7].
One of the primary functions of kinetochores is to create load-bearing attachments between the sister chromatids and microtubules. The kinetochore region that forms the interaction surface for spindle microtubules is known as the outer kinetochore. Microtubule attachment is predominantly mediated by the KMN-network, which is composed of KNL1 and the NDC80 and MIS12 complexes (Figure 2). This central hub of the outer kinetochore serves as the core microtubule-binding interface and is assembled onto kinetochores in prophase [8,9]. The NDC80 and KNL1 complexes individually have microtubule binding activities [9-13], while the MIS12 complex is required to ensure synergy in microtubule binding of the two complexes (Figure 2) [14]. The NDC80 complex is comprised of four proteins that form a rod-like structure. One end of the rod is composed of the globular regions of HEC1/NDC80 and NUF2 proteins that are folded into calponin-homology (CH) domains and that point outward to bind microtubules (reviewed in[15]). Extending beyond the CH domain of HEC1/NDC80 is a 80-amino acid unstructured sequence known as the tail that is essential for kinetochore-microtubule attachment [12,13]. This tail can be heavily modified by phosphorylation to regulate microtubule-binding affinity of the kinetochore (More on this below, in the section 'Kinetochore-Microtubule attachment stability'). In parallel to the KMN network, the SKA complex [14,16,17], the microtubule motor CENP-E [18-20], and CLIP-170 [21,22] facilitate the formation of kinetochore-microtubule attachments. It remains unclear, however, how these additional microtubule binding modules cooperate with the KMN-network to bind microtubules (Figure

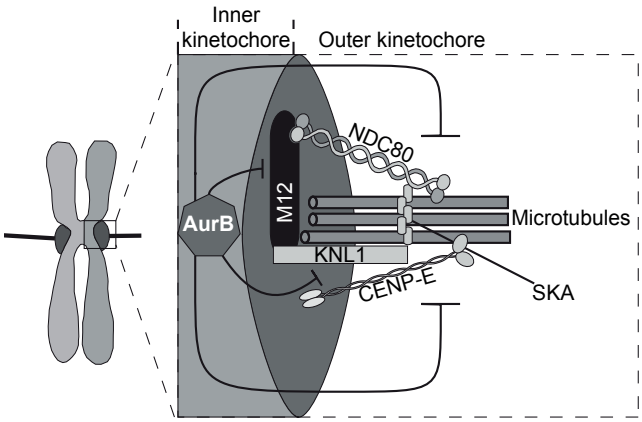

Figure 2. Kinetochore-microtubule attachment
The inner kinetochore, consisting of the CCAN (not shown), recruits microtubule binding proteins to the outer kinetochore. These include the kinesin-7 family microtubule motor protein CENP-E and the KMN network that together form the main microtubule binding sites of kinetochores. The KMN network consists of KNL1, MIS12 (M12) and NDC80/HEC1 (NDC80) subcomplexes, of which the NDC80 and KNL1 complexes possess microtubule-binding affinity. Aurora B (AurB) resides in the inner centromere and can destabilize microtubule attachment by phosphorylation of proteins of the KMN network and of CENP-E.

2).
The inner kinetochore provides linkage between the CENP-A containing chromatin and the outer kinetochore. A large group of proteins known as the constitutive centromere associated network (CCAN) make up the interface between the centromeric chromatin and the outer kinetochore and are required for proper kinetochore formation (reviewed in [23] and [24]). Two parallel pathways drive assembly of a functional kinetochore capable of binding microtubules. Firstly, a heterotetrameric complex of CENP-T-W-S-X binds and wraps centromeric DNA [25] and one of its components, CENP-T, associates via its N-terminus with the SPC24 and SPC25 subunits of the NDC80 complex [25,26]. Secondly, CENP-C directly interacts with CENPA as well as with the MIS12 complex, thereby linking the centromeric CENP-A nucleosome to the microtubule binding complex on the outer kinetochore [27].

Kinetochore-Microtubule attachment stability

Error-free chromosome alignment and segregation requires sister chromatid biorientation. Sister kinetochore biorientation is achieved through an error prone mechanism known as "search and capture" [28]. Dynamic microtubule plus ends grow and shrink from opposing spindle poles until they are captured and stabilized by a kinetochore. This process is not entirely random, as it is aided by molecular gradients that direct microtubules to kinetochores, as well as by microtubule growth from kinetochores and the so-called 'polar wind' that pushes chromosomes away from a pole closer to the opposite pole (reviewed in [29]). Despite these fast and regulated events of chromosome capture by the spindle, incomplete or incorrect microtubule attachments occur. These include chromosomes with one (monotelic) or two (syntelic) kinetochores attached to one spindle pole or one kinetochore attached to both poles (merotelic) (Figure 3) [30,31]. To ensure proper chromosome segregation in anaphase, correction of such erroneous attachments is carefully regulated. The inner centromeric chromosomal passenger complex (CPC) promotes biorientation by specifically destabilizing erroneous attachments, providing the chromosomes with a fresh opportunity to biorient [32-34]. The current view is that the CPC accomplishes this via its kinase component Aurora B that destabilizes kinetochore microtubule attachments that are not under tension from spindle-based pulling forces. In the absence of tension, Aurora B-mediated phosphorylation of the

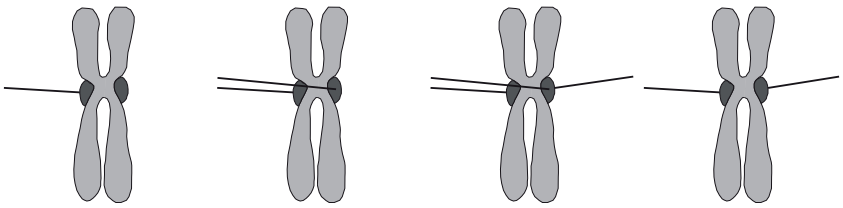

Figure 3. Types of chromosome attachments
Schematic representation of correct (Amphitelic) and incorrect (Monotelic, Syntelic and Merotelic) microtubule attachments by chromosomes.

KMN network including the NDC80 tail and the SKA complex strongly reduces microtubule-binding affinity of kinetochores (Figure 2) [9,10,13,14,17,35,36]. Establishment of tension between bioriented sister kinetochores spatially separates Aurora B at the inner centromere from its outer kinetochore substrates [37]. This view was recently challenged by a study in *S. cerevisiae*

that showed that error-correction by the CPC did not rely specifically on inner-centromere-localized CPC but could also be accomplished when it accumulates on the spindle [38]. As a result, it is currently unclear how CPC-based error-correction distinguishes bioriented attachments from erroneous ones.

A growing amount of evidence suggests that a dynamic balance between phosphorylation and dephosphorylation regulates biorientation. Protein phosphatase 1 (PP1) interacts with a conserved motif in the KMN-network member KNL1. PP1 recruitment opposes Aurora B activity at kinetochores by dephosphorylating Aurora B substrates and thus stabilizing microtubule attachment. Recruitment of PP1 to KNL1 is prevented by phosphorylation of Aurora B [39]. A similar mechanism is found for the outer kinetochore protein CENP-E: Phosphorylation of CENP-E by Aurora B decreases its affinity for microtubules and disrupts PP1 binding [40]. Finally, protein phosphatase 2a (PP2A) similarly counters Aurora B-dependent phosphorylation when it is bound to the BUBR1 protein [41,42]. It will be important to determine how, where and when the activity of PP1 and PP2A are coordinated to ensure proper biorientation.

The SAC and the APC/C

Besides facilitating microtubule attachment, the kinetochore also plays an essential role in relaying the microtubule binding status to a cell cycle surveillance mechanism that delays exit from mitosis when unattached kinetochores remain. Pioneering laser-ablation experiments in the 90's revealed that a mitotic checkpoint originating from unattached kinetochores delays anaphase progression until all kinetochores have attached spindle microtubules [43-45]. These experiments, performed in rat-kangaroo PtK2 cells, further showed that a single unattached kinetochore was sufficient to hold off anaphase onset for hours. The goal of the SAC therefore is to maintain sister chromatid cohesion and the mitotic state in order to buy time for the spindle to capture all chromosomes. We now know that the SAC accomplishes this by producing an inhibitor of the E3 ubiquitin ligase that specifically degrades Securin and Cyclin B, to cause sister separation and mitotic exit, respectively. This E3 ubiquitin ligase is known as the anaphase promoting complex or APC/C.

APC/C

The APC/C is a large E3 ubiquitin ligase which is composed of 15 subunits, which are conserved throughout evolution [46]. The core subunits form two subcomplexes that are held together by the large APC1 scaffold. One module containing APC2 and APC11 accounts for the catalytic activity, while the other subcomplex is involved in co-activator binding mediated by multiple tetratricopeptide repeats (TPR) containing subunits (reviewed in [47]) that include APC3, APC6, APC7 and APC8 [46]. The APC/C requires multiple E2 conjugating enzymes. UBCH5 and UBCH10 [48,49] prime APC/C substrates while UBE2S is responsible for elongation of the ubiquitin chains [50-52]. Substrate recognition by the APC/C relies on motif-based degrons within proteins. Although a large set of degron sequences exist, most can be divided into two classes, the Destruction or D-box (Arg-x-x-Leu) and the KEN box (Lys-Glu-Asn). Both D- and KEN-box containing substrates are recognized by the two main APC/C co-activators, CDC20 and CDC20-homologue1 (CDH1) that recruit and position substrates to the APC/C core for ubiquitination [53,54]. These structurally related co-activators contain WD40 domains that interact with the D-box degrons and act as co-receptors with the

APC/C subunit APC10 [55-57]. The sequential actions of the two co-activators provide temporal regulation of degradation of specific sets of APC/C substrates. CDC20 activates the APC/C during early mitosis to degrade among others Cyclin A [58,59] in prometaphase and Cyclin B and Securin at metaphase [60,61], while CDH1 directs APC/C activity at the last phases of mitosis and the subsequent G1 [62,63] to specific late-mitotic substrates such as Plk1 and Aurora B [64,65]. Upon entry in mitosis the APC/C is activated through phosphorylation by CDK1 and PLK1 [66]. Despite this, though, the APC/C needs to be kept from targeting its metaphase substrates until all kinetochores are correctly attached to the microtubule spindle, and that is the job of the SAC.

The SAC

The SAC, which is conserved across eukaryotes [67], prevents premature degradation of Securin and Cyclin B by inactivation of the APC/C co-activator CDC20. The first components of the SAC were identified in the early 90's in yeast. Two independent budding yeast screens identified mitotic arrest deficient (MAD) and budding uninhibited by benzimidazole (BUB) genes, which are essential for survival after treatment with spindle poisons [68,69]. Unattached kinetochores have a central role in the establishment and maintenance of APC/C inhibition by the production of a soluble inhibitory complex. The pseudokinase BUBR1, BUB3 and MAD2 mediate the inactivation of APC/C through their association with CDC20. BUBR1, BUB3, MAD2 and CDC20 form the mitotic checkpoint complex (MCC), which directly interacts with the APC/C. The MCC complex binds a site that partially overlaps with the CDC20 binding site and locks the otherwise flexible APC/C in a closed state preventing binding and ubiquitination of APC/C substrates [70,71]. The recently resolved crystal structure of fission yeast MCC, showed that the BUBR1 KEN box is positioned toward the KEN-box receptor of the CDC20 WD40 domain, which agrees with a previously proposed role for BUBR1 as a pseudosubstate inhibitor of the APC/C [72-74].

Unattached kinetochores are essential for SAC signaling and catalyze the production of the MCC [75]. Upon mitotic entry the protein kinase MPS1 is recruited and activated at the kinetochore, and is subsequently responsible for the recruitment of most of the other key SAC proteins, including MAD1, MAD2, BUBR1, BUB3, the kinase BUB1 and the RZZ complex (Figure 4) [76]. For more detail on MPS1 function, see the section 'MPS1' below. Key for MCC production is the recruitment of MAD1 and MAD2 to kinetochores, which, besides MPS1, additionally requires BUB1 and the RZZ complex (Figure 4) [77-80]. MAD1 forms a stable homodimer that binds two MAD2 molecules [81]. The MAD1/MAD2 hetero-tetramer then serves as a platform for structural MAD2 conversion from an inactive 'open' (O-MAD2) to an active 'closed' (C-MAD2) conformation (reviewed in [75,82]) which is essential for the production of the MCC. C-MAD2 binds CDC20, and MAD2-bound CDC20 is then capable of binding the BUBR1-BUB3 complex, thus forming the MCC (Figure 4) [83,84]. While both

MAD2 and BUBR1-BUB3 independently can inhibit the APC/C, they are a far more potent inhibitor when complexed in the MCC [62,71,83,85]. Despite this, recent evidence suggests that the main function of C-MAD2 is to create a CDC20-BUBR1 complex, which may represent the true SAC effector complex [84,86]. While C-MAD2, BUBR1 and BUB3 all have been found to be complexed with CDC20 during SAC mediated arrest [24,71], evidence from the Pines lab showed that most CDC20 is complexed with BUBR1, rather than MAD2 [86]. MAD2 can

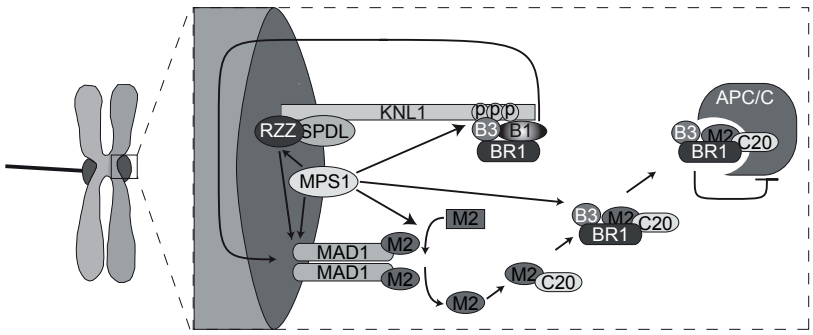

Figure 4. The SAC

In the absence of microtubule attachment, the SAC signaling network at kinetochores produces MCC complexes to inhibit the APC/C. The MCC consists of MAD2 (M2), CDC20 (C20), BUBR1 (BR1) and BUB3 (B3). Central in the regulation of the SAC is MPS1, which recruits RZZ/SPINDLY (SPDL) and BUB1 (B1) to unattached kinetochores as well as the MAD1/MAD2 platform that catalyzes the production of the MCC. MPS1 also promotes structural conversion of MAD2 from an open (square) to a closed (circle) form.

enhance the association between BUBR1 and CDC20 [83,87], possibly because this promotes a functional switch in CDC20 that exposes a previously inaccessible site for BUBR1 binding. Once the BUBR1-CDC20 binding is established C-MAD2 becomes dispensible for the inhibition of the APC/C [84]. MAD2 might thus function as a catalytic amplifier of BUBR1-CDC20 formation, but may not take part in APC/C inhibition directly.

MCC-mediated inhibition of the APC/C relies on several addition molecular mechanisms. During mitosis, CDC20 is continuously synthesized and degraded, and several studies have shown that destruction of CDC20 is required for efficient APC/C inhibition, since stabilization of CDC20 causes SAC override [86,88]. Additionally, BUB1 has been proposed to phosphorylate CDC20, thereby directly inhibiting its APC/C-activating ability [89]. This function is however debated since other studies have shown that BUB1 catalytic activity is dispensable for SAC regulation [77]. Finally, MPS1 activity promotes MCC formation by mediating MAD2 structural conversion [90] while simultaneously ensuring MCC stability (Figure 4) [91]. The underlying molecular mechanisms, however, remain to be elucidated. A more detailed description of MPS1 function in the SAC and mitosis can be found below.

Silencing the SAC

Although it is of great importance to maintain SAC activity while kinetochores are unattached, rapid extinguishing of the SAC signaling pathway and the breakdown of the SAC effector - the MCC - is of equal importance once kinetochores become attached. Evidence for an essential role of extinguishing the signal from kinetochores comes from the observation that failure to remove the MAD1 scaffold by artificially maintaining MAD1 on attached, bioriented kinetochores strongly delays anaphase onset [92]. Removal of MAD1 and MAD2 is, at least in part, done by dynein. In prometaphase dynein is localized to unattached kinetochores until microtubule attachment is established. Subsequently, dynein disconnects from kinetochores carrying SAC proteins as cargo and moves towards the spindle poles where its cargo is released (Figure 5A) [93]. This process is commonly referred to as stripping or streaming. Interfering with dynein activity consequently results in SAC silencing defects and a prolonged time spent in metaphase [93]. Besides MAD1 and MAD2, dynein has been shown to remove

several other SAC proteins including MPS1, BUBR1, the RZZ complex and SPINDLY (Figure 5A) [93,94]. Dynein is recruited to the kinetochore by proteins like NDE, NDEL1, the RZZ complex and SPINDLY and all have been proposed to be essential for dynein-dependent SAC silencing (reviewed in [95]). However, due to a role for dynein in kinetochore-microtubule attachment [96,97] and chromosome movement [98,99], depletion of dynein recruiters creates spindle assembly problems that indirectly stimulate a SAC response, making a role for these recruiters in the direct removal of SAC proteins difficult to interpret. Two recent studies however circumvented these issues elegantly. Dynein recruitment is mediated by a conserved motif within SPINDLY, known as the spindly box. Although unknown how this spindly box is involved, mutations in its sequence cause failure to recruit dynein to kinetochores without apparent effects on chromosome alignment, and cause a significant delay in the onset of anaphase with high levels of MAD1 and MAD2 on attached kinetochores. As stated above, SPINDLY depletion also results in dynein recruitment defects and spindle assembly issues. Interestingly, however, MAD1 and MAD2 removal from kinetochores once chromosomes finally align appears normal. SAC silening and SAC protein removal from kinetochores upon microtubule attachment may thus occur by a mechanism independent of kinetochore dynein [100,101]. Therefore, the removal of SPINDLY by dynein seems to be important for the extinguishing of SAC signaling at kinetochores. The RZZ complex plays an intriguing role in SAC signaling. By recruiting MAD1 to unattached kinetochores it serves in SAC activation, while indirectly, by localizing SPINDLY and dynein to kinetochores, is also responsible for MAD1 stripping and the subsequent inactivation of the SAC.

Besides the removal of SAC proteins from attached kinetochores, the dissociation of the

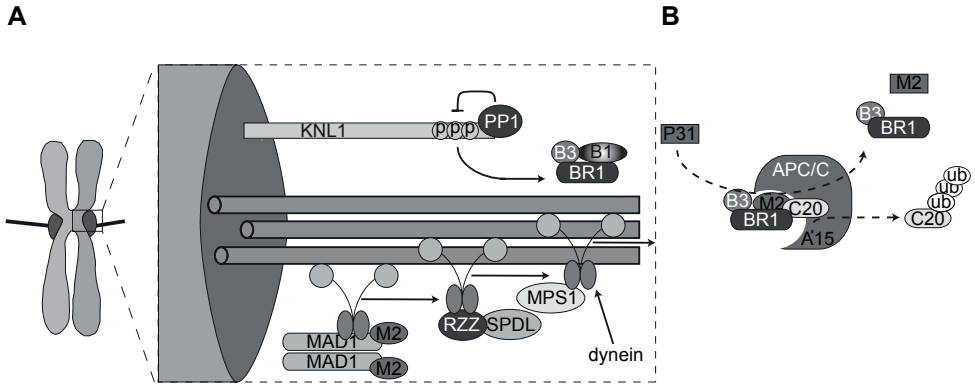

Figure 5. SAC silencing

A) Kinetochore-microtubule attachment causes dynein-dependent poleward stripping of SAC proteins such as MAD1, MAD2 (M2), SPINDLY (SPDL), the RZZ complex and MPS1. In addition, microtubule attachment further promotes the recruitment of PP1-like phosphatases that bind the N-terminus of KNL1 and dephosphorylate key SAC substrates. **B)** Once all kinetochores have made stable attachments, parallel and possibly intertwined activities of both p31^{comet} (P31) and APC15 (A15) promote the disassembly of the MCC and the MCC-APC/C complexes.

SAC effector, the MCC, is also required to rapidly exit mitosis after all kinetochores have attached. While the exact mechanisms are still unclear, it is generally accepted that the APC/C itself drives the disassembly of the MCC. Even though CDC20 ubiquitination and degradation has been proposed to maintain the SAC [86], it was recently shown that multi-ubiquitination of CDC20 by the APC/C causes dissociation of the MCC [102]. The current model therefore is that continuous, non-degradative CDC20 ubiquitination and MCC turnover on the

APC/C allows the SAC to rapidly respond to the attachment status of kinetochores [103-105]. The APC/C subunit APC15 plays a crucial role in this, as APC15 depletion was shown to prevent SAC silencing by locking MCC (including ubiquitinated CDC20) onto the APC/C. Since no defects in APC/C activity per se were seen upon APC15 depletion, APC15 may therefore be a subunit specifically required only for SAC silencing (Figure 5B) [104,105]. Removal of MCC from APC/C further requires the actions of a C-MAD2 mimetic, p31^{comet}. Since it directly binds C-MAD2 [106-108] and competes with O-MAD2 [109], it was first proposed to act as an inhibitory cap on the MAD1-C-MAD2 scaffold at kinetochores, preventing MAD2 conversion and thus MCC assembly. Evidence for this is lacking, however, and recent studies suggested that p31^{comet} extracts MAD2 from the MCC [110] to somehow facilitate ubiquitination of CDC20 and subsequent MCC disassembly (Figure 5B) [111,112]. As is clear from the discussion above, it is by no means clear how MCC disassembly comes about or how this is regulated, and a proper understanding of this likely requires in vitro reconstitution of the process.

Protein phosphatases participate in various aspects of mitosis and mitotic exit. In human cells, protein phosphatases at kinetochores dephosphorylate Aurora B substrates to stabilize kinetochore microtubule attachments [39,41]. PP2A-B56 is thought to dampen excessive Auroroa B activity in prometaphase, allowing establishment of attachments, while PP1 is thought to stabilize attachments on bioriented chromosomes specifically in metaphase [39,41,42,113,114]. The interplay between these phosphatases is an interesting line for future research. PP1-like phosphatases in yeast are also involved in mitotic control, but this appears more related to SAC silencing. *S. pombe* cells require PP1 to exit mitosis after forced mitotic exit by Aurora B inhibition [115], and *S. cerevisiae* cannot exit from mitosis in the absence of the PP1-like Glc7 phosphatase [116,117]. In addition to dephosphorylation of Aurora B substrates, Glc7 also counteracts Mps1 activity and thereby regulates recruitment of Bub1 to the KNL1/Spc105/Spc7 scaffold (Figure 5A)[118-120]. Though not yet proven, conservation of this mechanism in humans seems likely since the recruitment of PP1 to kinetochores in both yeast and human cells is virtually identical, occuring through PP1 docking motifs within the N-terminal part of KNL1 [117,121,122]. In addition to its role in PP1 recruitment, KNL1 may also regulate SAC silencing via its microtubule-binding site. Removal of microtubule-binding capacity of *C. elegans* KNL1 did not affect the ability of kinetochores to form load-bearing attachment formation but prevented SAC silencing [123] Lastly, the role of PP1 in SAC silencing in *S. pombe* also relies on the kinesin-8 family members KLP5-KLP6. Interestingly, KLP5-KLP6 motor activity is non essential for its function in SAC silencing suggesting that this role is independent of its role in chromosome segregation [122]. An important avenue for research will be the identification of PP1 substrates in the SAC. Does PP1 shut off MCC formation at kinetochores, does it assist in MCC disassembly, or both? It is in this regard of interest to note that phosphorylation of dynein intermediate chain (DIC) mediates dynein binding to the kinetochore and failure to dephosphorylate DIC causes retention of dynein at the kinetochore upon attachment and reduced stripping of SAC proteins [124].

MPS1

Although not part of the MCC, mitotic protein kinases are essential for MCC production and SAC signaling. Protein kinase such as BUB1 and MPS1 are known to promote SAC signaling in multiple ways and their signaling pathways are often intertwined with multiple other protein kinases. We here will focus on the role of MPS1 in the SAC and mitosis.

The protein kinase MPS1 was originally identified as an allele required for spindle pole duplication in budding yeast, hence its name Monopolar spindle 1 [125], While inactivation of MPS1 in yeast clearly results in monopolar spindle formation [125,126], it is debated whether this function is conserved in higher eukaryotes. MPS1 localizes to centrosomes and MPS1 overexpression in both mouse and human cells results in over duplication of centrosomes [127,128]. Other studies, however, were unable to reproduce these data [129,130], and detailed MPS1 RNAi and inhibitor studies have not reported overt centrosome defects [90,131-134]. In contrast to its proposed role in centrosome function, the importance of MPS1 to SAC signaling and to chromosome biorientation are undisputed [121,129,131-133,135-138]. MPS1 most likely carries out these functions at the kinetochore, and hence, spatiotemporal regulation of MPS1 localization and activation is critical. In human cells MPS1 protein, although present throughout the cell cycle, is upregulated as cells approach mitosis [129] and decline after anaphase onset [139,140]. As cells enter mitosis MPS1 accumulates in prophase at unattached kinetochores [129,131,135,141]. This is mediated by an N-terminal localization module in MPS1 [130,142,143] and further requires PRP4 [144], HEC1 [78,142,145,146] and Aurora B activity [142,146]. N-terminal deletion mutants defective in kinetochore localization are unable to activate the SAC in response to unattached kinetochores [142,143]. It is believed that kinetochore localization is important for two aspects of MPS1 function. First, kinetochore localization is important for MPS1 activation since local clustering of MPS1 promotes activating *in trans* and *in cis* autophosphorylation events [131,147,148]. Second, kinetochore localization is critical for function. The N-terminal truncation mutant mentioned before does not localize to kinetochores but is active when overexpressed (presumably by facilitating cross-phosphorylation in the cytoplasm) yet cannot sustain SAC activity [142]. Interestingly, MPS1 inhibition results in an accumulation of MPS1 at unattached kinetochores suggesting that MPS1 promotes its own release from kinetochores [90,149]. This is likely important to allow efficient shut-off of MCC production once kinetochores attach, as preventing MPS1 release by constitutively tethering it to kinetochores results in sustained SAC activation [149]. MPS1 inhibition has also been implication in irreversible SAC shut-off at anaphase onset. In yeast, Mps1 is degraded at anaphase and this was essential to allow proper anaphase progression and APC/C substrate degradation. In human cells, too, MPS1 appears to be degraded in mitosis and failure to do so properly caused mitotic abnormalities [140].

Once localized and activated, MPS1 exerts its control of the SAC in multiple ways. First, MPS1 regulates recruitment of multiple SAC proteins, including MAD1, MAD2, BUBR1, BUB1 and the RZZ complex (Figure 4) (reviewed in [76]). Second, MPS1 promotes MAD2 dimerization [90] and thus release of soluble C-MAD2 that is indispensible for MCC assembly. Finally, MPS1 activity maintains MCC stability (Figure 4) [91]. For most of these functions, it is unclear how MPS1 accomplishes its influence, since few functional phosphorylation sites in substrates have been reported. MPS1 has been shown to phosphorylate MAD1 and NDC80 in budding yeast but the molecular consequences of this have not been reported and these events do not appear to be conserved. A few notable relevant phosphorylations that explain aspects of MPS1 function have recently been reported, however. The first is the mechanism by which MPS1 controls BUB1 localization. Several recent studies showed that MPS1 phosphorylates conserved MELT-like motifs within KNL1. BUB1 recruitment to kinetochores relies on KNL1, most likely via direct interactions, and MPS1-dependent phosphorylation of these motifs is an essential component in this recruitment [118-120]. The second is phosphorylation of MAD2 by MPS1 in fission yeast. Mps1 was found to phosphorylate Mad2 on several residues. While a C-terminal phosphorylation promotes the dissociation of Mad2 from Mad1, a more

N-terminally located serine is phosphorylated to promote MCC stability [150]. It remains to be uncovered if these mechanism are conserved in humans.

Like the SAC, the conserved role of MPS1 in biorientation also likely involves multiple pathways. In human cells MPS1 phosphorylates the CPC member Borealin to promote Aurora B activity [131,132,151,152], and additionally contributes to centromere localization of Aurora B by promoting the BUB1-dependent phosphorylation of histone H_2A [153]. It is moreover highly likely that the control of MPS1 over BUBR1 localization affects PP2A levels at kinetochores, with ensuing alterations to Aurora B substrate phosphorylation and stability of kinetochore-microtubule interactions [41]. In yeast, phosphorylation of Dam1p by Mps1 has been shown to regulate efficient coupling of kinetochores to microtubules [154]. Although Dam1p is not present in animals, an analogous function may be performed by the vertebrate SKA complex, and it would be interesting to examine whether regulation of SKA by MPS1 exists in human cells. Finally, *Xenopus* CENP-E, which is important for chromosome congression, is heavily phosphorylated by MPS1 in the C-terminal tail *in vitro*, and this relieves auto-inhibition of the recombinant kinesin motor protein [155]. It is, again, unknown, if this occurs in cells and if this type of regulation is present in other species.
Besides regulation of the SAC and biorientation, some studies have implicated MPS1 in G2-phase DNA damage signaling through phosphorylation of multiple targets including BLM, CHK2 and p53 [156-158]. For sake of focus, however, this role of MPS1 will not be further discussed.

Outline of this thesis

Although the importance for MPS1 activity in the regulation of the SAC is well established, the underlying molecular mechanisms remain largely unknown. With the exception of KNL1, many MPS1 substrates that would explain its central role in SAC signaling remain elusive. The research described in this thesis focuses on the elucidation of the molecular mechanisms of MPS1 signaling in the SAC. **Chapter 2** describes the use of chemical genetics to specifically inhibit an engineered version of MPS1 in a penetrant and reversible manner, in order to probe MPS1 function in mitosis. This study showed for the first time which mitotic roles of MPS1 depend on its catalytic activity. In **Chapter 3** we investigated the pathways that were reported to control MAD1 kinetochore recruitment. We reveal that feedback control between MPS1, BUB1 and ZW10 regulates MAD1 localization and subsequently SAC activity. In **Chapter 4** we describe a way to find novel auxiliary SAC regulators. We provide evidence that PLK1, although dispensable for SAC signaling per se, modulates the SAC by promoting MCC stability when SAC activity is low. **Chapter 5** describes the application of several quantitative mass spectrometry-based proteomics approaches to identify novel MPS1 substrates. Finally we summarize the result of this thesis in **Chapter 6** and will discuss our findings in the light of current literature and propose future research directions.

Chapter 2

Chemical genetic inhibition of MPS1 in stable human cell lines reveals novel aspects of MPS1 function in mitosis

Tale Sliedrecht[1,2], Chao Zhang[3], Kevan M. Shokat[3], Geert J. P. L. Kops[1,2]

1 Department of Physiological Chemistry and Cancer Genomics Centre, UMC Utrecht, Utrecht, The Netherlands, **2** Netherlands Proteomics Centre, Utrecht, The Netherlands, **3** Department of Cellular and Molecular Pharmacology, University of California San Francisco, San Francisco, USA

Adapted from PLoS ONE 5(4): e10251

Abstract

Background: Proper execution of chromosome segregation relies on tight control of attachment of chromosomes to spindle microtubules. This is monitored by the mitotic checkpoint that allows chromosome segregation only when all chromosomes are stably attached. Proper functioning of the attachment and checkpoint processes is thus important to prevent chromosomal instability. Both processes rely on the mitotic kinase MPS1.

Principal finding: We present here two cell lines in which endogenous MPS1 has been stably replaced with a mutant kinase (MPS1-as) that is specifically inhibited by bulky PP1 analogs. MPS1 inhibition in these cell lines is highly penetrant and reversible. Timed inhibition during bipolar spindle assembly shows that MPS1 is critical for attachment error-correction and confirms its role in Aurora B regulation. We furthermore show that MPS1 has multiple controls over mitotic checkpoint activity. MPS1 inhibition precludes MAD1 localization to unattached kinetochores but also accelerates mitosis. This acceleration correlates with absence of detectable mitotic checkpoint complex after MPS1 inhibition. Finally, we show that short-term inhibition of MPS1 catalytic activity is sufficient to kill cells.

Conclusions/Significance: MPS1 is involved in the regulation of multiple key processes that ensure correct chromosome segregation and is a promising target for inhibition in anti-cancer strategies. We report here two cell lines that allow specific and highly penetrant inhibition of MPS1 in a reproducible manner through the use of chemical genetics. Using these cell lines we confirm previously suggested roles for MPS1 activity in mitosis, present evidence for novel functions and examine cell viability after short and prolonged MPS1 inhibition. These cell lines present the best cellular model system to date for investigations into MPS1 biology and the effects of penetrance and duration of MPS1 inhibition on cell viability.

Introduction

To maintain a stable genome, cells have evolved a variety of processes that ensure accurate chromosome segregation. In early mitosis, kinetochores of sister chromatids attach to microtubules emanating from opposite spindle poles. Correct end-on attachment of microtubules to kinetochores relies on the error-correction machinery that destabilizes improper attachments through the actions of the Aurora B kinase [58,59,159]. As long as unattached kinetochores persist, the onset of anaphase is prevented by a surveillance mechanism called the mitotic checkpoint that will halt cell cycle progression until all chromosomes are stably attached to the mitotic spindle [60,61,75]. The mitotic checkpoint will be satisfied upon stable biorientation of all chromosomes, after which chromosome segregation is allowed to proceed. Proper execution of chromosome biorientation and mitotic checkpoint signaling relies on a set of multifunctional kinases, one of which is the dual specificity kinase MPS1[29,62,63]. First discovered to regulate spindle pole body duplication in budding yeast [64,65,125], MPS1 was subsequently found to additionally regulate the mitotic checkpoint [66,136] and spindle assembly [67,160]. Regulation of the mitotic checkpoint by MPS1 is evolutionary conserved and has been shown in fission yeast, fruit flies, *Xenopus* egg extracts and human cells [68,69,129,135,161-163]. MPS1 exerts this control, at least in part, through regulating kinetochore localization of several checkpoint proteins including MAD1 and MAD2 [70,71,135,163,164]. Recently, MPS1 was also reported to regulate sister chromatid biorientation in both budding yeast and humans [72-74,138,164]. In human cells, MPS1 promotes biorientation by regulating Aurora B activity through phosphorylation of the chromosomal passenger complex (CPC) member Borealin [75,152,164].

Due to its central role in mitosis, misregulation of MPS1 kinase activity results in chromosomal instability (CIN) and subsequent aneuploidy, a hallmark shared by cells from solid tumors [76,131,165]. Inefficient activation of MPS1 results in weakened mitotic checkpoint activity and the persistence of falsely attached chromosomes, causing frequent but non-lethal chromosome segregation errors [77-80,131]. Conversely, reduction of MPS1 activity has recently been shown to sensitize tumor cells but not normal cells to low doses of taxol by elevating the frequency of chromosome missegregations to near-lethal levels [81,166]. Partial inhibition of MPS1 might therefore be an effective anti-cancer therapy.

Although RNAi studies have uncovered several aspects of human MPS1 biology, the multifunctional character of MPS1 has prevented detailed and temporally controlled investigations into the different roles MPS1 might play in mitosis. Inhibition using the small molecules SP600125 and cincreasin has proved to be useful [75,82,134,167], but cincreasin does not inhibit MPS1 in human cells [83,84,167] and the non-specific nature of SP600125 makes it an unfavorable choice to study MPS1. A more controlled approach is the use of chemical genetics, in which endogenous kinase is replaced by an engineered protein containing a mutated gatekeeper residue [62,71,83,85,168]. These gatekeeper mutants render the kinase specifically sensitive to inhibition by non-hydrolysable bulky ATP analogs such as chemically modified variants of the Src inhibitor PP1. This approach has previously been described for MPS1 in budding yeast [84,86,138,160] and in human cells in combination with transient RNAi [24,71,169]. The use of transient RNAi, however, introduces uncertainties regarding efficiency of knock down and reproducibility.

We present two cell lines in which endogenous MPS1 has been stably replaced with gatekeeper mutants. In-depth analysis of these clonal cell lines showed that addition of

bulky PP1 analogs allowed rapid and reversible inhibition of MPS1 kinase activity in a highly penetrant and reproducible manner. Using these cell lines we dissected the different roles of MPS1 in mitosis, further establishing known functions in checkpoint regulation and error-correction and providing novel insights in the function of MPS1 catalytic activity in checkpoint regulation.

Results

MPS1 is selectively inhibitable in two engineered cell lines

To study the role of MPS1 in different mitotic processes, we created cell lines in which MPS1 kinase activity could specifically and reversibly be inhibited. For this, we engineered the ATP-binding pocket of MPS1 to create a kinase with unique preference for bulky ATP-like small molecules [86,168]. As previously shown for MPS1 in a transient expression system [83,87,169], MPS1^{M602A} signifies such an analog sensitive (as) version. In addition to M602A, we also tested M602G, which similarly enlarges the ATP-binding pocket of MPS1 and may provide stronger inhibition [84,160]. To ensure that mutation of the gatekeeper residue did not affect MPS1 functionality, the ability of both MPS1^{M602A} and MPS1^{M602G} to sustain an active checkpoint in MPS1 RNAi cells was investigated. Similar to LAP-Mps^{WT}, both LAP-MPS1^{M602A} and LAP-MPS1^{M602G} reconstituted checkpoint signaling in response to nocodazole when endogenous MPS1 was transiently replaced with these proteins (Figure S1A).

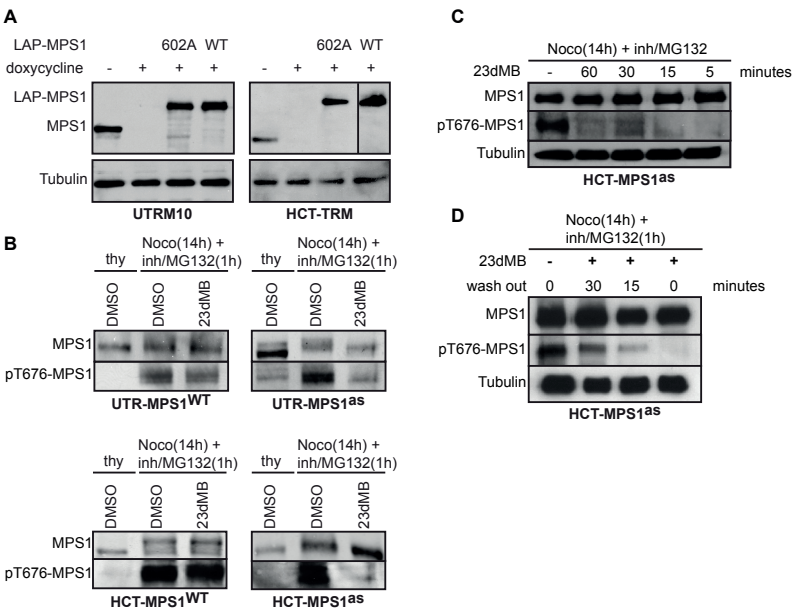

Figure 1. Stable expression of LAP-MPS1^{as} renders selective sensitivity to 23dMB-PP1

(A) MPS1 and tubulin immunoblots of lysates of UTRM10 and HCT-TRM cells in which endogenous MPS1 is removed by doxycycline-induced expression of MPS1 shRNA and replaced with the indicated LAP-MPS1 mutants. **(B-D)** pT676-MPS1 and MPS1 immunoblots of UTR-MPS1^{as} **(B)** and HCT-MPS1^{as} **(B-D)** cell lines treated with nocodazole and MG132 in combination DMSO/23dMB-PP1 for 1 hour **(B)**, with nocodazole and MG132 for 1 hour in combination with an additional 23dMB-PP1 treatment for the indicated amounts of time **(C)**, or with nocodazole and MG132 in combination with 23dMB-PP1 for 1 hour, followed by PBS wash after which cells were left for 15 or 30 minutes in media without 23dMB-PP1 **(D)**.

To create stable cell systems in which MPS1 could be inhibited in a potent and reproducible manner, we stably expressed LAP-MPS1^{M602A} (hereafter referred to as MPS1^{as}) or LAP-MPS1^{M602G} in UTRM10 (U2OS-derived) and HCT-TRM (HCT116-derived) cell lines in which endogenous MPS1 could be removed by doxycycline-induced expression of MPS1 shRNA [86,88,166]. Continuous growth in doxycycline and clonal selection resulted in stable, viable clonal cell lines in which endogenous MPS1 was undetectable and replaced with MPS1^{WT} or MPS1^{as} (Figure 1A). No HCT-TRM clones expressing MPS1^{M602G} were obtained and only one such UTRM10 clone grew out. We suspect that the low activity of MPS1^{M602G} (see below) significantly decreased the chance of survival of cells expressing only this form of MPS1. Nevertheless, one UTRM10 cell line expressing MPS1^{M602G} was established, showing that under certain circumstances, MPS1^{M602G} can support viability. All cell clones (renamed HCT-MPS1^{WT}, HCT-MPS1^{as}, UTR-MPS1^{WT}, UTR-MPS1^{as} and UTR-MPS1^{M602G}) have been kept in culture for months, showing that replacement of MPS1 is stable.

Human MPS1 auto-activates by phosphorylating T676 in its activation loop. T676 phosphorylation is essential for full kinase activity [89,131,147,148], and the phosphorylation status of T676 serves as a read-out for MPS1 kinase activity [77,131]. To investigate if MPS1^{as} activity could be inhibited by bulky PP1 analogs in our engineered cell lines, we examined MPS1 T676 phosphorylation in different conditions. Following tests on the potency of different PP1 analogs to inhibit MPS1^{as} (Figure S1B), we settled on 23dMB-PP1 (1-(*tert*-butyl)-3-(2,3-dimethylbenzyl)-1*H*-pyrazolo[3,4-*d*]pyrimidin-4-amine) as the MPS1^{as} inhibitor of choice. As expected, MPS1^{WT} and MPS1^{as} displayed a mobility shift and phosphorylation of T676 upon nocodazole addition in both HCT and UTR cell types (Figure 1B). Whereas addition of 23dMB-PP1 did not affect the mobility or T676 phosphorylation of MPS1^{WT}, 23dMB-PP1 prevented hyperphosphorylation as well as T676 phosphorylation of MPS1^{as} (Figure 1B). Full inhibition of MPS1^{as} was established within 5 minutes after addition of 23dMB-PP1 (Figure 1C). Furthermore, T676 phosphorylation could be detected 15 minutes after removal of 23dMB-PP1, showing that this rapid inhibition was reversible (Figure 1D). Interestingly, very little T676 phosphorylation and weak mobility shift was detected in the UTR-MPS1^{M602G} clone, indicating this engineered MPS1 kinase has strongly reduced activity compared to MPS1^{WT} and MPS1^{as} (Figure S2A). Although any residual activity and all MPS1 functions could be efficiently inhibited by treatment of the UTR-MPS1^{M602G} cells with PP1 inhibitors (Figure S2 and S3B), we focused our investigations on studies with the MPS1^{as} clones.

MPS1^{as} inhibition by 23dMB-PP1 disables mitotic checkpoint signaling

MPS1 kinase activity is needed for the mitotic checkpoint to delay mitosis when unattached kinetochores persist [90,134,135,160,164,169]. We next studied the ability of the cell lines to maintain a mitotic checkpoint response in the presence of 23dMB-PP1. In absence of 23dMB-PP1, all HCT-MPS1^{WT} and HCT-MPS1^{as} cell lines sustained checkpoint activity in the presence of nocodazole as scored by mitotic index (Figure 2A). The ability to maintain a nocodazole-induced mitotic delay was not lost in MPS1^{WT} cells upon treatment with 23dMB-PP1, showing 23dMB-PP1 did not have off-target effects that could disable the mitotic checkpoint. In contrast to MPS1^{WT}-expressing cells, 23dMB-PP1 completely abolished mitotic checkpoint activity in MPS1^{as} cells. Similar results were obtained with the UTR-MPS1^{M602G} cells (Figure S2B).

To ensure that MPS1 inhibition decreased mitotic index by inhibiting mitotic checkpoint activity rather than, for instance, preventing entry into mitosis, mitotic progression in the

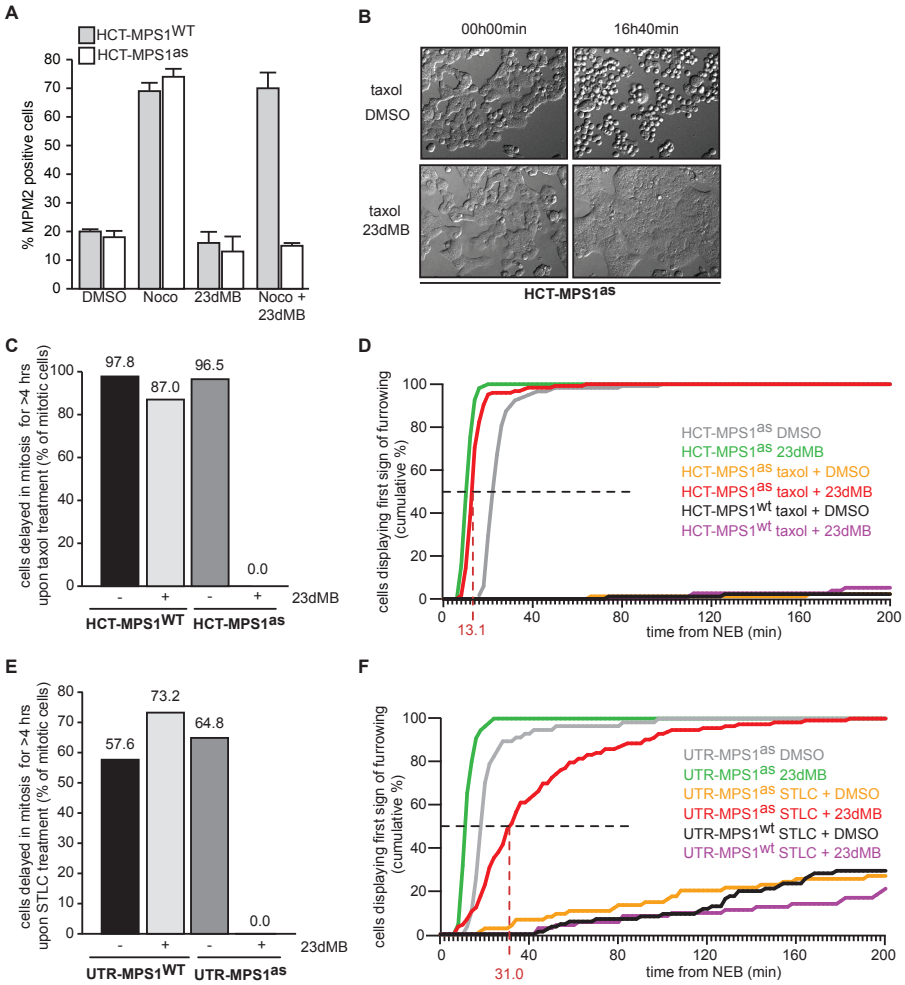

Figure 2. MPS1 activity is essential for the mitotic checkpoint

(A) Quantification of flow cytometric analysis of the fraction of mitotic cells treated with DMSO or 23dMB-PP1 alone or in combination with nocodazole for 14 hours. Graph represents average of three experiments (+/-SD).

(B-F) Time-lapse analysis by DIC microscopy of HCT- and UTR-derived cells treated with taxol (HCT-derived cells) or STLC (UTR-derived cells) in combination with DMSO or 23dMB-PP1. Images in B display morphology of HCT-MPS1^{as} cells imaged at the indicated timepoints after addition of taxol in combination with DMSO or 23dMB-PP1. Graphs in **(C)** and **(E)** represent percentages of cells delayed in mitosis for 4 hours or longer. Percentages are indicated at top of each column. Line graphs in **(D)** and **(F)** show cumulative percentages of cells that display first signs of furrowing at indicated times after NEB. Dashed lines indicate half-time to furrowing of inhibited drug-treated MPS1^{as} cells.

presence of spindle poisons was monitored by live cell differential interference contrast (DIC) microscopy. As a measure for time spent in mitosis, the time from nuclear envelope breakdown (NEB) to the first signs of furrow ingression was scored. Engaging the mitotic checkpoint in these cells by treatment with the spindle drugs nocodazole or taxol, or the Eg5 inhibitor STLC caused all cell lines to delay mitosis for hours (Figure 2B-F and S3). Delays were most pronounced in cells with the HCT-TRM background where ~95% of cells

maintained the arrest for at least 4 hours (Figure 2C, D and S3A, C) and ~55% for at least 10 hours (data not shown). In stark contrast, addition of 23dMB-PP1 caused all HCT-MPS1^{as} but not HCT-MPS1^{WT} cells to exit mitosis within 60 minutes (Figure 2D and S3A, C). These data show that the ability of cells to delay mitotic progression absolutely requires MPS1 kinase activity. Moreover, the finding that all 23dMB-PP1-treated HCT-MPS1^{as} cells had lost this ability illustrated the clonality of this cell line.

MPS1 kinase activity promotes localization of MAD1, MAD2, CDC20 and BUB1 to unattached kinetochores.

Proper functioning of the mitotic checkpoint requires the recruitment of checkpoint proteins to the kinetochore. Kinase activity of MPS1 is required for the recruitment of MAD2 to unattached kinetochores, at least partly explaining its necessity for checkpoint signaling [91,135,164,169]. There is, however, discrepancy between reports on the requirement of MPS1 for the recruitment of MAD1 [92,145,163,164,169], BUB1 [93,145,163,164,170], BUBR1 [93,121,134,147,164] and CENP-E [93,94,128,135,145,164,169] to kinetochores.

To examine how MPS1 catalytic activity contributes to recruitment of these and other checkpoint proteins, we assayed their kinetochore association after inhibition of MPS1^{as} in our cell lines. Like the ability to delay mitosis, kinetochore recruitment of MAD1, MAD2, BUBR1, BUB1, CENP-E and CDC20 was altered neither in DMSO-treated MPS1^{WT} or MPS1^{as} cells, nor in 23dMB-PP1-treated MPS1^{-WT} cells (Figure 3 and S4). However, addition of 23dMB-PP1 to MPS1^{as} cells significantly reduced the level of MAD1, MAD2, BUB1 and CDC20 at unattached kinetochores, but only marginally affected BUBR1 levels and did not influence CENP-E levels (Figure 3). These data show that MPS1 kinase activity promotes kinetochore-binding of MAD1, MAD2, BUB1 and CDC20.

MPS1 inhibition strongly diminishes MCC levels in mitotic cells

The mitotic checkpoint functions through the production of an inhibitory complex called the mitotic checkpoint complex (MCC). The MCC targets CDC20, the main activator of the anaphase promoting complex or cyclosome (APC/C) in prometaphase, thereby preventing exit from mitosis [75,95]. The amplification of MCC assembly by unattached kinetochores is dependent on kinetochore localization of MAD1 and MAD2 [83,96,97,171]. Since inhibition of MPS1 resulted in loss of kinetochore-bound MAD1/MAD2, we set out to investigate if MPS1 inhibition influences the amount of MCC in nocodazole-treated cells. As expected, CDC20 immunoprecipitations from cells treated with DMSO contained the MCC subunits MAD2, BUBR1 and BUB3 (Figure 4A). Although inhibition of MPS1 did not alter the levels of coprecipitated BUBR1 and BUB3, the amount of CDC20-bound MAD2 in mitotic cells was reduced to interphase levels after treatment with 23dMB-PP1 (Figure 4A). Similarly, MAD2 immunoprecipitations displayed little bound CDC20 in cells treated with 23dMB-PP1 when compared to DMSO-treated cells (Figure 4B). These data show that MPS1 catalytic activity is needed for formation and/or stability of MCC.

MPS1 inhibition decreases the time spent in mitosis

To get more detailed insight in the functions of MPS1 kinase activity during mitosis, we examined various aspects of chromosome segregation in our cell lines by time-lapse microscopy. MPS1^{WT} cells treated with DMSO or 23dMB-PP1 progressed through mitosis normally. In addition, 23dMB-PP1 treatment of MPS1^{as}-expressing cells caused no overt problems in mitotic entry, bipolar spindle formation or cytokinesis in neither cell line.

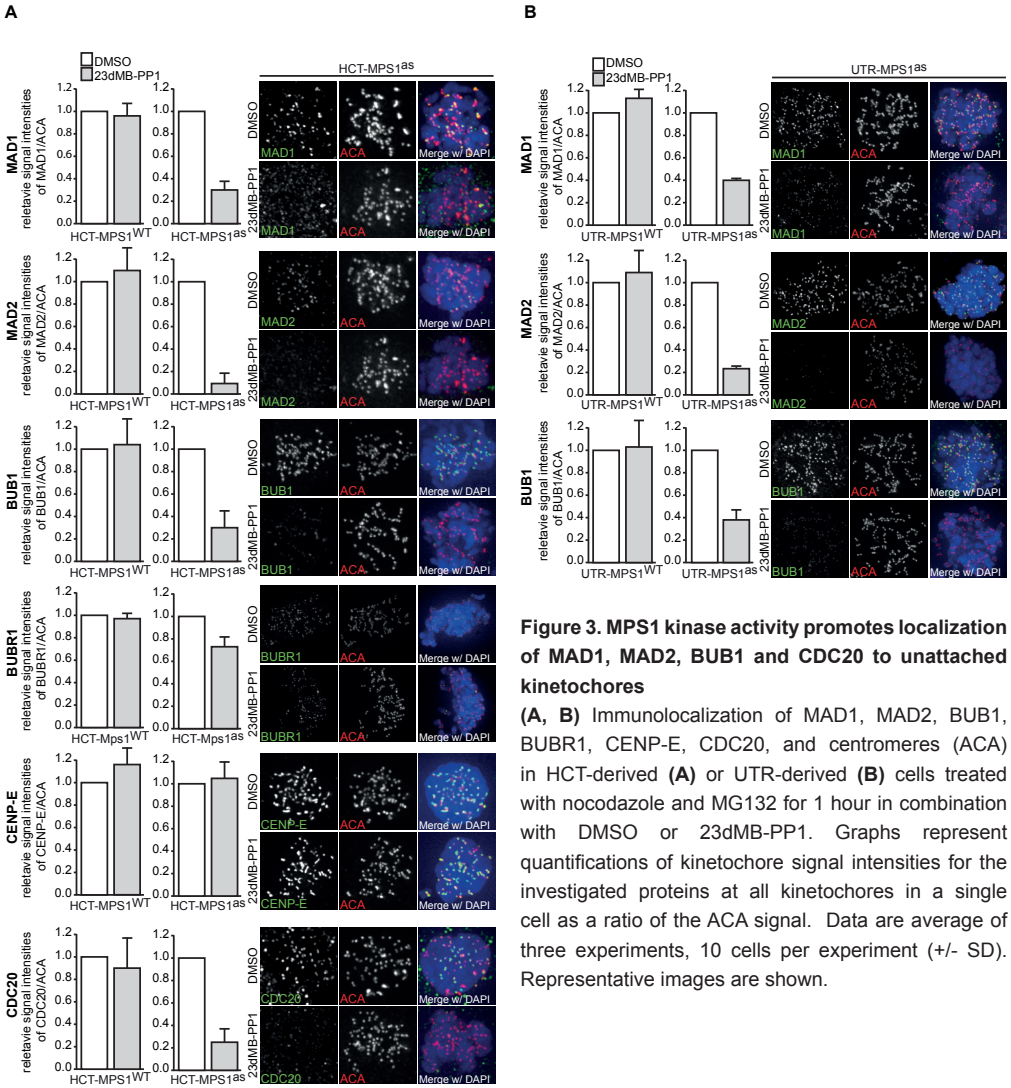

Figure 3. MPS1 kinase activity promotes localization of MAD1, MAD2, BUB1 and CDC20 to unattached kinetochores

(A, B) Immunolocalization of MAD1, MAD2, BUB1, BUBR1, CENP-E, CDC20, and centromeres (ACA) in HCT-derived **(A)** or UTR-derived **(B)** cells treated with nocodazole and MG132 for 1 hour in combination with DMSO or 23dMB-PP1. Graphs represent quantifications of kinetochore signal intensities for the investigated proteins at all kinetochores in a single cell as a ratio of the ACA signal. Data are average of three experiments, 10 cells per experiment (+/- SD). Representative images are shown.

Strikingly, however, 23dMB-PP1-treated MPS1^{as} cells sped through mitosis (Figure 5A). To more carefully quantify this phenotype, the time from NEB to the first signs of furrowing was measured. Half of DMSO-treated HCT-MPS1^{WT} and HCT-MPS1^{as} cells had proceeded to furrow ingression 26 and 22 minutes after NEB, respectively (Figure 5B). Strikingly, whereas addition of 23dMB-PP1 had no effect on the time to furrow ingression of HCT-MPS1^{WT} cells, half the 23dMB-PP1-treated HCT-MPS1^{as} cells showed signs of furrow ingression in as little as 10 minutes and no cell took longer than 20 minutes to reach this furrowing stage of mitosis (Figure 5A, B). Further evidence for the high penetrance of MPS1 inhibition in these cells was illustrated by the fact that exit from mitosis in taxol was within a similar timeframe as these unperturbed mitosis: 13 vs. 10 minutes, respectively (Figure 2D). A similar, albeit less consistent effect was apparent in the UTR-derived cell lines: Half-time to furrowing in UTR-MPS1^{as} cells was reduced from 18 to 12 minutes by treatment with 23dMB-PP1, whereas this was not altered by 23dMB-PP1 in UTR-MPS1^{WT} cells (Figure 5C).

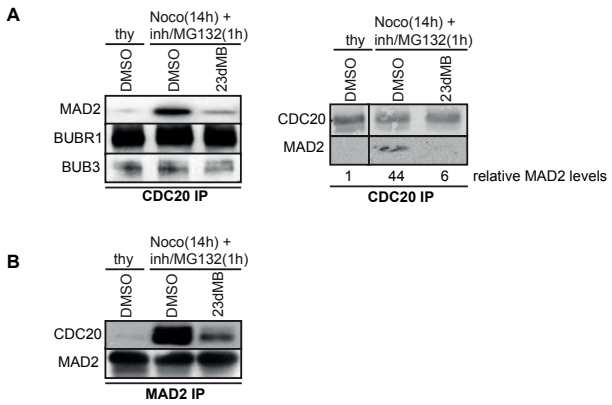

Figure 4. MPS1 inhibition reduces MAD2-CDC20 interaction

(A, B) Immunoblots of the indicated proteins in immunoprecipitations of CDC20 **(A)** or MAD2 **(B)**. Immunoprecipitations were preformed on interphase cell lysates (thymidine, thy) or mitotic cell lysates (nocodazole, noco) of HCT-MPS1^{as} cells treated with DMSO or 23dMB-PP1 in combination with MG132 for 1 hour. Quantification of MAD2 levels in CDC20 immunoprecipitates, relative to interphase levels, is indicated in **(A)**, right panel.

MPS1 activity facilitates attachment error-correction

MPS1 is critical for chromosome biorientation in yeast and humans [98,99,138,164] and our previous results using MPS1 RNAi supported the hypothesis that MPS1 facilitates error-correction by promoting Aurora B activity at inner centromeres [100,101,164]. Nevertheless, a true display of the role for MPS1 in error-correction requires inhibition of MPS1 activity solely during the error-correction process. Our analog-sensitive cell lines provided the opportunity to test this. We first verified that MPS1 inhibition prevented efficient chromosome alignment on the cell's equator. Cells were treated with MG132 for 60 minutes to prevent exit from mitosis and provide cells with sufficient time to align all chromosomes. Roughly 30% of DMSO- or 23dMB-PP1-treated HCT-MPS1^{WT} cells or DMSO-treated HCT-MPS1^{as} cells displayed misaligned chromosomes within this time (Figure 6A). In agreement with our previous studies [86,164], addition of 23dMB-PP1 to HCT-MPS1^{as} cells caused severe alignment problems in ~70% of cells. Similar results were obtained by MPS1 inhibition in UTR-MPS1^{M602G} cells (Fig S2C).
We next investigated if the generated cells lines were able to correct faulty attachments when MPS1 was inhibited during error-correction rather than prior to the establishment of errors. To this end, cells were treated with the Eg5-inhibitor monastrol to create monopolar spindles with large numbers of chromosomes that have syntelic or monotelic attachments [102,172]. Monastrol can efficiently be removed from cell, which allows the formation of a bipolar spindle in which full chromosome alignment requires correction of the improper attachments by Aurora B [34,103-105,173]. All attachment errors were corrected and full chromosome alignment was restored in 87% of HCT-MPS1^{WT} cells 50 minutes after removal of monastrol (Figure 6B, C). Addition of 23dMB-PP1 during monastrol washout of MPS1^{as} cells however, caused significant problems with chromosome alignment (Figure 6B, C). Importantly, the non-aligned chromosomes were often seen to have retained syntelic attachments, indicative of error-correction deficiency. These data solidify the notion that MPS1 activity is needed for efficient correction of erroneous attachments.

MPS1 enhances Aurora B activity

Erroneous kinetochore-microtubule attachments cause a lack of tension between sister centromeres which allows Aurora B kinase activity to destabilize such attachments [32-34,37,104,105,174,175]. We and others previously found that MPS1 enhances Aurora B activity up to 4-fold by phosphorylating the CPC component Borealin, explaining the contribution of MPS1 to error-correction [106-108,152,164]. We next set out to examine the link between MPS1 and Aurora

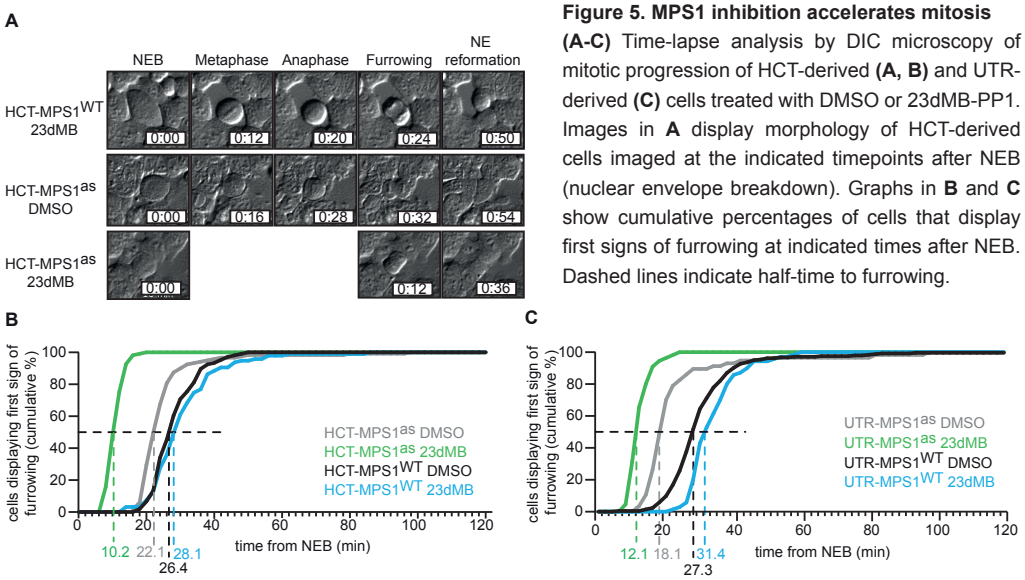

Figure 5. MPS1 inhibition accelerates mitosis
(A-C) Time-lapse analysis by DIC microscopy of mitotic progression of HCT-derived **(A, B)** and UTR-derived **(C)** cells treated with DMSO or 23dMB-PP1. Images in **A** display morphology of HCT-derived cells imaged at the indicated timepoints after NEB (nuclear envelope breakdown). Graphs in **B** and **C** show cumulative percentages of cells that display first signs of furrowing at indicated times after NEB. Dashed lines indicate half-time to furrowing.

B activity in our analog-sensitive cell lines. Using phosphate-affinity gel electrophoresis [109,176], Borealin displayed a prominent mobility shift in mitotic samples of nocodazole-treated cells (Figure 6D). This shift was reduced upon inhibition of MPS1^{as} by 23DMB-PP1, showing for the first time that phosphorylation of endogenous Borealin is under control of MPS1 activity. To investigate the consequences of MPS1 inhibition on Aurora B activity, mitotic cells were collected by shake-off after 14 hours of taxol treatment and subsequently treated with 23dMB-PP1 or DMSO in combination with MG132 for an additional hour, after which mitotic lysates were examined for phosphorylation of Serine 10 in Histone H3 (pS10-H3) by immunoblot. Surprisingly, addition of 23dMB-PP1 to UTR- or HCT-MPS1^{as} cells that had been arrested in mitosis for hours did not significantly reduce pS10-H3, even though MPS1 activity, as measured by mobility shift, was inhibited (Fig 6E, F). These findings are in seeming contrast to our previous report, in which MPS1 RNAi reduced pS10-H3 levels in HeLa cells [110,164]. Since one difference between these experiments is whether or not cells entered mitosis with intact MPS1 activity, we next examined pS10-H3 levels in cells that had seen 23dMB-PP1 prior to mitotic entry. For this, cells were treated with DMSO or 23dMB-PP1 for 1 hour, after which taxol/MG132 was added for an additional 2 hours. Analysis of these mitotic samples showed significant reduction of pS10-H3 levels in 23dMB-PP1-treated MPS1^{as} cells but not MPS1^{WT} cells (Figure 6E, F and S5). The magnitude of this decrease is less prominent than direct inhibition of Aurora B activity using ZM447439 (Figure 6E, F and S5) [33,111,112], which is in line with our previous observations that showed that while MPS1 could enhance Aurora B activity, it was not absolutely critical [39,41,164].

Selective, short-term inhibition of MPS1 kills cells

Long-term MPS1 RNAi kills U2OS, HCT116 and LS174T cells [16, 17] and MPS1 inhibition has been proposed as an effective way to induce a lethal dose of chromosome segregation errors [39,41,42,79,113,114,166,177]. To examine if selective and penetrant inhibition of the catalytic activity of MPS1 is lethal, UTR- and HCT-derived MPS1^{wt} and MPS1^{as} cells were treated with 23dMB-PP1 for 8 days after which colony outgrowth was scored. 23dMB-PP1 had no off-target effect on viability during this period, as MPS1^{wt} cells remained fully viable despite

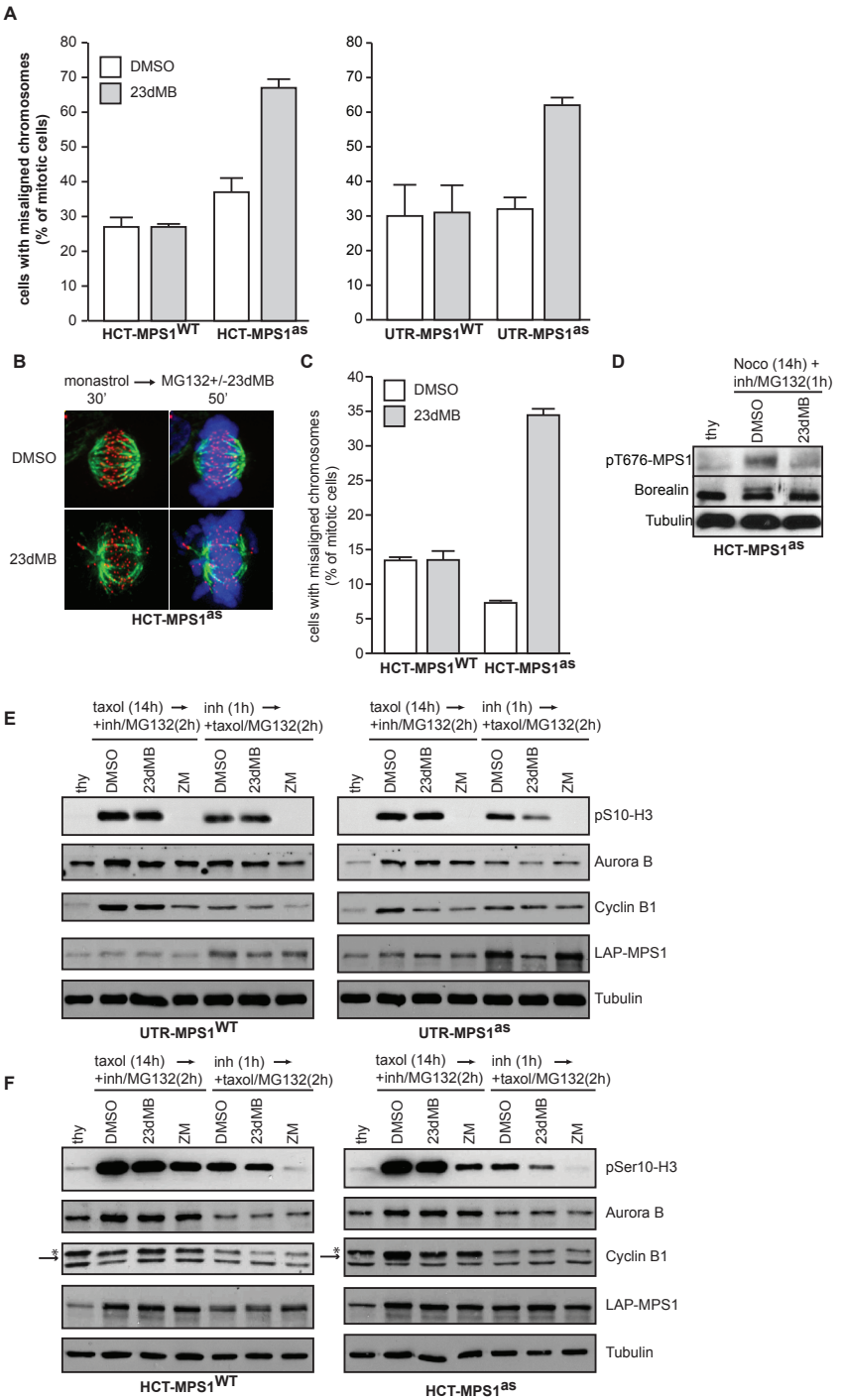

Figure 6. MPS1 activity is required for efficient correction of erroneous attachments

(A) Chromosome alignment in HCT- and UTR-MPS1^{WT} and -MPS1^{as} cell lines treated with MG132 for 60 minutes in combination with DMSO or 23dMB-PP1. Graphs display percentages of cells with misaligned chromosomes,

averages of three experiments, at least 50 mitotic cells per experiment (+/-SD). **(B, C)** Immunostainings of HCT-MPS1^{WT} and HCT-MPS1^{as} cells treated with monastrol for 30 min followed by a release from monastrol into MG132 with or without 23dMB-PP1 for 50 minutes. Cells in B were immunostained for tubulin (green) and centromeres (ACA, red). DNA (DAPI) is in blue. Graph in **(C)** indicates the percentage of mitotic cells with misaligned chromosomes 50 minutes after monastrol washout, averages of two experiments, at least 100 mitotic cells per experiment (+/-SD). **(D)** Immunoblots of Borealin after phosphate-affinity gel electrophoresis of lysates from nocodazole-treated HCT-MPS1^{as} cells to which DMSO or 23dMB-PP1 and MG132 was added during the final hour. **(E, F)** Immunoblots of the indicated proteins in lysates of the UTR- **(E)** and HCT-MPS1 **(F)** variant cell lines. Cells were treated either with thymidine (thy), with taxol for 14 hours followed by the indicated inhibitors for an additional 2hrs, or with the indicated inhibitors for 1 hour followed by taxol/MG132 treatment for an additional 2 hrs ZM, ZM447439. Arrow in F points to Cyclin B. Asteriks indicates aspecific band in thymidine sample.

prolonged exposure to 23dMB-PP1 (Figure 7A). As shown in Figure 7B, however, no MPS1^{as} cells survived prolonged MPS1 inhibition. To approach a more relevant duration of inhibition in potential future clinical settings, we next tested the effect of short-term inhibition of MPS1 on cell viability. Addition of 23dMB-PP1 for 2 days and subsequent removal of the inhibitor until day 8 left no (HCT-MPS1^{as}) or very few (UTR-MPS1^{as}) cells alive (Figure 7B). These data show that efficient inhibition of MPS1 for a relatively short period of time is sufficient to kill cells

Discussion

In the present study we investigated the different roles of MPS1 in mitosis of human cells through the use of chemical genetics. We report here two clonal cell lines expressing analog-sensitive versions of MPS1 in which endogenous MPS1 was stably removed by doxycycline-induced shRNA expression. Use of these cell lines circumvents experimental limitation in reproductivity and penetrance associated with transient RNAi reconstitutions [115,169] and allows temporal control of MPS1 activity.

Chemical genetic inhibition of MPS1 was previously used to uncover novel aspects of MPS1 in *S. cerevisiae* mitosis [138,160]. A yeast strain carrying the analog-sensitive M516G mutation (similar to the M602G mutation in human MPS1, included in the present study) allowed analysis of MPS1 functions after the moment of spindle pole body duplication, a critical function of MPS1 in budding yeast [125,160]. Using this strain (*MPS1-as1*), it was verified that MPS1 inhibition prevents mitotic checkpoint activity and causes cell death [160]. In addition, MPS1-inhibited yeast cells were found to display spindle morphology defects and chromosome mispositioning [160], possibly as a consequence of errors in chromosome biorientation [138].

In agreement with these and other reports [138,160,164], chemical genetic inhibition of MPS1 in our human cell lines verified that MPS1 kinase activity is critical for chromosome biorientation. Although our data using MPS1 RNAi supported the hypothesis that MPS1 facilitated error-correction by promoting Aurora B activity at inner centromeres [164], we now show that error-correction is also prevented when MPS1 kinase activity is inhibited only during the error-correction process in cells undergoing spindle bipolarisation after monastrol wash-out. Additionally, through the use of phosphate-affinity gel electrophoresis we show that phosphorylation of endogenous Borealin is under the control of MPS1. Borealin phosphorylation enhances Aurora B activity [152,164] yet inhibition of MPS1 did not affect pS10-H3 levels under conditions that showed an increase in Borealin mobility. pS10-H3 was only found reduced when cells entered mitosis without MPS1 activity. These results suggest

that partial reduction in Aurora B activity caused by MPS1 inhibition is difficult to detect once pS10-H3 is fully established, possibly because of low turnover of the phosphate group on S10-H3. In support of this, inactivation of Aurora B by a 2 hour exposure of our HCT-derived cells to ZM447439 only caused a moderate reduction of pS10-H3 levels. These data indicate that pS10-H3 serves as a good readout for MPS1-dependent regulation of Aurora B activity when pS10-H3 is not fully established at mitotic entry. Nevertheless, since MPS1 inhibition during mitosis affects Borealin phosphorylation and error-correction, it is likely that acute effects on Aurora B activity by MPS1 inhibition can be visualised with antibodies to the relevant error-correction substrates.

The function of MPS1 kinase activity in the regulation of the mitotic checkpoint has previously been established by various labs including ours, and the present data fully agree with this [134,135,160,164,169]. As expected [145,163,164], MPS1 inhibition in our cell lines caused mislocalization of MAD1 and MAD2. This disagrees with the study by Tighe et al., in which chemical genetic inhibition of MPS1 in cells transiently transfected with MPS1 shRNA plasmids had little effect on MAD1 recruitment [169]. This discrepancy may be due to differences in penetrance of MPS1 inhibition. Whereas inhibition of MPS1 with 1NM-PP1 in the Tighe et al. study left mitotic progression unaffected in a large proportion of cells, mitosis was disturbed in the vast majority (UTR-MPS1^{as}) or all (HCT-MPS1^{as}) cells in our cell lines (Figure 2 and 5). This difference in penetrance may be due to inefficient RNAi by transient shRNA transfection or potency of 1NM-PP1 in the Tighe et al., study. In our hands, 1NM-PP1 was significantly less capable of inhibiting MPS1 than 23dMB-PP1 or 3MB-PP1 (Figure S2). Besides MAD1/MAD2, our data further indicate that MPS1 is essential for recruitment of CDC20 as well as BUB1 to unattached kinetochores, in agreement with some [163,170] but not other [145,164] previous reports using MPS1 RNAi or MPS1 protein depletion.

MPS1 inactivation affects the quality of chromosome segregation in unperturbed mitosis [131,169]. Using time-lapse microscopy we show that inactivation of MPS1 accelerates mitosis. A similar phenotype was reported for cells depleted of MAD2 or BUBR1 [78]. The regulation of mitotic timing by MAD2 and BUBR1 is kinetochore-independent, since MAD1 depletion, while disabling the mitotic checkpoint, did not affect normal mitotic timing [78]. It is therefore unlikely that lack of recruitment of MAD1 and MAD2 to kinetochores in MPS1-inhibited cells contributes to accelerated mitosis. An explanation for the timing phenotype, proposed by Meraldi et al., and in agreement with experimental data [71], is the possibility that sufficient MCC exists in interphase to constrain APC/C activity long enough to allow full chromosome

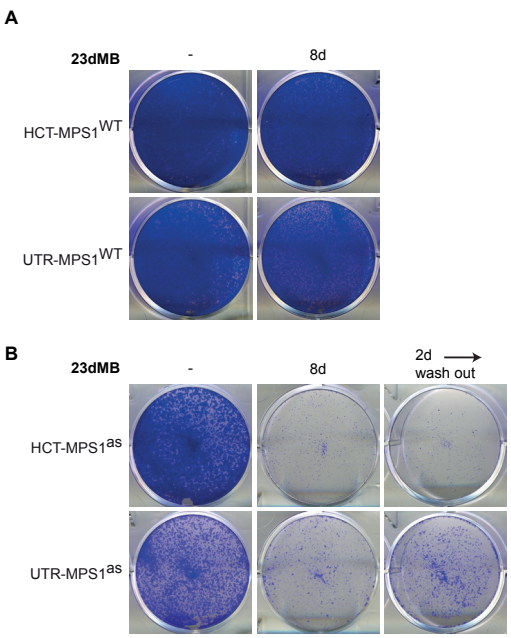

Figure 7. Specific inhibition of MPS1 enzymatic activity causes cell death

HCT-MPS1^{WT} and UTR-MPS1^{WT} cells **(A)** and HCT-MPS1^{as} and UTR-MPS1^{as} cell **(B)** were treated with or without (-) 23dMB-PP1 for 8 days (8d), or with 23dMB-PP1 for 2 days (2d) followed by wash-out and continued growth until day 8.

biorientation in the majority of cells. In this model, only presence of persistent unattached kinetochores requires additional MCC formation to further prolong mitosis. Given the timing phenotype of MPS1-inhibited cells, it is therefore possible that MPS1, in addition to influencing MAD1-dependent MCC formation, affects stability or inhibitory potential of pre-assembled MCC. Further studies are needed to examine this hypothesis.

Due to its central role in mitosis, MPS1 is an attractive target for anti-cancer therapies. A recent study from our lab proposed that elevating the frequency of chromosome segregation errors by partial MPS1 reduction can be of clinical relevance, especially with other treatments that affect fidelity of chromosome segregation [166]. We show here for the first time that specific inhibition of MPS1 enzymatic activity efficiently kills human cells. Moreover, a short pulse of inhibition followed by recovery caused lethality in a significant fraction of cells. As such a pulse of MPS1 inhibition is more relevant to potential future clinical situations than potent, long-term kinase inhibition, these data illustrate that specific and penetrant inhibition of MPS1 activity might indeed be a promising anti-cancer strategy.

Material & Methods

Tissue Culture and Treatments

UTR-MPS1^{WT}, UTR-MPS1^{as}, HCT-MPS1 ^{WT} and HCT-MPS1 ^{as} cells were derived from UTRM10 [131,164,166] and HCT-TRM (named HCT-116-TetRMPS1 clone#2 in Ref. [166]) cell lines, respectively. Briefly, these cell lines stably express TetR and carry pSuperior-retro-puro-MPS1, resulting in depletion of MPS1 protein upon addition of doxycycline. To generate the derivative cell lines that express MPS1^{WT} and MPS1^{as}, UTRM10 and HCT-TRM cells were transfected using the calcium phosphate method with the different LAP-MPS1 alleles and selected with doxycycline (1 μg/ml). Single colonies were selected after limiting dilution. HCT-TRM-derivative cells were grown in RPMI (Lonza) with 6% Tet-approved FCS (Clontech), supplemented with pen/strep (Invitrogen). UTRM10-derivative cells were grown in DMEM (Lonza) with 8% Tet-approved FCS (Clontech), supplemented with pen/strep (Invitrogen) and Ultra-Glutamine (Lonza).

Thymidine (2.5 mM), nocodazole (660 nM), taxol (1 μM), MG132 (10 μM), monastrol (200 μM), STLC (10 μM), doxycycline and puromycin (1 μg•ml^{-1}) were all from Sigma, ZM447449 (Tocris Bioscience) was added at 2 μM and 23dMB-PP1 at 1 μM.

Antibodies

The following primary antibodies were used for immunoblotting, immunofluorescence imaging and FACS analyses: MPS1-NT (Upstate), pT676-MPS1 [16], BUBR1-300A (Bethyl), MAD2 (custom polyclonal Rb antibody. Briefly, His_6-MAD2 (pQE80L-hMAD2) was expressed in BL21 cells, purified using Ni-agarose (Qiagen) and injected into New Zealand rabbits (Covance). MAD2 antibody was affinity purified from rabbit serum using His_6-MAD2), BUB1 (Abcam), MAD1 (SantaCruz Biotechnology), a-tubulin (Sigma), CREST (Cortex Biochem), MPM2 (Upstate), CDC20 (SantaCruz Biotechnology), BUB3 (BD Trans Lab) and Borealin (a gift of W. Earnshaw). Secondary antibodies included anti-human Alexafluor647 and anti-rabbit Alexafluor488 (Molecular Probes) for immunofluorescence studies, anti-mouse-Cy5 (Jackson) for FACS and anti-Mouse/Rabbit Alexa680/800 (Molecular Probes) for immunoblotting.

Flow cytometry

HCT- and UTR-derived cell lines were released from a 24 hours thymidine block into nocodazole or 23dMB-PP1 or a combination of both for 18 hours, harvested and fixed in 70% ice-cold ethanol for 24 hours, and analyzed using MPM2 immunostains as described [79].

Immunofluorescence and live cell imaging

For immunolocalization studies, cells were plated on 12 mm coverslips, pre-extracted with 0.2% TritonX-100 in warm PEM (100 mM PIPES pH6.8, 1mM MgCl2 and 5mM EGTA) for 1 minute, fixed with 3% PFA in PBS, blocked with 3% BSA in PBS for 1 hour, incubated with primary antibody for 16 hrs at 4°C, washed with PBS/0.1% TritonX-100 and incubated with secondary antibodies for an additional 1 hour at room temperature. Coverslips were washed and submerged in PBS containing DAPI, washed again and mounted using ProLong Antifade (Molecular Probes). All images were acquired on a DeltaVision RT system (Applied Precision) with a 100X/1.40NA UPlanSApo objective (Olympus) using SoftWorx software. Images are maximum intensity projections of deconvolved stacks. For quantification, all images of similarly stained experiments and acquired with identical illumination-settings were analyzed using ImageJ. Average pixel intensities of the total of all regions encompassing centromeres plus kinetochores were determined in the various channels and corrected for background.
For live cell imaging, cells were plated in 4-well chambered glass-bottom slides (LabTekII) or 24-well glass bottom plates (MatTek), transfected and imaged in a heated chamber (37°C and 5% CO_2) using a 20X/0.5NA UPLFLN objective on a Olympus IX-81 microscope, controlled by Cell-M software (Olympus). 16 bits DIC (5 msec exposure) images were acquired every 2 minutes using a Hamamatsu ORCA-ER camera. Images were processed using Cell-M software.

Immunoprecipitation

HCT-MPS1^{as} cells were released from a 24 hours thymidine block into nocodazole for 18 hours, harvested and lysed in 50 mM Tris 7.5, 150 mM NaCl, 1% TX-100, 2 mM MgCl2, 5 mM EDTA, supplemented with protease inhibitors and phosphatase inhibitors for 10 minutes on ice. The cleared extract was incubated with 10% protein A-agarose beads (Roche)/antibody mix for 2 hours at 4°C on a rotating wheel. The beads were washed twice with lysis buffer. Supernatant and beads were processed for SDS-PAGE and the proteins were transferred to nitrocellulose membranes for immunoblotting.

Colony Formation Assays

Cells (50,000/well) were plated in 6-well plates (Costar). Cells were grown in media supplemented with DMSO or 23dMB-PP1 (1 mM) for 8 days or for 2 days followed by inhibitor wash-out and continued incubation in media without 23dMB-PP1 for an additional 6 days. At day 8, plates were washed with PBS, fixed for 5 minutes with 96% methanol and stained with 0.1% crystal violet in water for 30 minutes.

Acknowledgments

The authors thank Aniek Janssen for providing the HCT-TRM cell line, Prasad Jallepalli for providing initial stocks of 3MB-PP1, Bill Earnshaw for providing Borealin antibody and the Kops, Lens and Medema laboratories for insights and discussions.

Supplemental Figures

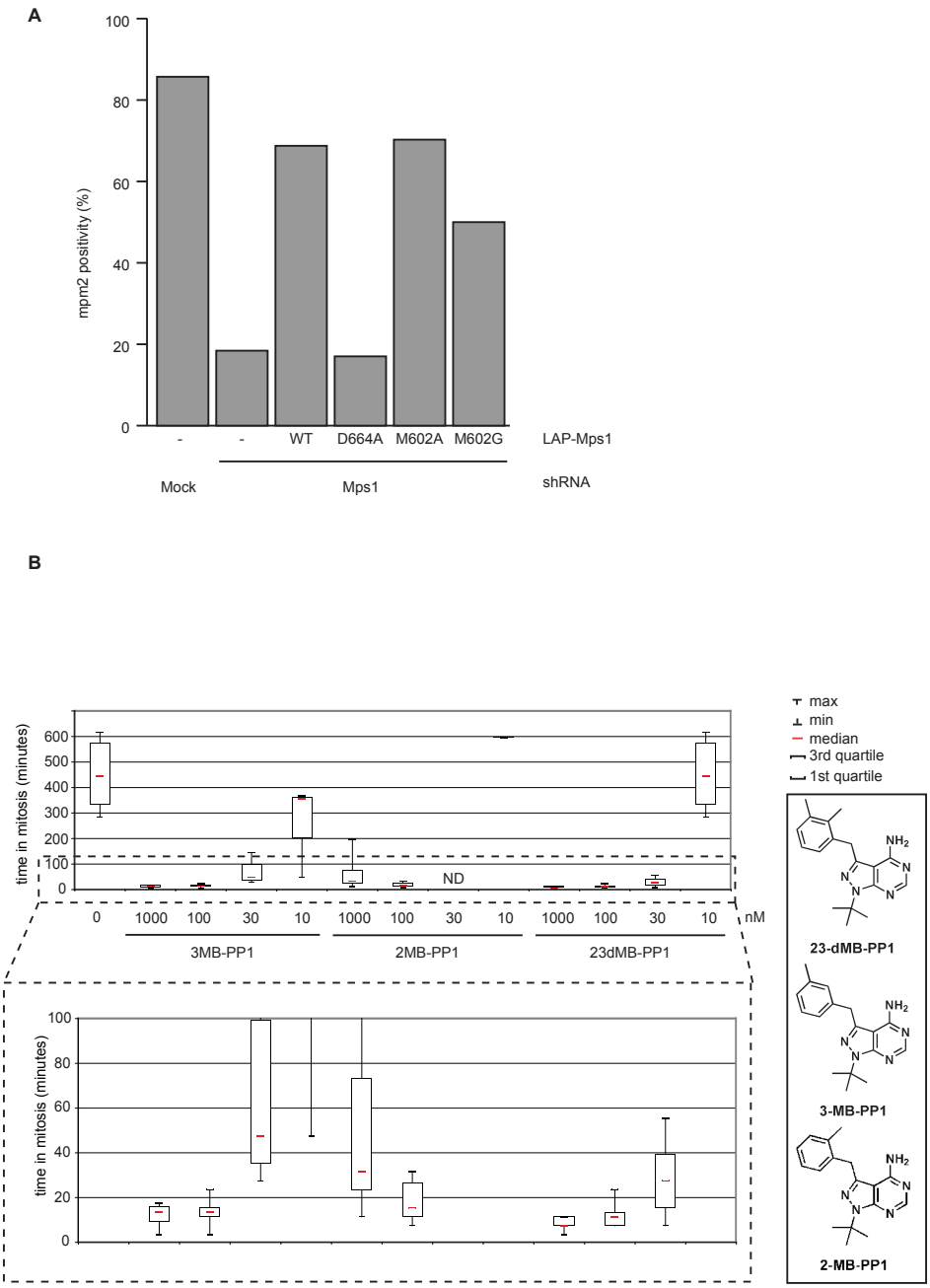

Figure S1

(A) Quantification of flow cytometric analysis of fraction of mitotic cells treated with nocodazole for 18 hours. Cells were transiently transfected with indicated LAP-MPS1 constructs. D664A is an enzymatically inactive mutant. **(B)** Box-and-whisker diagrams of time spent in mitosis of UTR-MPS1as cell treated with taxol in combination with increasing concentrations of different bulky PP1 inhibitors. ND; not determined. (molecular structures displayed in right panel).

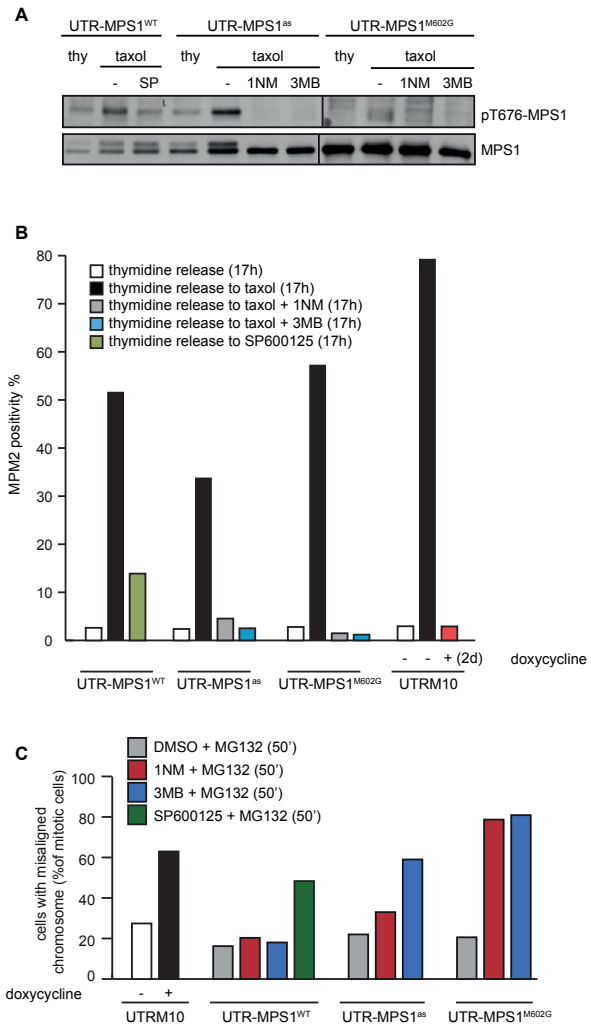

Figure S2

(A) pT676-MPS1 and MPS1 immunoblot of UTR-MPS1WT, UTR-MPS1as and UTR-MPS1M602G cells treated with thymidine (thy) for 20 hours or with taxol and MG132 in combination with indicated inhibitors for 1 hour. 1NM, 1NM-PP1; 3MB, 3MB-PP1; SP, SP600125. **(B)** Quantification of flow cytometric analysis of fraction of mitotic UTRM10, UTR-MPS1WT, UTR-MPS1as and UTR-MPS1M602G cells treated with taxol in combination with indicated inhibitors for 17 hours. **(C)** Chromosome alignment in UTRM10, UTR-MPS1WT, UTR-MPS1as and UTR-MPS1M602G cells treated with MG132 for 50 minutes in combination with the indicated inhibitors. Graph displays percentages of cells with misaligned chromosomes.

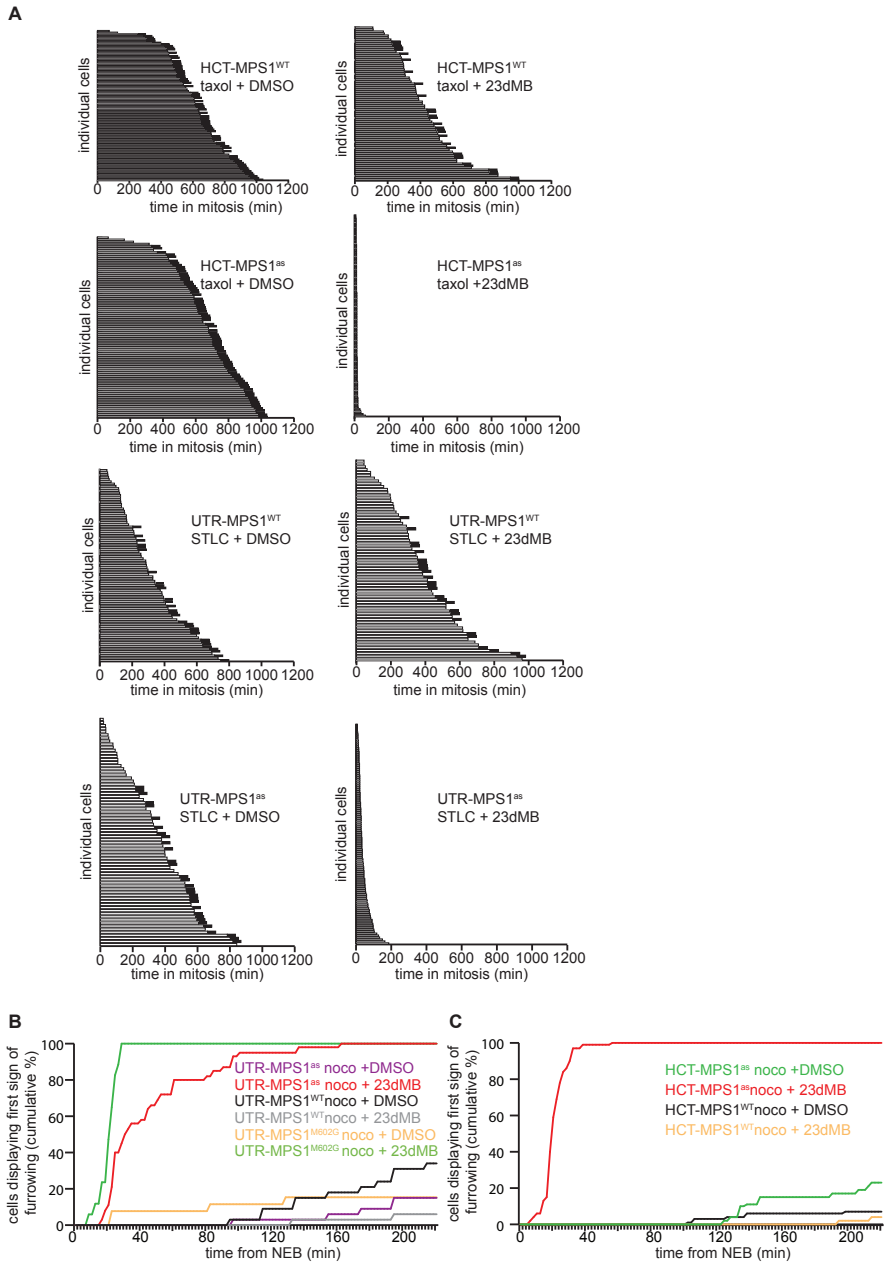

Figure S3:

(A-C) Time-lapse analysis by DIC microscopy of HCT- and UTR-derived cells treated with **(A)** taxol (HCT-derived cells) or STLC (UTR-derived cells) in combination with DMSO or 23dMB-PP1, or nocodazole **(B, C)** in combination with DMSO or 23dMB-PP1. Graphs in A display the time from NEB to the first signs of furrow ingression for individual cells. Black bars indicate end of time-lapse acquisition. Line graphs in **B** and **C** show cumulative percentages of UTR-derived cells **(B)** and HCT-derived cells **(C)** displaying first signs of furrowing at indicated times after NEB.

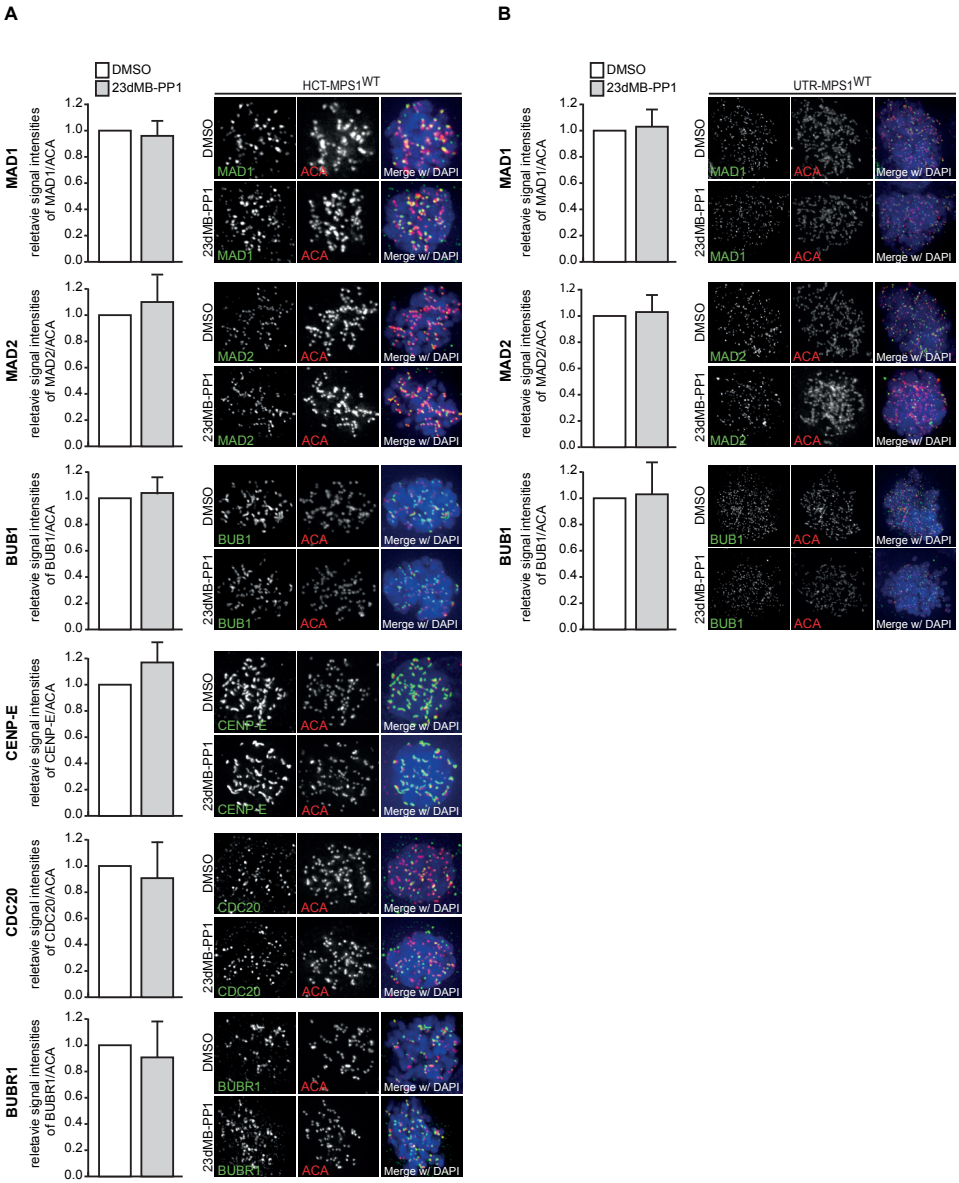

Figure S4:

Immunolocalization of MAD1, MAD2, BUB1, BUBR1, CDC20 and CENP-E and centromeres (ACA) in HCT-MPS1WT **(A)** and UTR-MPS1WT **(B)** cells treated with nocodazole and MG132 for 1 hour in combination with DMSO or 23dMB-PP1. Graphs represent quantifications of kinetochore signal intensities for the investigated proteins at all kinetochores in a single cell as a ratio of the ACA signal. Data are average of three experiments, 10 cells per experiment (+/- SD). Representative images are shown. DNA (DAPI) is in blue.

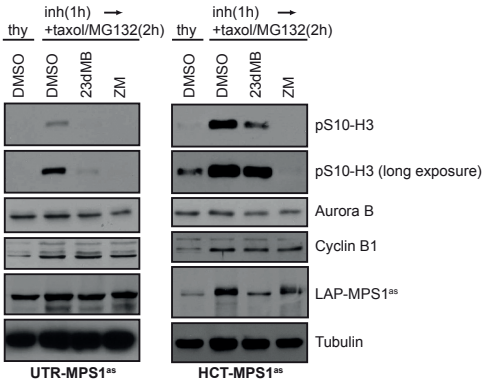

Figure S5:
Immunoblots of the indicated proteins in lysates of the HCT- and UTR-MPS1 variant cell lines. Cells were treated with thymidine (thy), or with the indicated inhibitors for 1 hour followed by taxol/MG132 treatment for an additional 2 hrs. ZM, ZM447439.

Chapter 3

Feedback control between MPS1, BUB1 and ZW10 regulates SAC activity by establishing MAD1 kinetochore binding.

Tale Sliedrecht[1,4], Mathijs Vleugel[1], Vincent Groenewold[1], Geert J.P.L. Kops[1,2,3,4,]

[1]Molecular Cancer Research and [2]Department of Medical Oncology and [3]Cancer Genomics Netherlands, University Medical Center Utrecht, 3584 CG, Utrecht.[4] The Netherlands. Netherlands Proteomics Centre, Utrecht, The Netherlands

To be submitted

Abstract

Correct chromosome distribution during mitosis is facilitated by the spindle assembly checkpoint (SAC) that restrains anaphase until all chromosomes are attached to the mitotic spindle. Essential for SAC activity is kinetochore localization of MAD1 that catalyzes the production of an anaphase inhibitor by conformationally activating MAD2. MPS1, the ROD-ZW10-ZWILCH (RZZ) complex and BUB1 control MAD1 kinetochore binding, but their relative contributions are unknown. We show that MAD1 localization by MPS1 is mediated by BUB1 and ZW10. BUB1 regulates ZW10 localization, and ZW10 in turn controls MAD1 kinetochore binding. This pathway is complemented by a feedback in which ZW10 additionally controls MPS1 levels at kinetochores through stabilization of the KMN network. Finally, SAC defects resulting from the absence of BUB1 or ZW10 can be rescued by artificially tethering MAD1 to kinetochores. We thus propose the existence of an MPS1-BUB1-RZZ pathway that is reinforced by feedback stabilization of the KMN network and that promotes SAC activity predominantly by establishing MAD1 kinetochore binding.

Introduction

To maintain genomic stability during cell divisions, a cell must faithfully segregate its chromosomes in mitosis. The evolutionary conserved SAC has evolved to safeguard against errors in chromosome segregation by preventing premature mitotic exit. Chromosomes that are unattached to microtubules of the mitotic spindle activate the SAC by producing a diffusible inhibitor, the mitotic checkpoint complex (MCC). The MCC then inhibits CDC20-dependent activation of the E3 ubiquitin ligase anaphase-promoting complex/cyclosome (APC/C) towards key mitotic substrates. This ensures persistent CDK1 activity and sister chromatid cohesion, thus allowing cells more time to connect to spindle microtubules [46,67]. A key step in MCC formation is the recruitment of the checkpoint protein MAD1 to kinetochores of unattached chromosomes [141,171,178-180]. MAD1 forms a stable homodimer that binds two MAD2 molecules, enabling catalysis of MAD2 structural conversion from an inactive 'open' to an active 'closed' form (reviewed in [82]). Although the exact composition of the MCC is debated [70,72,83,84,86], a core component is BUBR1, a pseudokinase that prevents substrate access to APC/C-CDC20 in a pseudosubstrate manner[73,74,181,182]. Closed MAD2 is critical for establishing [83,84] and possibly also maintaining [70,72] BUBR1 binding to APC/C-CDC20.

SAC activation relies on MAD1 binding to unattached kinetochores, but it is unknown what the MAD1 receptor at kinetochores is. Nevertheless, several proteins contribute to MAD1 kinetochore localization, including the conserved mitotic kinases MPS1 and BUB1, and the poorly understood RZZ complex [76-78,80,177,183,184]. The RZZ complex consists of the extended coiled-coil protein ROD, the well-conserved ZW10 protein and the more recently evolved ZWILCH protein [67,185,186]. Neither of these have recognizable protein domains or catalytic activities and it is presently unknown how the RZZ complex performs its mitotic functions. Besides activating the SAC by establishing and maintaining kinetochore localization of MAD1, the RZZ complex is also involved in silencing the SAC in metazoans by localizing the dynein complex to kinetochores [101,187,188]. Once microtubules are bound, kinetochore-dynein proceeds to remove the MAD1/MAD2 scaffold as well as other SAC proteins from kinetochores[93,94,189].

The BUB1 kinase [190] phosphorylates Histone2A on T120 to enable inner-centromere localization of SGO1 that in turn protects centromeric cohesion and establishes inner-centromere localization of the chromosomal passenger complex [191,192]. In addition, BUB1 impacts the SAC by yet undefined mechanisms. It has been proposed that BUB1 phosphorylates CDC20, thereby directly inhibiting its APC/C-activating ability [85], but others have suggested that BUB1 kinase activity is dispensable for its role in the SAC [77]. Interestingly, BUB1 is needed for MAD1 localization to unattached kinetochores [77,184,193], and this too does not require its catalytic activity [77].

Like BUB1, MPS1 performs various critical functions in mitosis. It is essential for chromosome bi-orientation [138,151,164] as well as for SAC activation and maintenance [90,91,129,135,151,164] MPS1 impacts the SAC on multiple levels, ranging from regulating MAD1 localization [76], MAD2 'activation' [90], and MCC stabilization [91]. These functions all depend on its kinase activity [76]. As a result, depletion or catalytic inhibition of MPS1 results in premature activation of the APC/C and rapid exit from mitosis [129,135,151,164]. Besides MAD1 and MAD2, MPS1 has been shown to be required for the kinetochore recruitment of multiple other mitotic regulators, including the RZZ complex, CDC20, BUBR1 and BUB1 [76]

An important unresolved question is how microtubule attachment and SAC signaling are integrated at kinetochores. The KMN network (KNL1-MIS12–NDC80 complex) constitutes

the major microtubule binding activity of mitotic kinetochores (reviewed in [15]), and several of its components have been shown to be required for SAC protein localization. MPS1 kinetochore binding, for instance, relies on the CH domain of NDC80 [142,145,146], and both BUB1 and BUBR1 localize to kinetochores by interacting with the KNL1 protein [194-196]. This interaction is promoted by MPS1-dependent phosphorylation of MELT-like sequences in KNL1, thus explaining the causal relationship between MPS1 activity and BUB1 kinetochore localization [118-120]. It is unknown, however, how MPS1, BUB1 or the RZZ direct MAD1 localization, whether there is a more direct role in this for the KMN network, and how these various contributions interconnect.

Results

Kinetochore tethered MPS1 continuously recruits MAD1, BUB1, ZW10 and SPINDLY

MAD1 localization to unattached kinetochores is regulated by MPS1, BUB1 and RZZ [76,77,79,184,193]. We and others have shown that BUB1 and RZZ in turn depend on MPS1 activity for their localization [91,133,151]. To investigate how MPS1 controls MAD1 localization and if these three regulators of MAD1 localization operate in one pathway, we made use of our prior observation that high levels of MAD1 are retained on metaphase kinetochores to which MPS1 was artificially tethered [149]. We created cell lines with inducible expression of the kinetochore-tethered MIS12-MPS1$^{\Delta 200}$ fusion protein [142,146], permitting examination specifically of MPS1-driven MAD1 localization.

In addition to MAD1 and MAD2 (Figure 1A, and [149]) induced expression of MIS12-MPS1$^{\Delta 200}$ also retained high levels of BUB1, ZW10 and SPINDLY on metaphase kinetochores (Figure

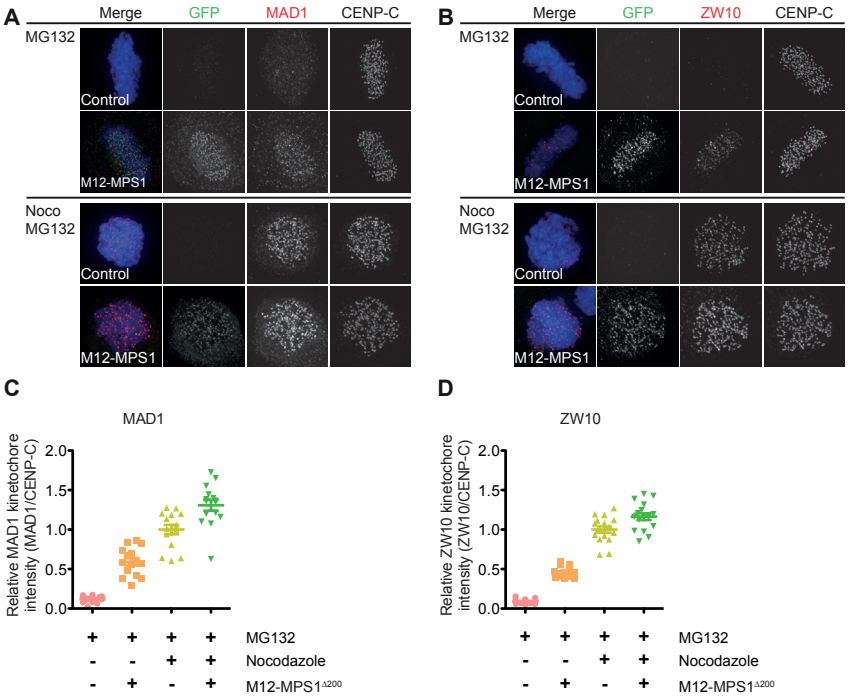

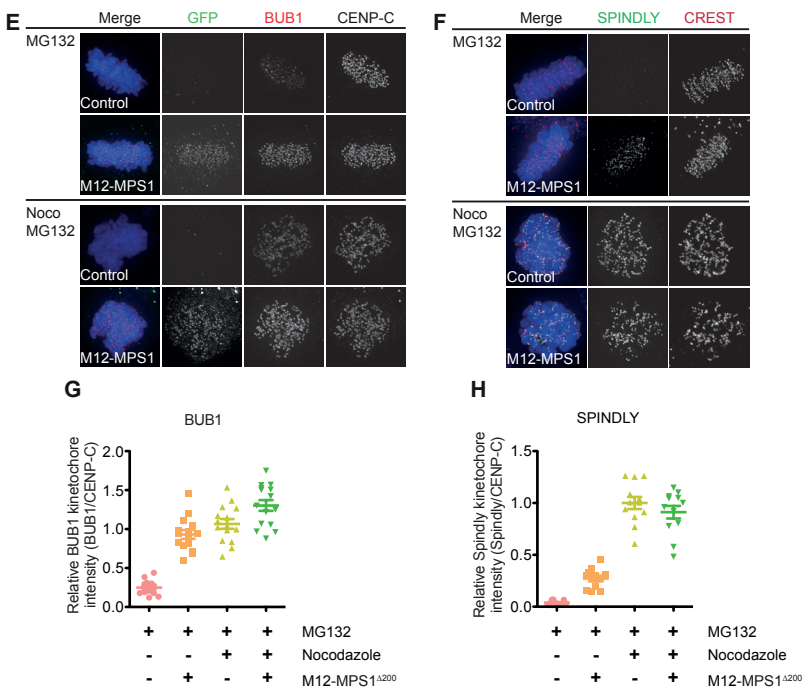

Figure 1. Kinetochore tethered MPS1 continuously recruits MAD1, BUB1, ZW10 and SPINDLY

(A-F) Immunolocalisation of MAD1, ZW10, BUB1, SPINDLY, GFP and centromeres (CENP-C/CREST) in U2OS cells, non-induced or induced to express LAP-MIS12-MPS1$^{\Delta 200}$ (indicated as M12-MPS1), and treated with MG132 alone or in combination with nocodazole for 1 hour. Representative images are shown in **A, B, E, F**. Graphs represent total kinetochore intensity of MAD1 **(C)**, ZW10 **(D)** BUB1 **(G)** and SPINDLY **(H)** relative to centromeres (CENP-C/CREST) ±SD. All data are from ≥ 15 cells per experiment and are representative of three experiments.

1B-H). Since MPS1 is required for their initial recruitment in prometaphase [76], this may indicate that MIS12-MPS1$^{\Delta 200}$ continuously recruits these proteins to bioriented kinetochores. Alternatively, since MAD1, ZW10 and SPINDLY have been described as cargo for dynein in metaphase [93,94], MIS12-MPS1$^{\Delta 200}$ could act predominantly to prevent their dynein-mediated stripping from bioriented kinetochores, either directly or indirectly by maintaining kinetochore SPINDLY [101,188]. To examine this more closely, we tested the activity of the dynein-dependent stripping pathway by treating cells with nordihydroguaiaretic acid (NDGA), a drug that interferes with cargo release by dynein. If dynein-dependent kinetochore stripping occurs, NDGA treatment results in accumulation of dynein cargo at spindle poles [94]. Addition of NDGA caused accumulation of ZW10 at spindle poles in control cells and more strikingly so in MIS12-MPS1$^{\Delta 200}$ expressing cells as well (Figure 2A). These results suggest that dynein-dependent stripping occurs normally in MIS12-MPS1$^{\Delta 200}$-expressing metaphase cells.

Maintenance of MAD1, BUB1 and ZW10 at kinetochores requires MPS1 activity

Since stripping occurs normally in MIS12-MPS1$^{\Delta 200}$ expressing cells, the accumulation of checkpoint proteins at metaphase kinetochores of these cells is likely due to their continued recruitment by MPS1. In line with this, the intense ZW10 signals at poles of NDGA-treated MIS12-MPS1$^{\Delta 200}$ cells can be explained by ongoing cycles of recruitment and stripping without eventual cargo release at poles. To examine this further, we next addressed whether MPS1

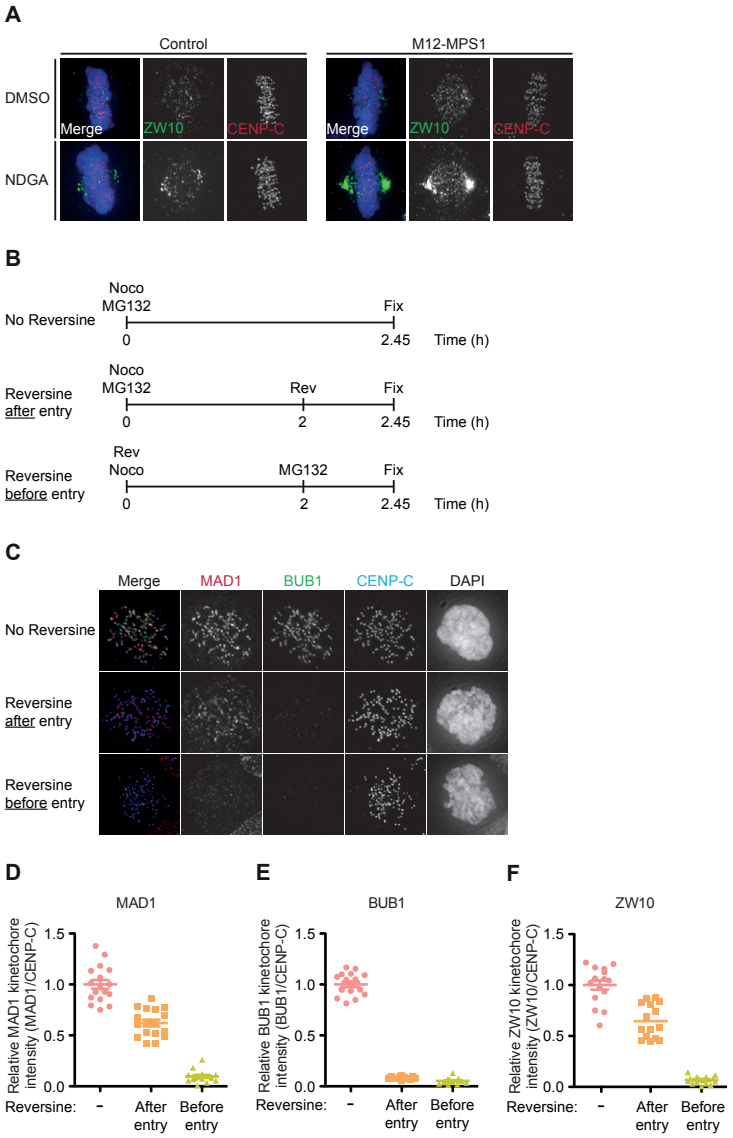

Figure 2. Maintenance of MAD1, BUB1 and ZW10 at kinetochores requires MPS1 activity

(A) Immunolocalisation of ZW10 and centromeres (CENP-C) in HeLa cells, non-induced or induced to express mcherry-MIS12-MPS1Δ200 (indicated as M12-MPS1), and treated with either DMSO or NDGA for 30 minutes. **(B-F)** Representative images **(C)** and quantification **(D-F)** of immunolocalisation of MAD1 **(C, D)**, BUB1 **(C, E)**, ZW10 **(F)**(representative images not shown) and centromeres (CENP-C) in HeLa cells treated with the indicated drugs as schematically displayed in **(B)**. Graphs represent total kinetochore intensity of indicated antigens relative to centromeres (CENP-C) ±SD. All data are from ≥15 cells per experiment and are representative of three experiments.

is normally required to maintain high levels of SAC proteins at unattached kinetochores. Addition of the MPS1 inhibitor reversine [133] prior to mitotic entry prevented kinetochore binding of MAD1, BUB1 and ZW10 (Figure 2C bottom panel, 2B-F), as observed previously by us and others [76]. Addition of reversine after entry into mitosis similarly abolished BUB1 localization, and decreased kinetochore MAD1 and ZW10 levels by roughly 50% (Figure

2C middle panel, 2B-F). This was reminiscent of the observations shown in Figure 1, where MIS12-MPS1 was able to cause full recruitment of BUB1 to metaphase kinetochores (as compared to nocodazole-treatment) but no more than approximately 50% of ZW10 and MAD1 (Figure 1A-H) These data show that while it impacts the maintenance of BUB1, ZW10 and MAD1 to different extents, MPS1 activity is required to establish and maintain high levels of the three SAC proteins at unattached kinetochores.

MPS1 regulates MAD1 and ZW10 recruitment through BUB1

Thus far, our observations are compatible with a signaling pathway in which MPS1 activity promotes MAD1 kinetochore binding indirectly by localizing BUB1 and RZZ. In support of this, RNAi of ZW10 or BUB1 in MIS12-MPS1-expressing cells abolished MAD1 binding to metaphase kinetochores (Figure 3A-C). Moreover, as shown by others [77,79,184,193], BUB1 or ZW10 depletion diminished MAD1 kinetochore binding in normal prometaphase cells (Figure 3D, E). A point mutant of BUB1 that kills kinase activity (KD) was equally proficient as wild-type BUB1 in restoring MAD1 localization in BUB1-depleted cells, showing BUB1 activity was not required for this (Figure 3F, G).

Yeast BUB1 has been shown to directly bind MAD1 [197], suggesting that BUB1 might function as direct recruiter of MAD1 at the kinetochore. Since MPS1 inhibition in mitosis completely clears BUB1 from kinetochores while only partially affecting MAD1 kinetochore levels (Figure 2B-E) we suspect that this is not conserved in humans. Furthermore, expression of BUB1 fused to the Lac repressor protein (LacI-LAP-BUB1) in cells containing a stably integrated tandem Lac-Operator (LacO) array [198] is unable to recruit MAD1 (Figure 3H), while known interactor BUBR1 does bind BUB1 at these sites (Figure 3I). In line with this, constitutive localization of BUB1 to kinetochores using a MIS12-BUB1 fusion protein does also fail to recruit MAD1 while efficiently phosphorylating Histone 2A and recruiting BUBR1 and BUB3 (data not shown). Finally, proteomic analysis of LAP-BUB1 pull-downs failed to reveal a direct interaction between BUB1 and MAD1 while known interactors are identified (Figure 3J). These data strongly suggest that BUB1 does not function as a scaffold for direct binding of MAD1.

To examine if the MPS1-BUB1/RZZ-MAD1 pathway is linear or whether RZZ and BUB1 operate in parallel pathways, we depleted BUB1 or ZW10 and analyzed kinetochore localization of the other in nocodazole-treated cells. As shown in Figure 4A and B, BUB1 depletion prevented ZW10 kinetochore binding to a similar degree as MAD1 (Figure 3D, E), in agreement with an MPS1-BUB1-ZW10-MAD1 hierarchy. Like MAD1, ZW10 kinetochore recruitment also did not require BUB1 kinase activity (Figure 4C, D). Unexpectedly, ZW10 depletion in turn significantly reduced BUB1 levels at kinetochores (Figure 4E-G), albeit to a lesser extent than its effect on MAD1 levels (Figure 3D, E).

ZW10 regulates MPS1 kinetochore levels by stabilizing association of the KMN network with kinetochores.

BUB1 localization at mitotic kinetochores relies on phosphorylation of the outer-kinetochore scaffold KNL1 by MPS1 [118-120]. KNL1 is an integral component of the KMN network that constitutes the microtubule binding interface of kinetochores, and which includes the MIS12 and NDC80/HEC1 complexes (reviewed in [23]). We had noticed that the MIS12-MPS1$^{\Delta 200}$ protein displayed consistently lower kinetochore-binding capacity when ZW10 was depleted from cells (Figure 3C). Indeed, the amount of endogenous KNL1 and HEC1 at kinetochores

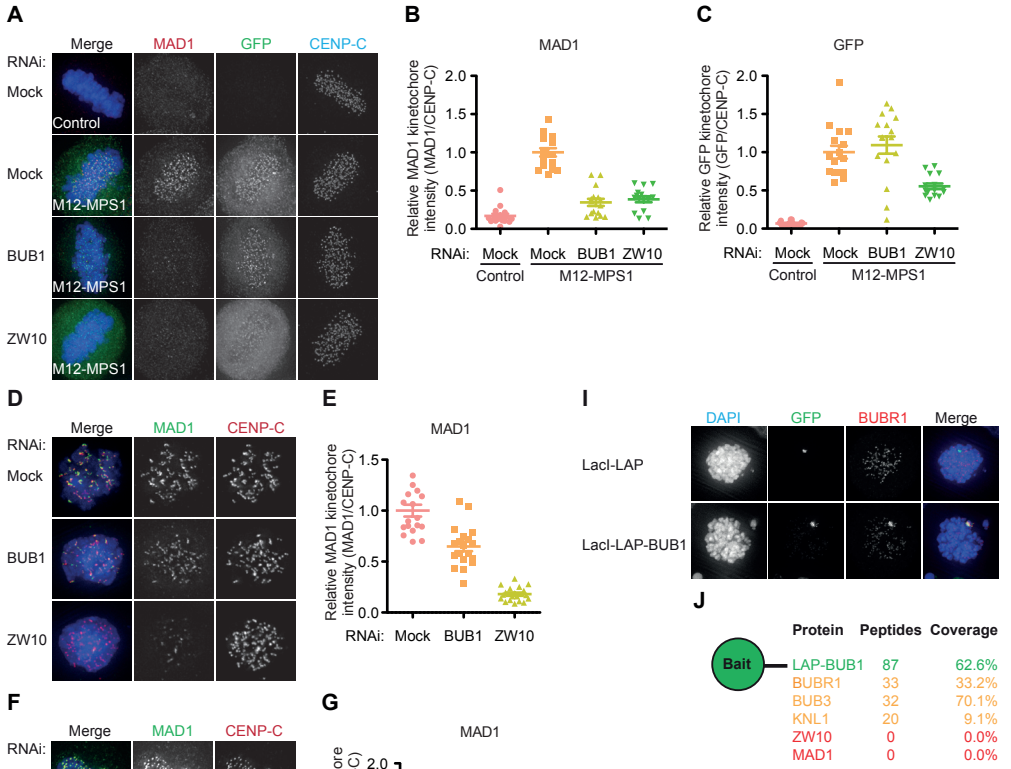

Figure 3. MPS1 regulates MAD1 recruitment through BUB1.

(A-C) Immunolocalisation of MAD1, GFP and centromeres (CENP-C) in U2OS cells non-induced or induced to express LAP-MIS12-MPS1$^{\Delta 200}$ (indicated as M12-MPS1), transfected with indicated siRNAs and treated with MG132 for 1 hour. Representative images are shown in A. Graphs **(B, C)** represent total kinetochore intensity of MAD1 **(B)** and GFP **(C)** relative to centromeres (CENP-C) ±SD. **(D-E)** Immunolocalisation of MAD1 and centromeres (CENP-C) in HeLa cells transfected with indicated siRNAs and treated with nocodazole and MG132 for 1 hour. Representative images are shown in **D**. Graph represent total kinetochore intensity of MAD1 **(E)** relative to centromeres (CENP-C) ±SD. **(F, G)** Immunolocalisation of MAD1 and centromeres (CENP-C) in HeLa cells, non-induced or induced to express LAP-BUB1-WT or -KD, transfected with indicated siRNAs and treated with nocodazole and MG132 for 1 hour. Representative images are shown in F. Graph represents total kinetochore intensity of MAD1 **(G)** relative to centromeres (CENP-C) ±SD. **(H, I)** Immunolocalisation of MAD1 BUBR1, GFP and centromeres (CREST) in U2OS-LacO cells transfected with indicated plasmids, treated with nocodazole and MG132 for 1 hour. All data are from ≥15 cells and are representative of three experiments. (J) Recovered peptides (amount and coverage) in mass spectrometric analysis of LAP-BUB1 affinity purifications. Color coding: Green=bait, orange=known interactors, red=ZW10 or MAD1.

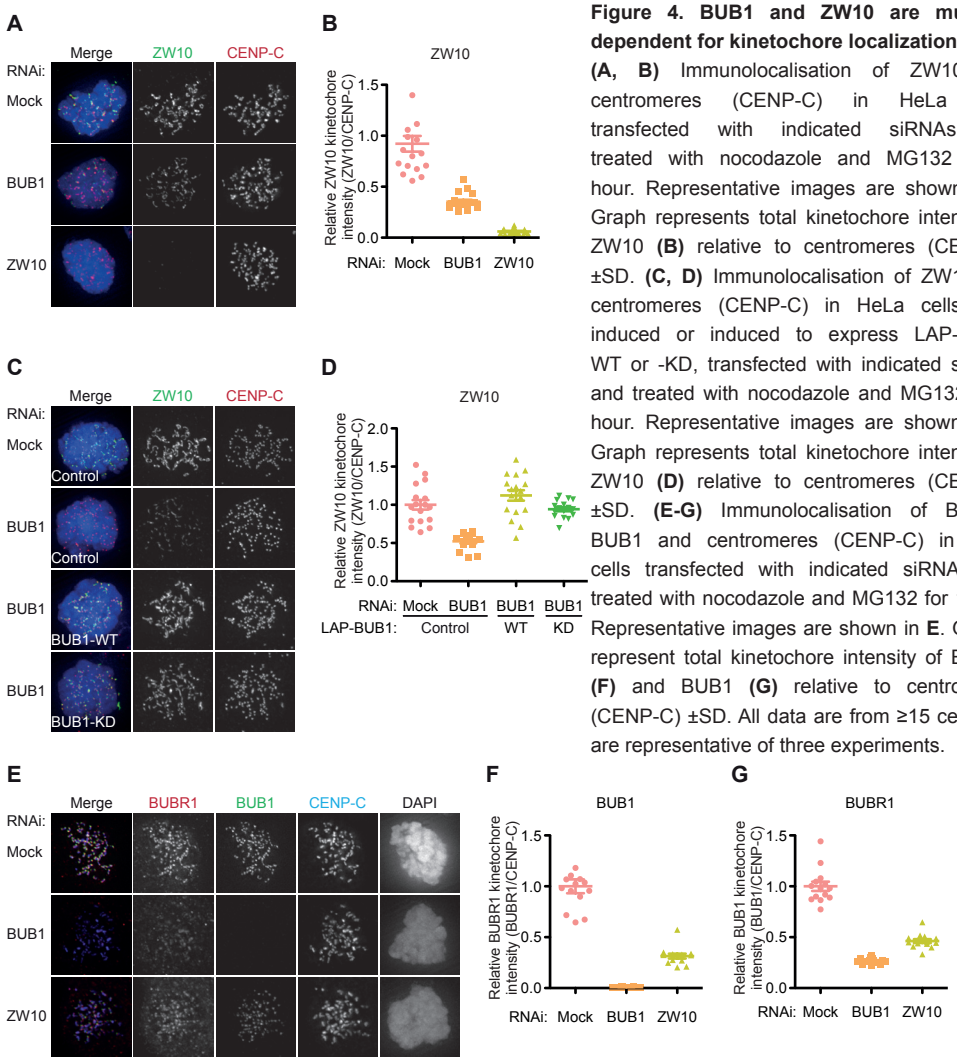

Figure 4. BUB1 and ZW10 are mutually dependent for kinetochore localization

(A, B) Immunolocalisation of ZW10 and centromeres (CENP-C) in HeLa cells transfected with indicated siRNAs and treated with nocodazole and MG132 for 1 hour. Representative images are shown in A. Graph represents total kinetochore intensity of ZW10 **(B)** relative to centromeres (CENP-C) ±SD. **(C, D)** Immunolocalisation of ZW10 and centromeres (CENP-C) in HeLa cells non-induced or induced to express LAP-BUB1-WT or -KD, transfected with indicated siRNAs and treated with nocodazole and MG132 for 1 hour. Representative images are shown in **C**. Graph represents total kinetochore intensity of ZW10 **(D)** relative to centromeres (CENP-C) ±SD. **(E-G)** Immunolocalisation of BUBR1, BUB1 and centromeres (CENP-C) in HeLa cells transfected with indicated siRNAs and treated with nocodazole and MG132 for 1 hour. Representative images are shown in **E**. Graphs represent total kinetochore intensity of BUBR1 **(F)** and BUB1 **(G)** relative to centromeres (CENP-C) ±SD. All data are from ≥15 cells and are representative of three experiments.

was significantly reduced upon depletion of ZW10 but not BUB1 (Figure 5A-C). The reduction in kinetochore HEC1 levels upon ZW10 depletion further correlated with reduced MPS1 levels (Figure 5D, E), in agreement with an essential role for HEC1 in MPS1 kinetochore localization [142,145,146]. These data suggest that ZW10 impacts BUB1 kinetochore levels indirectly, by ensuring high levels of MPS1 at kinetochores through stabilizing the association of the KMN network with kinetochores. Importantly, tethering MPS1 to kinetochores using the MIS12-MPS1$^{\Delta 200}$ protein significantly restored BUB1 kinetochore levels in the absence of ZW10 (Figure 5F, G), despite a small reduction in the amount of MIS12 that could be incorporated into the KMN network (Figure 5H).

Our finding that in MIS12-MPS1$^{\Delta 200}$-expressing cells ZW10 depletion precludes MAD1 kinetochore binding without significantly affecting kinetochore BUB1 leads us to conclude that ZW10 controls MAD1 kinetochore recruitment independent of its feedback to the MPS1-BUB1 pathway. Since BUB1 depletions do not affect kinetochore MPS1 [78,129], we propose

that a MPS1-BUB1-RZZ pathway controls MAD1 localization, and that RZZ reinforces this by feedback, stabilizing kinetochore binding of the KMN network.

MPS1, ZW10 and BUB1 cooperate to maintain SAC activity.

Our data show that MAD1 kinetochore localization relies on a MPS1-BUB1-RZZ feedback pathway. Although it is known that depleting any of the individual components of the pathway abrogates SAC activity, we wished to examine if their role in this pathway is critical for SAC activity. To this end, we tested the ability of cells compromised for the pathway to delay mitotic exit in response to microtubule depolymerization by nocodazole. We have previously shown that inefficient depletion or inhibition of any component of the Aurora B-HEC1-MPS1 pathway sensitizes the SAC response to depletion or inhibition of any other component of that pathway [142,146]. For example, RNAi of Aurora B or HEC1 abrogates SAC signaling only when MPS1 activity is slightly reduced by low dose of the MPS1 inhibitor reversine. We reasoned that if BUB1 and ZW10 operate in one pathway that further includes MPS1, the SAC response in ZW10- or BUB1-depleted cells should become highly sensitive to additional depletion/inhibition of any of the other components of the pathway. Depletion of either BUB1 or ZW10 or treatment with low dose (250 nM) reversine could not abolish SAC activity, as evidenced by persistent mitotic delays of nocodazole-treated cells (Figure 6A). Strikingly, however, codepletion of BUB1 and ZW10 caused noco-treated cells to rapidly exit mitosis and this was true also for cells depleted of either BUB1 or ZW10 and treated with 250 nM reversine (Figure 6A). Thus, reducing the activity of any two components of the pathway is synthetic lethal to the SAC response.

Regulating MAD1 kinetochore binding is the predominant role of ZW10 and BUB1 in the SAC

We next tested whether control of MAD1 kinetochore localization is critical for regulation of the SAC response by the MPS1-BUB1-RZZ pathway, by artificially re-locating MAD1 to kinetochores in cells deficient for components of the pathway. To this end, we created a cell line expressing MIS12-FRB-tagRFP and eYFP-FKBP-MAD1, permitting conditional MAD1 kinetochore tethering by rapamycin-induced heterodimerization of FRB and FKBP [199] (Figure 6B). Remarkably, the rapid exit from mitosis of nocodazole-treated cells upon combinatorial inhibition of MPS1 (250 nM reversine) and either ZW10 or BUB1 was completely prevented by induced tethering of MAD1 to kinetochores (Figure 6C). Taken together, these data show that MPS1, BUB1 and ZW10 operate in one pathway that promotes SAC activity predominantly by localizing MAD1 to kinetochores.

Discussion

MAD1 stands at the core of SAC signaling, yet how MAD1 kinetochore localization is regulated remains largely unknown. Our data show that MPS1, BUB1 and ZW10, all previously implicated in MAD1 regulation, operate in a linear pathway to recruit MAD1 to unattached kinetochores (Figure 6D). We show that ZW10 and BUB1 are mediators of MPS1's control over MAD1 kinetochore localization, and that ZW10 is likely downstream of BUB1 in this pathway. Besides controlling MAD1 kinetochore localization, ZW10 in parallel promotes stability of the KMN network and thereby indirectly promotes MPS1 localization (Figure 6D). We furthermore show that tethering MAD1 to kinetochores rescues SAC defects in ZW10- or

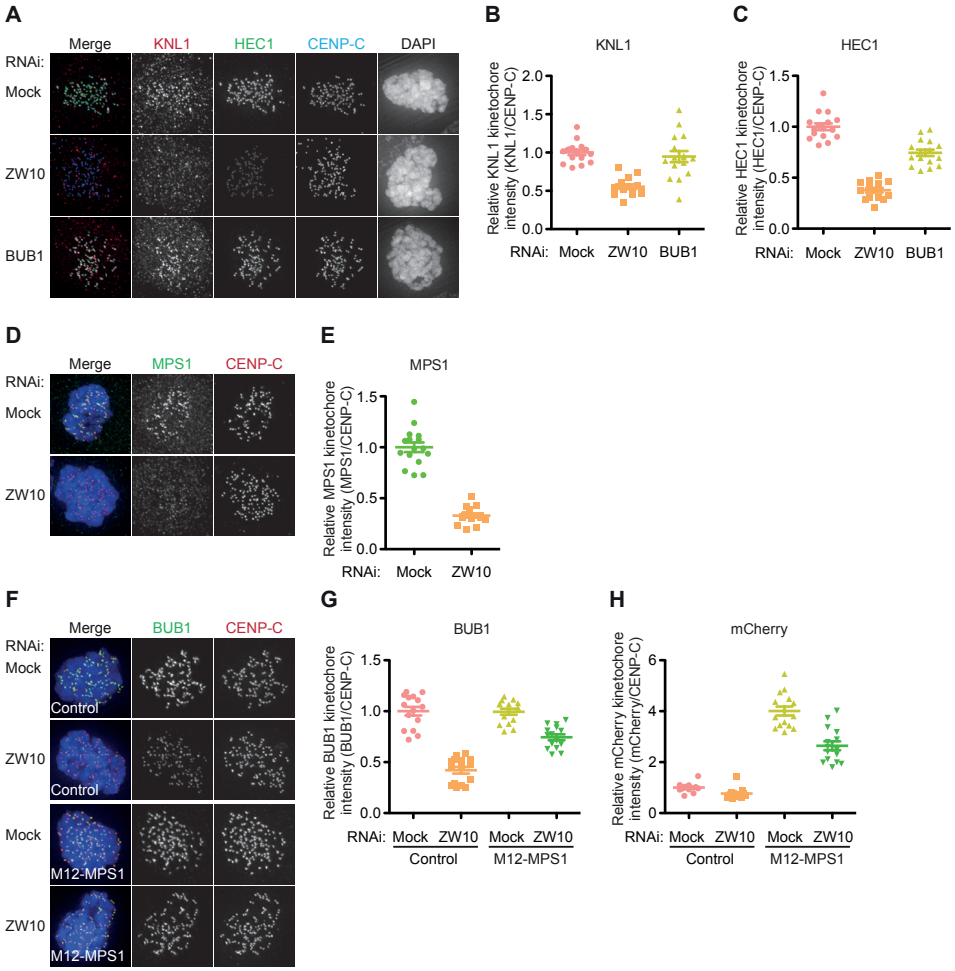

Figure 5. ZW10 regulates MPS1 kinetochore levels by regulating KMN network stability

(A-C) Immunolocalisation of KNL1, HEC and centromeres (CENP-C) in HeLa cells transfected with indicated siRNAs and treated with nocodazole and MG132 for 1 hour. Representative images are shown in **A**. Graphs represent total kinetochore intensity of KNL1 **(B)** and HEC1 **(C)** relative to centromeres (CENP-C) ±SD. **(D-E)** Immunolocalisation of MPS1 and centromeres (CENP-C) in HeLa cells transfected with indicated siRNAs and treated with nocodazole, 500 nM reversine and MG132 for 1 hour. Representative images are shown in **D.** Graph represent total kinetochore intensity of MPS1 **(E)** relative to centromeres (CENP-C) ±SD. **(F-H)** Immunolocalisation of BUB1, mCherry and centromeres (CENP-C) in HeLa cells non-induced or induced to express mCherry-MIS12-MPS1$^{\Delta 200}$ (indicated as M12-MPS1), transfected with indicated siRNAs and treated with nocodazole and MG132 for 1 hour. Representative images are shown in **F.** Graphs represent total kinetochore intensity of BUB1 **(G)** and mCherry **(H)** relative to centromeres (CENP-C) ±SD. All data are from ≥15 cells and are representative of three experiments.

BUB1-depleted cells. This argues strongly in favor of the hypothesis that MAD1 kinetochore binding is the primary function of the MPS1-BUB1-RZZ pathway and feedback in the SAC response, and argues against a role for BUB1 in the SAC downstream of MAD1 [89]. Since BUB1 also recruits the MCC component BUBR1, these results may furthermore indicate that either BUBR1 kinetochore localization is not essential for the SAC or that BUBR1 has a major contribution to MAD1 recruitment. In support of the former, an N-terminal fragment

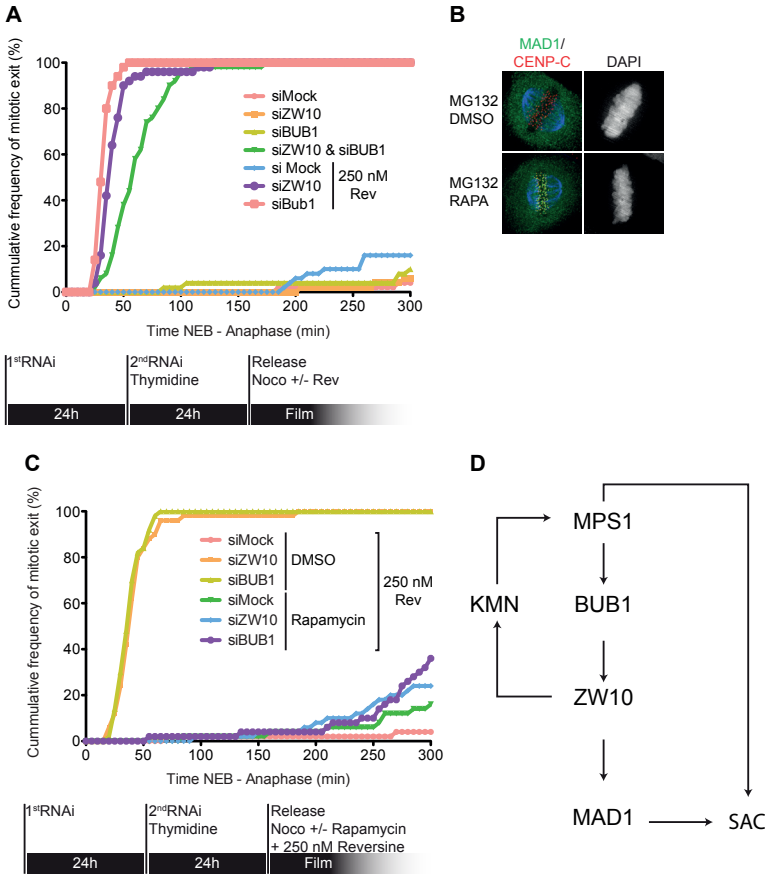

Figure 6. Regulating MAD1 kinetochore binding is the predominant role of ZW10 and BUB1 in the SAC
(A, C) Time-lapse analysis of duration of mitotic arrest in HeLa cells transfected with (combinations of) indicated siRNAs and treated with nocodazole and/or reversine or rapamycin, as indicated. Graphs (50 cells per treatment) show cumulative frequency of mitotic exit (scored as cell flattening) at the indicated times after NEB, and are representative of 3 independent experiments. **(B)** Immunolocalisation of MAD1 and centromeres (CENP-C) in HeLa cells, treated with MG132 alone or in combination with Rapamycin for 30 minutes. Data is representative of two experiments **(D)** Model of MAD1 kinetochore regulation. MAD1 kinetochore recruitment and SAC response is regulated by MPS1 via BUB1 and ZW10. ZW10 functions to establish MAD1 localization while simultaneously regulating MPS1 localization through stabilizing the KMN network.

of BUBR1 that fails to localize to kinetochores is able to maintain a SAC response [200], and kinetochore BUBR1 has been implicated in SAC-independent regulation of kinetochore-microtubule interactions [41,201].

What is or are the kinetochore receptor(s) for MAD1? Central to the localization of checkpoint proteins to kinetochores is the KMN network. The CH domain of HEC1 is important for recruitment of MPS1 [142,145,146], which in turn phosphorylates KNL1 to recruit BUB1 [118-120]. An initial observation of a yeast-2-hybrid interaction between MAD1 and HEC1 could not be verified in cells [145], and extensive tandem-affinity purifications of the KMN network has not found any co-precipitating MAD1 [8,202]. In budding yeast, MAD1 forms a mitosis-specific

interaction with BUB1 [197,203], and human MAD1 kinetochore localization depends on an evolutionary conserved domain within BUB1 but does not require BUB1 catalytic activity [77]. Although these data suggest that BUB1 might act as a RZZ/MAD1 binding platform on kinetochores, we and others [184] observed that efficient depletion of BUB1 (by either RNAi or MPS1 inhibition) reduces MAD1 kinetochore levels by only half. We could furthermore observe no direct interaction between BUB1 and MAD1, and could find no MAD1 on ectopic chromosome sites to which BUB1 was bound. These observations do not exclude a direct interaction between BUB1 and MAD1 but suggest that BUB1 is not or not the only kinetochore receptor for MAD1 in human cells. If ZW10 is downstream of BUB1 in the pathway towards MAD1 kinetochore binding, could the RZZ complex perhaps be the MAD1 receptor? Inhibition of MPS1 affects the RZZ complex and MAD1 in a similar manner, and although recently disputed [101] ZW10 may be stably bound to unattached kinetochores [204] and is removed upon microtubule attachment, much like MAD1 [94,141,205]. Finally, the RZZ-controlled protein SPINDLY has been proposed as the direct MAD1 receptor in *C. elegans* [206], but SPINDLY depletion in human cells does not prevent MAD1 kinetochore binding [100,101,188]. In conclusion, a direct receptor for MAD1 at mitotic kinetochores has yet to be found, and perhaps the mode of MAD1 kinetochore binding is multifactorial, with contributions from all of the above-mentioned proteins. It is of interest to note in this respect that the N-terminal coiled coil of MAD1 as well as its conserved C-terminal domain (CDT) contribute independently to kinetochore binding[184,207].

We provide evidence that BUB1 regulates localization of the RZZ complex, and does so independently of its capacity to phosphorylate proteins. RZZ kinetochore binding is, like MAD1, likely multifactorial. It depends entirely on the ZW10-interacting protein 1 (ZWINT1), but a mutant of ZW10 unable to bind ZWINT-1 still localizes to kinetochores, albeit with a reduced time of residency [204]. Suggesting that ZWINT1 forms multiple sites of interaction with RZZ. ZWINT1 is recruited to kinetochores by KNL1, a large scaffold and member of the KMN network that also recruits BUB1 to kinetochores [196,208]. In contrast to RZZ, kinetochore binding of ZWINT1 does not appear to be regulated during mitosis [91,133,209], and we thus suspect that BUB1, in a non-catalytic fashion, impinges on one or more of the ZWINT1-RZZ interaction sites. As chromosomes congress, microtubule binding of the KNL1 N-terminus might interfere with BUB1 binding and subsequently the ZWINT-1-ZW10 interaction, thus enabling dynein-dependent stripping of checkpoint proteins. Interestingly, *C. elegans* KNL1 mutants lacking microtubule binding activity are able to form load-bearing attachment but fail to silence the checkpoint while being able to recruit dynein [123]. It will be interesting to investigate kinetochore levels of BUB1 and the RZZ complex in these mutants.

Unexpectedly, our data show that the RZZ complex is required for stable association of the KMN network with kinetochores. Studies in *C. elegans* and in human cells have recently shown a functional connection between the RZZ complex and the KMN network [100,101]. Depletion of SPINDLY causes severe chromosome alignment defects due to strong reduction in the ability of kinetochores to form load-bearing attachments, a function of the KMN network. These defects were largely rescued by co-depletion of the RZZ complex. As a result, the authors proposed that RZZ inhibits the formation of load-bearing attachments by the KMN network by a yet unknown mechanism, and that this inhibition is repressed by SPINDLY/dynein [100]. It is unclear if this is mechanistically linked to our observations that ZW10 depletion affects KMN levels at kinetochores, but it is not unlikely that the effects

of RZZ on KMN function can cause compromised KMN integrity. It would be of interest to examine KMN levels upon SPINDLY and dynein depletion, and potential interaction between components of the RZZ compelx and the KMN network.

Materials & Methods

Cell Culture and transfection

U2OS, U2OS LacO cells (a gift from S. Janicki) and HeLa cells were grown in DMEM supplemented with 8% FBS, 50 µg/ml penicillin/streptomycin, and 2 mM L-glutamine. HeLa Flp-in cells (a gift from S. Taylor) were cultured in the same medium but containing 8% tetracycline-approved FBS (Clontech) supplemented with hygromycin (200 µg/ml) and blasticidin (4 µg/ml). U2OS-TR cells (a gift from M. Timmers) were cultured in the same medium but containing 8% tetracycline-approved FBS (Clontech) supplemented Zeocin (100 µg/ml). Plasmids were transfected using Fugene HD (Roche) according to the manufacturer's instructions. To generate stably-integrated HeLa Flp-In cells, pCDNA5-constructs were co-transfected with Ogg44 recombinase in a 10:1 ratio [77] and selected with Blasticidin and Hygromycin. Constructs were expressed by addition of 1 µg/ml doxycyclin for 24h. siBUB1 (5'-GAAUGUAAGCGUUCACGAA-3') siZW10 (5'-UGAUCAAUGU-GCUGUUCAA-3') were transfected using Hiperfect (Qiagen) at 20 nM and 100 nM respectively for 2 days according to manufacturer's instructions.

Cell lines

HeLa Flp-in cells were transfected with pcDNA5 (Invitrogen) encoding for LAP-BUB1-WT or BUB1-KD, mCherry–MIS12–MPS1$^{\Delta 200}$, eYFP-FKBP-MAD1-WT and selected with hygromycin and blasticidin to establish polyclonal cell lines. Stable HeLa Flp in cells harboring eYFP-FKBP-MAD1-WT were subsequently transfected with pcDNA3 (Invitrogen) encoding for MIS12-FRB-FLAG. The U2OS-TR cell line was transfected with pcDNA4 vector (Invitrogen) encoding LAP–MIS12–MPS1$^{\Delta 200}$ and selected with Zeocin. Monoclonal cell lines were then established by limited dilution (Clone 9B; LAP–MIS12–MPS1 $^{\Delta 200}$)

Immunofluorescence, antibodies and reagents

Cells were plated on 12-mm coverslips and treated as described in figure legends, cells were pre-extracted with PEM/TX (100 mM PIPES [pH 6.8], 1 mM $MgCl^2$, 5 mM EGTA, 0.2% Triton X-100) for 1 min. before a 5 min. fixation in 3.7% formaldehyde in PEM/TX-100. Coverslips were blocked with 3% BSA in PBS for 1 hr., incubated with primary antibody for 16 hr. at 4 C °, washed with PBS/0.1% TX-100 and incubated with secondary antibodies for an additional 1 hr. at room temperature. Coverslips were washed and submerged in PBS containing DAPI and mounted using ProLong Gold antifade (Molecular Probes). Image acquisition and quantification were done as described [146], using a DeltaVision RT system (Applied Precision) with a 1003/1.40 numerical aperture (NA) UPlanSApo objective (Olympus) for acquiring images, ImageJ software for quantification and Photoshop CS5 (Adobe) for image processing.

The following primary antibodies were used for immunofluorescence imaging: MPS1–NT (EMD Millipore, 05-682, 1;1000), CREST (Cortex Biochem, CS1058 1:2000), CENP-C (Sanbio, PD030, 1:1000) HEC1 9G3 (Abcam, ab3613 1:1000), GFP (custom rabbit

polyclonal, 1:10.000), GFP (Roche, 11814460001 mouse monoclonal, 1:1000), KNL1 (Abcam, ab70537, 1:1000), BUB1 (Bethyl, A300-373A, 1:1000), BUBR1 (Bethyl, A300-386A, 1:1000), MAD1 (Custom anti-mouse, a gift from Andrea Musacchio, 1:50), ZW10 (Abcam, ab21582, 1:1000). Secondary antibodies were high-crossed goat anti–human and anti–guinea pig Alexa Fluor 647 and goat anti–rabbit and anti–mouse Alexa Fluor 488 and Alexa Fluor 568 (Molecular Probes) for immunofluorescence experiments. Thymidine (2.5 mM), nocodazole (830 nM), MG132 (5 μM), reversine (various doses), doxycycline, STLC (10 μM) were all obtained from Sigma. Zeocin (100 μg/ml) was obtained from Invitrogen, Rapamycin and Blasticidin were obtained from PAA Laboratories.

Live-cell imaging

Cells were plated in 8 well chambered glass-bottom slides (LabTek), transfected, and imaged in a heated chamber (37°C and 5% CO2) using a 20×/0.5 NA UPLFLN objective (Olympus) on a microscope (IX-81; Olympus) controlled by Cell-M software (Olympus). Images were acquired using a camera (ORCA-ER; Hamamatsu Photonics) and processed using Cell-M software.

Mass spectrometry.

HeLa Flp-in cells inducibly expressing LAP-BUB1 and LAP–MAD1 were synchronized in mitosis by a 24h thymidine block followed by o/n treatment with nocodazole. Cells were harvested, lysed and prepared for immunoprecipitation and mass spectrometry as described [182].

Chapter 4

PLK1 promotes SAC activity by stabilizing the mitotic checkpoint complex.

Tale Sliedrecht[1,4], Saskia J.E. Suijkerbuijk[1,5], Vincent Groenewold[1], Geert J.P.L. Kops[1,2,3,4]

[1]Molecular Cancer Research and [2]Department of Medical Oncology and [3]Cancer Genomics Netherlands, University Medical Center Utrecht, 3584 CG, Utrecht, The Netherlands. [4]Netherlands Proteomics Centre, Utrecht, The Netherlands, [5]Present address: The Wellcome Trust/Cancer Research UK Gurdon Institute, University of Cambridge, Tennis Court Road, Cambridge CB2 1QN, United Kingdom

Manuscript in preparation

Abstract

The spindle assembly checkpoint (SAC) ensures correct chromosomes distribution during mitosis by preventing the onset of anaphase until all chromosomes are attached to the mitotic spindle. Robust SAC signaling relies on an intimately intertwined signaling network that is assembled on unattached kinetochores. In addition to the essential SAC components, some proteins are known to fine-tune the SAC. Their auxiliary function in SAC signaling is revealed when the SAC is functionally compromised. Using a sensitized assay in which partial MPS1 inhibition weakens SAC activity, we found that Polo like kinase 1 (PLK1) modulates the SAC in a non-essential manner. PLK1 activity does not regulate MPS1 function or kinetochore binding of core SAC components, but regulates the SAC downstream of MAD1 function. PLK1 activity promotes stability of the diffusible SAC effector complex known as MCC and we report a novel PLK1-like phosphorylation site in BUBR1 that regulates the BUBR1 - BUB3 interaction known to contribute to MCC function. Our findings reveal PLK1 as a kinetochore-independent auxiliary factor required for robust SAC signaling.

Introduction

When cells enter mitosis, their unattached kinetochores rapidly recruit and activate MPS1 in order to swiftly establish and maintain an effective spindle assembly checkpoint (SAC) response [146,201]. MPS1 initiates, among other things, recruitment of the SAC proteins MAD1 and MAD2, thus enabling production of the SAC effector complex known as the mitotic checkpoint complex (MCC) (reviewed in [75], chapter 3). The MCC prevents degradation of Cyclin B and Securin by the E3 ubiquitin ligase anaphase promoting complex/cyclosome (APC/C) [71,83] and as such delays mitotic progression when unattached kinetochores persist. As chromosomes attach and congress, the SAC is maintained with progressively fewer unattached kinetochores. It is currently unknown whether MCC levels follow the amount of unattached kinetochores or whether the proposed catalytic nature of MCC production ensures high levels of MCC regardless of how many kinetochores are unattached [75,210].
Efficient activation of the SAC depends on a network of mitotic kinases that predominantly localize to unattached kinetochores. These kinases include, but may not be limited to, MPS1, BUB1 and Aurora B. BUB1 regulates the SAC by recruiting MAD1 (Chapter 3, [77,78,184]) but it also involved in chromosome bi-orientation and sister chormatid cohesion by phosphorylation of Histone2A [192]. MPS1 is required for efficient SAC signaling by recruiting checkpoint proteins, including BUB1, to unattached kinetochores [76], by facilitating MAD2 dimerization [90], and by promoting MCC stability [91]. Simultaneously and independent of its role in the SAC, MPS1 coordinates attachment error-correction [90,133,138,146,151,153,164]. We and other recently reported that the kinase Aurora B, best known for its roles in chromosome bi-orientation and cytokinesis (reviewed in [211]) is also required for timely establishment of the SAC, by initiating efficient recruitment of MPS1 to kinetochores at the onset of mitosis [146,153,212]. This role, however, is not an essential one, as efficient depletion or inactivation of Aurora B does not abrogate the SAC but does significantly delay its timely establishment. As a result, cells without Aurora B activity enter mitosis without a SAC and need minutes to establish it. Once established, cells proceed through mitosis with a normal SAC but have permitted partial Cyclin B degradation during the early stages of mitosis. This low level of Cyclin B affects the ability of the SAC to delay mitosis for extended periods of time [146]. Aurora B is therefore and auxiliary factor in the SAC response, a role that was revealed in a sensitized SAC assay [146,212].

A kinase whose role in the SAC is controversial and not well established is Polo-like kinase 1 (PLK1). PLK1 regulates numerous processes in cell division, with essential roles in bipolar spindle assembly [213,214], centrosome maturation [215,216], regulation of kinetochore-microtubule attachment [41,114,217-219] and cytokinesis [220]. The diversity of PLK1 functions is accommodated by its wide range of sites to which it localizes. PLK1 targeting to subcellular locations is mediated by its C-terminal Polo-box domain (PDB), which recognizes proteins primed by CDK1 phosphorylation [221,222]. An example, PLK1 binds to CDK1-primed BUBR1 at mitotic kinetochores [217] and phosphorylates BUBR1 on multiple residues to create a docking site for the B56-PP2A phosphatase that is essential for formation of stable kinetochore-microtubule attachments [41,42,113]. As a result PLK1 inhibition weakens kinetochore attachments and subsequently causes a SAC-dependent mitotic delay [214,223,224]. Some reports suggest that PLK1 may regulate the SAC [225-227]. In human cells and *Xenopus* egg extracts, PLK1 has been suggested to regulate kinetochore binding of MAD1, MAD2 and/or BUBR1 [225,227], and in *Drosophila* S2 cells the PLK1 homolog Polo was suggested to regulate MPS1 localization

[228]. None of these studies, however, reported an effect of PLK1 inhibition/depletion on the ability of cells to delay mitosis in response to unattached kinetochores.

We cared to investigate if mitotic kinases other than Aurora B have an auxiliary role in the SAC. We here report PLK1 as such an auxiliary SAC regulator. We show that PLK1 inhibition does not affect kinetochore localization of SAC proteins such as MPS1 and MAD1 in human cells. Our data instead suggest that PLK1 is essential to maintain MCC stability, possibly by phosphorylation of the BUBR1 GLEBS domain that mediates the BUBR1-BUB3 interaction.

Results

PLK1 participates in maintaining a SAC response

Rapid maximal activation of the SAC in response to unattached kinetochores depends on a tightly regulated signaling network involving multiple layers of feedback control [67]. Many components of this network are essential and some are auxiliary. An example of the latter is the kinase Aurora B. Efficient inhibition of Aurora B (by combining RNAi with small molecule inhibitors) does not prevent SAC activation but delays its swift establishment at the onset of mitosis by delaying efficient MPS1 localization and subsequent activation [146]. As a result, cells enter mitosis with much reduced levels of Cyclin B, risking accelerated mitotic slippage. The effect of Aurora B on the SAC was revealed by a sensitized assay in which the SAC is weakened in nocodazole-treated cells by addition of a low dose of the MPS1 inhibitor reversine [133]. When assayed for mitotic duration using DIC time-lapse imaging, such cells normally maintain mitotic delays for many hours despite reduced MPS1 activity ([146], see also Figure 1A, B) but become extremely sensitive to additional perturbations that affect the SAC, such as Aurora B inhibitors [146,212]. We used this assay to find other mitotic kinases that promote SAC activity but may not be essential for it. To exclude indirect effects of kinase inhibition on the SAC from potential changes in kinetochore-microtubule interactions, these and all further experiments were performed in the presence of nocodazole. The majority of nocodazole-treated cells maintained extended mitotic delays upon addition of 125 nM of reversine (hereafter referred to as “low reversine”) or a high dose (50 nM) of the PLK1 inhibitor BI2536 [224] (Figure 1A, B). Strikingly, simultaneous treatment with low reversine and 50 nM BI2536 caused cells to rapidly exit mitosis (Figure 1A, B). The sensitization to BI2536 was due specific PLK1 inhibition, as it was recapitulated by PLK1 siRNA (Figure 1C). Weakening MPS1 activity by adding the Aurora B inhibitor ZM447439 instead of low reversine also sensitized the SAC to PLK1 inhibition (Figure 1D).

PLK1 is not required for timely SAC establishment

To gain further insight into how PLK1 affects SAC signaling, we measured the rate of Cyclin B degradation in cells treated with combinations of the various inhibitors. To this end, cellular fluorescence was monitored in a HeLa cell line in which endogenous Cyclin B1 was tagged with eYFP by inserting the eYFP cDNA sequence in the last exon of the *CCNB1* locus (Figure 2A). Nocodazole-treated Hela-CCNB1^{eYFP} cells maintained relatively stable Cyclin B1 levels for hours after NEB (Figure 2B). As shown before and similar to addition of ZM447439 [146], addition of low reversine before mitotic entry caused an initial drop in Cyclin B1 levels after NEB that subsequently stabilized to a degradation rate that was similar to control cells (Figure 2B) This initial drop is due to late establishment of SAC activity when MPS1 activity is compromised, either by inefficient MPS1 localization due to loss of Aurora B activity or by

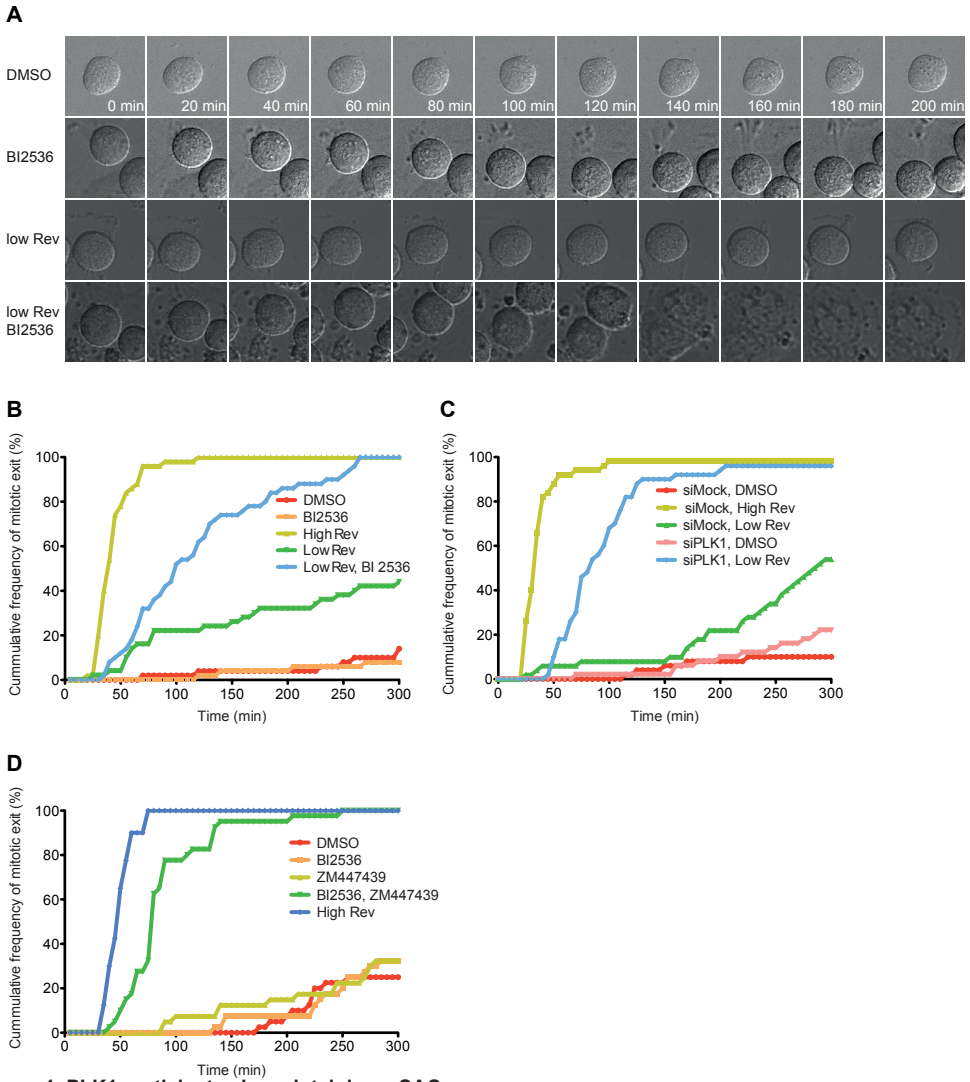

Figure 1. PLK1 participates in maintaining a SAC response

(A, B) Stills **(A)** and analysis **(B)** of mitotic exit by live imaging of HeLa cells, treated as indicated. Nocodazole was present in all conditions. Graph in (**B)** (50 cells per condition) shows cumulative frequency of mitotic exit, determined by cell flattening, versus time (min). t=0 indicates addition of indicated drugs. Data are representative of 3 independent experiments. **(C, D)** Analysis of mitotic exit by live imaging of U2OS cells, transfected and/or treated as indicated. Nocodazole was present in all conditions. Graphs (50 cells per condition) show cumulative frequency of mitotic exit, determined by cell flattening, versus time (min). t=0 indicates addition of indicated drugs. Data are representative of two independent experiments.

reductions in MPS1 activity [146]. Notably, addition of BI2536 had no effect on the rate of Cyclin B1 degradation in control cells but accelerated it in cells treated with low reversine (Figure 2B). The accelerated rate of Cyclin B degradation, although sufficient to explain rapid mitotic exit, was not as fast as the rate reached when the SAC was fully inactivated, for instance by high dose reversine (500 nM, hereafter referred to as 'high reversine') (Figure 2B). PLK1

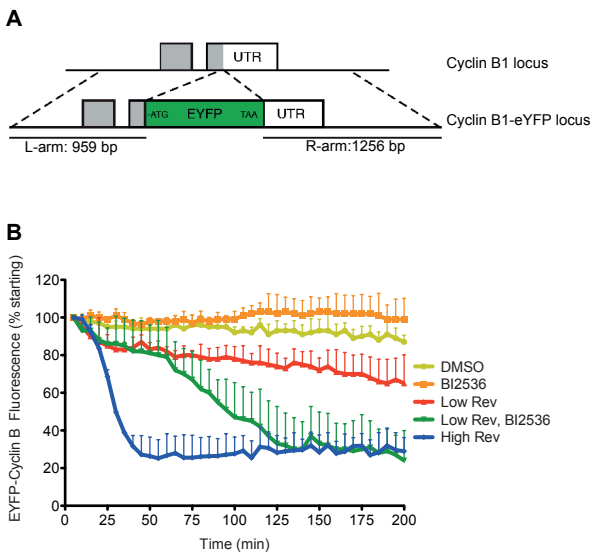

Figure 2. PLK1 is not required for timely SAC establishment

(A) Schematic overview of the insertion of EYFP in the *CCNB1* locus by homologous recombination. **(B)** Quantification of Cyclin B1–eYFP fluorescence in mitotic HeLa-CCNB1-eYFP cells treated with nocodazole and indicated inhibitors. Fluorescence at nuclear envelope breakdown (NEB: t=0) was set to 100%. Data represent the mean (+S.D.) of 5 cells, and is representative of two independent experiments. All drugs were added before mitotic entry.

inhibition may thus not fully inactivate the SAC response in MPS1-compromised cells, or, alternatively, maximal APC/C activation requires PLK1 activity independent of its effects on the SAC, as previously suggested [229,230].

MPS1 localization and activity are not regulated by PLK1

Like Aurora B [146,212], PLK1 could promote SAC activation by ensuring efficient recruitment of MPS1 to unattached kinetochores, as recently suggested for *Drosophila* Polo in S2 cells [228]. This would be in line with observations in human cells that PLK1 contributes to Aurora B activation [231] and accumulation of Aurora B on centromeres of unaligned chromosomes [232]. Several lines of evidence, however, strongly indicate that MPS1 localization and activation are normal in PLK1-inhibited human cells. First, even slight reductions in MPS1 activity cause accumulation of MPS1 on unattached kinetochores (Figure 3A, B, and [90,149]), yet PLK1 inhibition had no effect on MPS1 kinetochore levels, neither alone nor in combination with low reversine (Figure 3A, B). Second, tethering MPS1 to kinetochores by induced expression of MIS12-MPS1$^{\Delta 200}$ [142,146,149], while rescuing SAC inactivation by Aurora B inhibitors in our sensitized SAC assay [146], could not restore the SAC upon PLK1 inhibition (Figure 3C). Third, efficient reactivation of MPS1 in mitosis during recovery from transient inhibition of CDK1 using RO3306 [146,153] was unaffected by BI2536 (Figure 3D). Taken together, we conclude that PLK1 regulates the SAC independent of MPS1 localization or activation.

PLK1 does not regulate recruitment of SAC proteins to unattached kinetochores.

We next wished to examine at which level PLK1 activity exerted its effects on SAC signaling. Several SAC proteins including BUB1 and RZZ promote SAC signaling predominantly by ensuring MAD1 kinetochore binding (chapter 3), while others operate downstream of MAD1, for example in catalyzing MCC production (MAD2) or inhibiting APC/C-CDC20 activity (BUBR1-BUB3). PLK1 has been reported to affect MAD1 localization and to directly phosphorylate MAD1 [225]. To determine if PLK1 acted upstream or downstream of MAD1 kinetochore localization, we examined SAC activity after PLK1 inhibition in cells with kinetochore-tethered MAD1 [92], using the same cell line as introduced in chapter 3, (Figure

3.6B C). If PLK1 predominantly acts upstream of MAD1 function, the tethered MAD1 should rescue SAC defects in PLK1-inhibited cells, as is the case for SAC defects upon BUB1 or ZW10 depletion (chapter 3). As shown in Figure 4A, rapamycin-induced tethering of MAD1 to unattached kinetochores was unable to prevent the mitotic exit caused by simultaneous inhibition of PLK1 and MPS1. In support of a role for PLK1 downstream of MAD1 kinetochore binding, immunolocalization studies showed that PLK1 inhibition did not affect localization of MAD1 or MAD2 to kinetochores of nocodazole-treated cells (Figure 4B, D, E). Lack of an effect on localization of MAD1 by PLK1 inhibition was also apparent in cells with weakened MPS1 activity: Cells treated with low reversine displayed significantly diminished kinetochore levels of MAD1 and MAD2, but additional inhibition of PLK1 did not reduce this further (Figure 4B, D, E). Addition of BI2536 also did not affect kinetochore levels

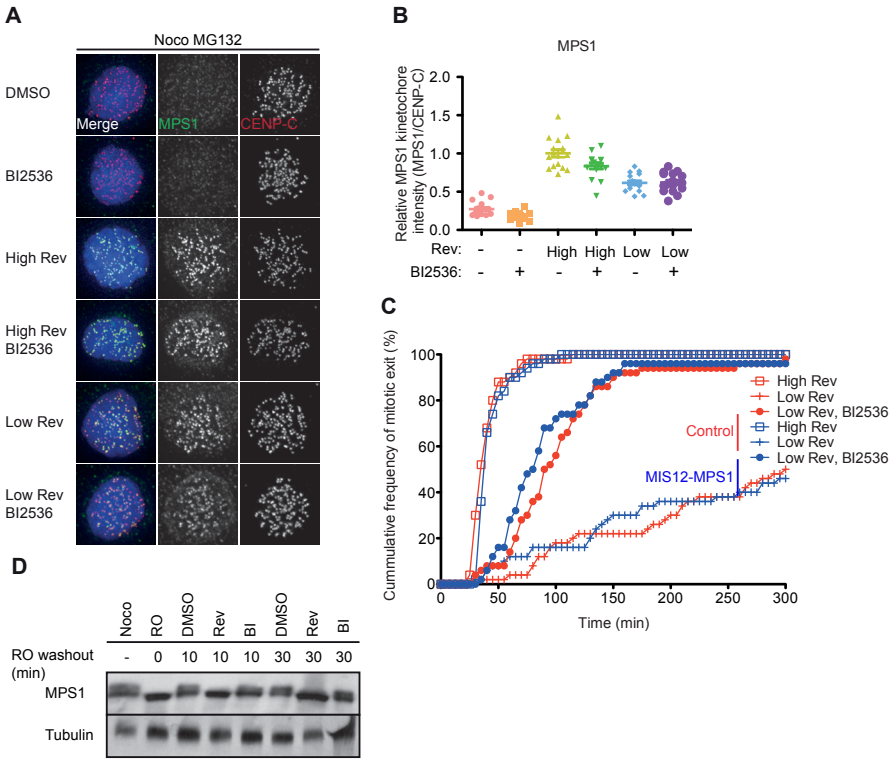

Figure 3. MPS1 localization is not influenced upon PLK1 inhibition

(A, B) Immunolocalization of MPS1 and centromeres (CENP-C) in HeLa cells treated with nocodazole, MG132 and indicated inhibitors for 2 hours. Representative images are shown in **A**. Graph in B represent total kinetochore intensity of MPS1 relative to centromeres (CENP-C) ±SD. All data are from ≥15 cells and are representative of three independent experiments. **(C)** Time-lapse analysis of duration of mitotic arrest in U2OS cells, non-induced or induced to express LAP-MIS12-MPS1$^{\Delta 200}$, and treated with nocodazole in combination with indicated inhibitors. Graph (50 cells per treatment) shows cumulative frequency of mitotic exit (scored as cell flattening) at the indicated times after addition of the inhibitors. Data is representative of 3 independent experiments. **(D)** Immunoblot of MPS1 and tubulin in whole cell lysates from HeLa cells treated with nocodazole without (-) or with RO3306 for 15 minutes (all other lanes) and subsequently released into nocodazole/ inhibitor for the indicated times. Lower-mobility MPS1 forms indicate phosphorylated, active MPS1.

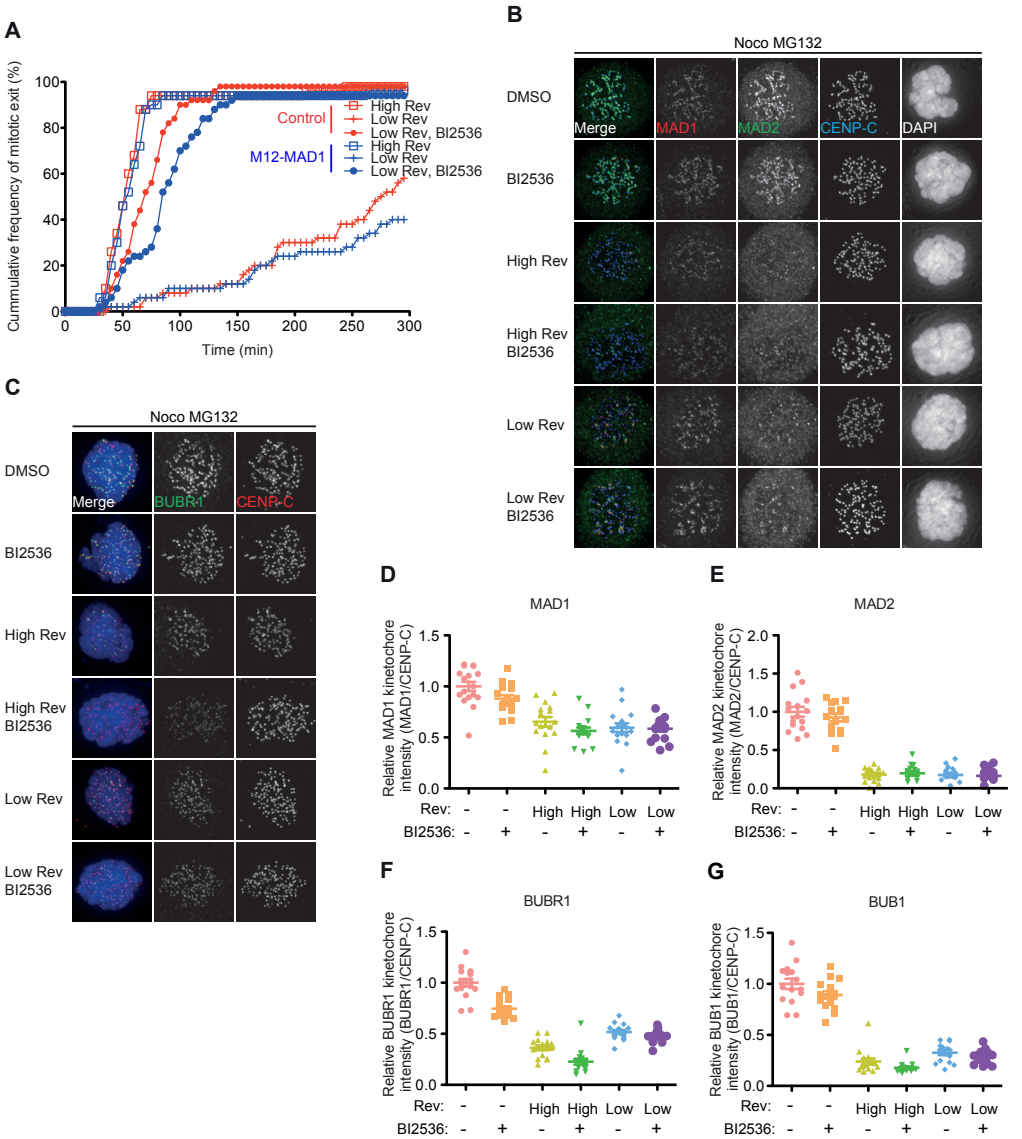

Figure 4. PLK1 does not influence the localization checkpoint proteins

(A) Time-lapse analysis of duration of mitotic arrest in HeLa cells stably expressing MIS12-FRB-tagRFP, induced to express eYFP-FKBP-MAD1, and treated with nocodazole in combination with DMSO or Rapamycin (to induce FRB-FKBP heterodimerination and indicated inhibitors. Graph (50 cells per treatment) shows cumulative frequency of mitotic exit (scored as cell flattening) at the indicated times after addition of the inhibitors. Data is representative of 3 independent experiments. **(B-F)** Representative images and quantifications of immunolocalization of MAD1 **(B, D)**, MAD2 **(B, E)**, BUBR1 **(C, F)**, BUB1 **(G)**(Representative images not shown) and centromeres (CENP-C) in HeLa cells treated with nocodazole, MG132 and the indicated inhibitors for 2 hours. Graphs represent total kinetochore intensities of indicated proteins relative to centromeres (CENP-C) ±SD. All data are from ≥15 cells and are representative of three experiments.

of BUB1 (Figure 4G) and only marginally affected kinetochore levels of BUBR1 (Figure 4C, F). Together, these data show that PLK1 does not significantly regulate kinetochore binding of the core SAC machinery.

PLK1 activity promotes MCC stability

Our observation that the SAC in cells expressing MIS12-MAD1 was still sensitive to PLK1 inhibition (Figure 4A) showed that PLK1 promotes SAC activation downstream of MAD1 function. The primary function of MAD1 is to enable conversion of MAD2 to its closed conformation, thereby catalyzing production of the MCC [75]. To explore the idea that PLK1 acts downstream of MAD1 function at kinetochores, we set out to assess MCC formation in PLK1-inhibited cells by immunoprecipitation. While either PLK1 inhibition or MPS1 inhibition did not or only marginally affect the amount of CDC20 that was co-precipitated with MAD2 from lysates of nocodazole-treated cells (Figure 5A and [91,151]), combined treatment with PLK1 inhibitor and low or high dose reversine drastically diminished CDC20 in MAD2 immunoprecipitates (Figure 5A). We furthermore found that the amount of BUB3 co-precipitating with BUBR1 was strongly decreased when MPS1 and PLK1 were simultaneously inhibited (Figure 5B), but not when either PLK1 or MPS1 alone were inhibited (Figure 5B). We thus conclude that PLK1 activity contributes to the formation and/or maintenance of a stable MCC.

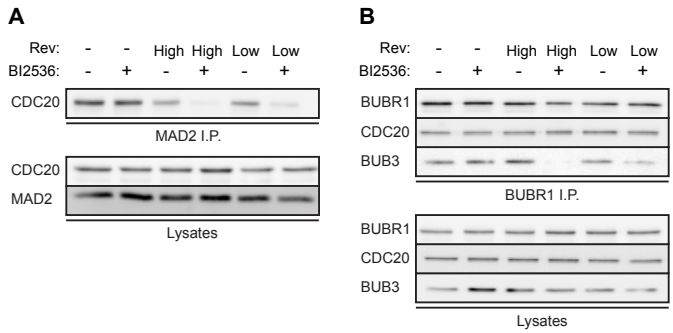

Figure 5. PLK1 activity is essential for MCC stability

(A, B) Immunoblots of CDC20, MAD2, BUB3 or BUBR1 in immunoprecipitates of endogenous MAD2 **(A)** or BUBR1 **(B)** (upper panels) or in lysates (bottom panels) from mitotic HeLa cells treated with nocodazole, MG132 and the indicated inhibitors for 2 hours.

Phosphorylation of BUBR1 on a conserved PLK1 consensus site promotes its interaction with BUB3

Spatiotemporal regulation of MCC formation or stabilization downstream of MAD2 conversion is poorly understood. Since our data suggest that PLK1 may play an auxiliary role in this, we wished to clarify the mechanism of action of PLK1 on MCC formation. It has recently been suggested that MPS1 activity maintains stability of cytoplasmic MCC [91]. However, since our data do not support a role of MPS1 in PLK1-mediated control of the SAC response, we chose to examine MCC components for phosphorylation on PLK1 consensus phosphorylation sites. We and other previously reported that PLK1 phosphorylates BUBR1 in the KARD motif to create a PP2A-B56 binding site [41,217-219,233]. Using mass spectrometric analyses of LAP-BUBR1 purified from mitotic U2OS cells (Figure 6A), we found many additional phosphorylated residues on BUBR1, including the previously reported pS435, pS543 and pS670 (not shown) [218,233], as well as a novel one, pS411 (Figure 6B, C). S411 and its neighbouring sequences are well-conserved (Figure 6C and [67]) and S411 resides in a PLK1 consensus motif (D/E-x-S/T-Φ-D/E, where x represents any amino acid and Φ a large hydrophobic amino acid [234,235]). Moreover, S411 is located within the GLEBS motif, which

mediates the interaction between BUBR1 and BUB3 (Figure 6C) [218,236].
Since combined inhibition of MPS1 and PLK1 decreased BUB3-BUBR1 interaction, we next examined a potential role in this for S411 phosphorylation. As expected, immunoprecipitation of BUBR1 co-precipitated BUB3, and this was abolished by deleting the GLEBS motif in BUBR1 (BUBR1-ΔGLEBS) (Figure 6D). Substitution of S411 to unphosphorylatable Alanine, although not abolishing it, also strongly decreased BUB3 binding (Figure 6D), suggesting that S411 phosphorylation contributes to the BUBR1-BUB3 interaction. Loss of BUB3 binding was even more pronounced when S411 was substituted for aspartate which potentially mimics phosphorylation (Figure 6D). All BUBR1 variants expressed normally, but only WT and S411A localized to kinetochores (Figure 6E). Lack of S411D binding to BUB3 and kinetochores may be due either to specific phosphorylation-dependent loss of the BUB3 interaction, or inadvertent disruption of GLEBS motif function by the substitution. Our data show that PLK1 promotes SAC activity downstream of MAD1 kinetochore localization, possibly by MCC stabilization through BUBR1-S411 phosphorylation to promote BUBR1-BUB3 binding.

Discussion

Our data show that PLK1 activity promotes SAC activation, a role that becomes essential when the SAC response is sub-optimal. PLK1 impacts SAC signaling downstream of MAD1 kinetochore localization, as PLK1 inhibitors do not prevent localization of MAD1, MAD2, MPS1 and BUB1 to kinetochores, and still affect SAC signaling when MAD1 is tethered to kinetochores. Instead, we provide evidence that PLK1 promotes MCC stability and show that this could, in part, be mediated by phosphorylation of S411 in the BUB3-interacting GLEBS motif of BUBR1.

Although a function for PLK1 in the SAC has been suggested previously [225-227], no functional SAC defect has been reported in cells lacking PLK1 activity. As we show here, this is likely due to the fact that PLK1 is an auxiliary factor whose role in the SAC is masked by its involvement in a multitude of other mitotic processes. For example, inhibition of PLK1 during normal mitotic progression will delay rather than shorten mitosis, because the effect of PLK1 inhibition on the stability of kinetochore-microtubule attachments [41,42,113,217-219,233] is likely dominant over its non-essential role in the SAC. A role for PLK1 in the SAC is revealed when its effects on attachments is negated by the use of nocodazole and when the SAC is weakened by compromising MPS1 activity. If not essential, under what conditions is PLK1 activity important for the SAC? We find that PLK1 activity is indispensable for MCC stability when the SAC is functionally compromised. A recent study proposed that as chromosomes congress, MCC composition shifts from a MAD2-containing MCC to one that lacks MAD2 [237]. Perhaps PLK1 might become important once the SAC becomes progressively weaker when MCC composition changes as more and more kinetochores attach and congress. Although technically challenging, examining this possibility will require ways to address whether the SAC is more sensitive to PLK1 inhibition in cells containing only few unattached kinetochores.

Previous studies have suggested that PLK1 promotes localization of MAD1/MAD2 and/or MPS1 to unattached kinetochores [225,228]. However, we and others failed to observe any effect on kinetochore levels of these proteins after PLK1 inactivation [184,224]. Furthermore, we find

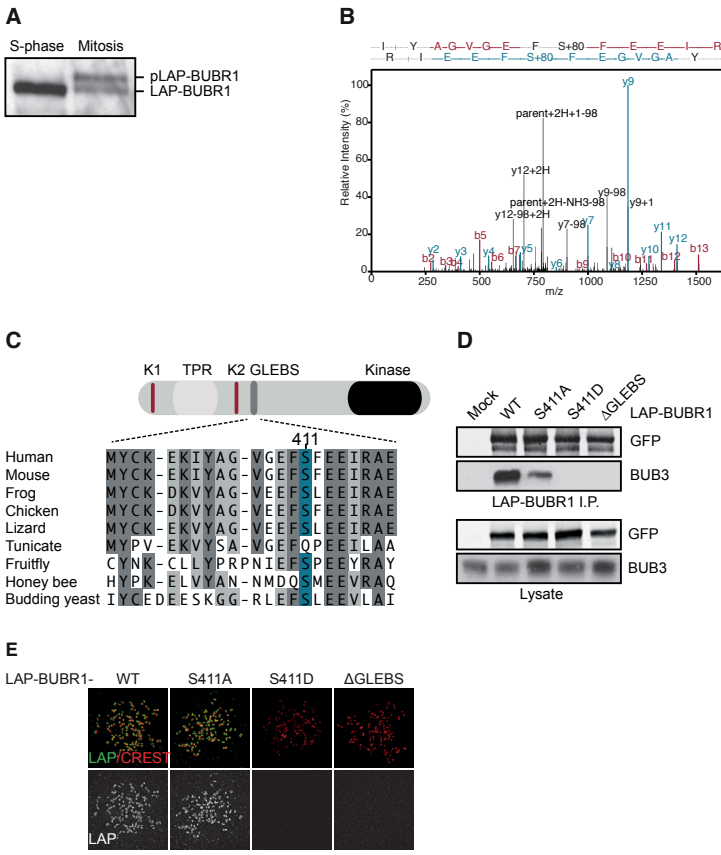

Figure 6. BUBR1 phosphorylation on S411 promotes BUB3 binding

(A) Immunoblot of lysates from S-phase (24 hours thymidine treatment) and mitotic (16 hours nocodazole treatment) HeLa cells transfected with LAP-BUBR1. **(B)** Schematic representation of domain architecture of BUBR1 and sequence alignment of the GLEBS motif. Conserved residues are indicated in grey. S411 based on the sequence of human BUBR1, is shown in blue. Human, *H. sapiens*; Mouse, *M. musculus*; Frog, *X. tropicalis*; Chicken, *G. gallus*; Lizard; *A. carolinensis;* Tunicate, *C. intestinalis*; Fruitfly, *D. melanogaster*; Honey bee, *A. mellifera*; Budding yeast, *S. cerevisiae*. **(C)** MS/MS spectrum of pS411 containing peptide of BUBR1 (aa 403-416) is shown. Identified b and y ions are indicated. **(D)** Immunoblots of LAP-BUBR1 variants pull-downs (upper panel) or of lysates (lower panel) from mitotic 293T cells transfected with indicated LAP-BUBR1 and treated with nocodazole, using anti-BUB3 and anti-GFP antibodies. **(E)** HeLa cells transfected with indicated LAP-BUBR1 variants and treated with nocodazole and MG132 for 30 minutes and immunostained for GFP and centromeres (CREST)

that PLK1 acts downstream of MAD1 localization, since PLK1 inhibition still affects the SAC when MAD1 is tethered to kinetochores.

We show here, as observed in *Drosophila* S2 cells [228] that PLK1 is required for maximal MAD2-CDC20 and BUBR1-BUB3 interaction under conditions of a weakened SAC. The latter may be mediated by a here newly identified mitotic phosphorylation site on BUBR1 that resides in a PLK1 consensus motif within the BUB3-binding GLEBS motif of BUBR1. Mutation of this S411 site disrupts BUBR1-BUB3 interaction. This could indirectly affect MAD2-CDC20 interaction and MCC stability, although it is somewhat puzzling why CDC20 retains its normal interaction with BUBR1. It remains to be established whether phosphorylation of S411 in the

GLEBS motif is due to PLK1 and proof of a causal link between this phosphorylation and the contribution of PLK1 to the SAC will require functional characterization of S411A, both in SAC activity and MCC stability.
An additional or alternative mechanism by which PLK1 may influence the SAC response is redundancy with MPS1 signaling. Interestingly, the kinase consensus motif of MPS1 [238,239] closely resembles that of PLK1 [234,235]. PLK1 could therefore theoretically reinforce MPS1 signaling by phosphorylating a subset of the same substrates. One of the few bona fide MPS1 substrates reported is KNL1. MPS1 phosphorylates MELT-like motifs in KNL1 that recruit BUB1 and thereby impact SAC activity [118-120]. However, since we observe no decrease in BUB1 localization upon PLK1 inhibition, it is unlikely that PLK1 targets these motifs. Other MPS1 substrates that impact the SAC have not yet been described, but potential candidates include those that affect MCC levels downstream of MAD1. In that respect it is of interest to note that MPS1 has been proposed to mediated conversion of MAD2 to its closed form [90], but mechanistic details of this are unknown.

A weakened SAC may promote tumor progression by causing low levels of chromosomal instability (CIN) [177,240]. Indeed several mouse models with reduced SAC display CIN and are more prone to tumor formation in particular sensitized backgrounds (reviewed in [241]). Although SAC defects do not appear to contribute to CIN in cultured human cancer cell lines [242,243], a weakened SAC may contribute to cancer phenotypes in human patients, as various alterations to SAC components in human tumors are regularly reported [244-246]. Our observation that PLK1 is important for a maximal SAC response under suboptimal conditions may have implications for the molecular origins of CIN in tumors, and for our interpretation of the effects of PLK1 inhibitors on cell viability in (pre)clinical settings. In this light it might be interesting to test the ability of CIN tumor cells to maintain SAC signaling in the presence of PLK1 inhibitors.

Materials & Methods

Cell Culture and Cell lines
U2OS cells, and HeLa cells were grown in DMEM supplemented with 8% FBS, 50 µg/ml penicillin/streptomycin, and 2 mM L-glutamine. Plasmids were transfected using Fugene HD (Roche) according to the manufacturer's instructions. To generate stably-integrated HeLa Flp-In cells, pCDNA5-constructs were co-transfected with Ogg44 recombinase in a 10:1 ratio and selected with hygormycin and blasticidin [77]. Constructs were expressed by addition of 1 µg/ml doxycyclin for 24h. HeLa Flp in cells were transfected with pcDNA5 (Invitrogen) encoding for mcherry–Mis12–Mps1$^{\Delta 200}$ and selected with hygromycin and blasticidin to establish polyclonal cell lines. Stable HeLa Flp in cells harboring eYFP-FKBP-MAD1 were subsequently transfected with pcDNA3 (Invitrogen) encoding for MIS12-FRB-FLAG. HeLa-CCNB1-EYFP cells: A single allele of CCNB1 was modified to contain EYFP by integrating the EYFP sequence directly 5' between the stop codon and 3'UTR in exon 9 using homologous recombination, as described [247]. The cassette encompassing the homology arms and eYFP sequence was synthesized (Genscript), validated and transferred to pAAV. The preparation of infectious AAV particles, transduction of cells, and subsequent sorting of EYFP-positive cells was previously described [248].

Immunofluorescence, antibodies and reagents

Cells were plated on 12-mm coverslips, treated as described in figure legends, and pre-extracted with PEM/TX (100 mM PIPES [pH 6.8], 1 mM $MgCl^2$, 5 mM EGTA, 0.2% Triton X-100) for 1 min before a 5 min fixation in 3.7% formaldehyde in PEM/TX. Coverslips were blocked with 3% BSA in PBS for 1 hr. incubated with primary antibody for 16 hr. at 4 C °, washed with PBS/0.1% Triton X-100, and incubated with secondary antibodies for an additional 1 hr. at room temperature. Coverslips were washed and submerged in PBS containing DAPI and mounted using ProLong Gold antifade (Molecular Probes). Image acquisition and quantification were done as described [146], using a DeltaVision RT system (Applied Precision) with a 1003/1.40 numerical aperture (NA) UPlanSApo objective (Olympus) for acquiring images, ImageJ software for quantification and Photoshop CS5 (Adobe) for image processing.

The following primary antibodies were used for immunofluorescence imaging: MPS1–NT (EMD Millipore, 05-682, 1;1000), CREST/ACA (Cortex Biochem, CS1058 1:2000), CENP-C (Sanbio, PD030, 1:1000), GFP (custom rabbit polyclonal, 1:10.000), GFP (Roche, 11814460001 mouse monoclonal, 1:1000), BUB1 (Bethyl, A300-373A, 1:1000), BUBR1 (Bethyl, A300-386A, 1:1000), MAD1 (Custom mouse, a gift from Andrea Musacchio, 1:50). Secondary antibodies were high-crossed goat anti–human and anti–guinea pig Alexa Fluor 647 and goat anti–rabbit and anti–mouse Alexa Fluor 488 and Alexa Fluor 568 (Molecular Probes) for immunofluorescence experiments. Thymidine (2.5 mM), nocodazole (830 nM), MG132 (5 μM), reversine (various doses), doxycycline, G-418 (1 mg/ml) and puromycin (1 μg/ml) were all obtained from Sigma. Zeocin (100 μg/ml) was obtained from Invitrogen, ZM447439 (2mM, Tocris Bioscience), BI2536 (50nM, Boehringer Ingelheim Pharma), RO3306 (1 μM, Enzo life sciences), Rapamycin and Blasticidin was obtained from PAA Laboratories. siPLK (5'-GCUCUGUGAUAACAGCGUG-3', custom Ambion) were transfected using Hiperfect (Qiagen) at 20 nM according to manufacturer's instructions.

Live-cell imaging

Cells were plated in 8 well chambered glass-bottom slides (LabTek), transfected, and imaged in a heated chamber (37°C and 5% CO2) using a 20×/0.5 NA UPLFLN objective (Olympus) on a micro- scope (IX-81; Olympus) controlled by Cell-M software (Olympus). Images were acquired using a camera (ORCA-ER; Hamamatsu Photonics) and processed using Cell-M software.

Mass spectrometry

For mass spectrometry, stable LAP-BUB1 and LAP–MAD1 HeLa cells were synchronized in mitosis by a 24h thymidine block, followed by o/n treatment with nocodazole and cells were harvested followed by immunoprecipitation and mass spectrometry as described in [41].

Immunoprecipitation

HeLa cells or U2OS and 293T cells transfected with LAP-BUBR1, were released from a 24-hour thymidine-induced block into nocodazole for 16 hours. Mitotic cells were harvested and subsequently treated with indicated inhibitors and lysed in lysis buffer (50mM HEPES pH7.5, 150mM NaCl, 5mM EDTA, 0.5% NP-40, 1mM Na_3VO_4, 1mM b-glycerophosphate, 1mM NaF and Complete protease inhibitor (Roche)). Anti-MAD2 or anti-CDC20 antibody were bound to Protein-G-Agarose (Roche), LAP-BUBR1 was bound to S-agarose (Novagen) for 2 hours, washed four times in lysis buffer and after removal of all buffer sample buffer was added and

boiled for 5 minutes. Samples were separated by SDS-page.

Chapter 5

Phosphoproteomics screens to identify mitotic MPS1 substrates

Tale Sliedrecht[1,4], Vincent Groenewold[1] Shabaz Mohammed [4,5], Albert J. R. Heck[4,5], Geert J. P. L. Kops[1,2,3,4,]

[1]Molecular Cancer Research and [2]Department of Medical Oncology and [3]Cancer Genomics Netherlands, University Medical Center Utrecht, 3584 CG, Utrecht. The Netherlands. [4]Netherlands Proteomics Centre, Utrecht, The Netherlands. Biomolecular Mass Spectrometry and Proteomics, Utrecht Institute for Pharmaceutical Sciences and Bijvoet Center for Biomolecular Research, Utrecht University, Padualaan 8, 3584 CH Utrecht, The Netherlands.

Abstract

Maintenance of genomic stability during cell divisions depends on tight spatio-temporal control of mitotic processes. Two of these, chromosome biorientation and the spindle assembly checkpoint (SAC), are regulated and integrated by a set of protein kinases and phosphatases that form a robust and sensitive network to ensure faithful segregation of chromosomes in mitosis. Despite identification of the important enzymes, many of the relevant phosphorylation events have not been mapped. Here we report our efforts to uncover substrates of MPS1, a mitotic protein kinase that is a central coordinator of both biorientation and the SAC. Using quantitative mass spectrometry-based phosphoproteomics on three experimental conditions that compared phospho-proteins in cells with and without MPS1 kinase activity, we have mapped 154 regulated phospho-sites. We discuss which of these are potential MPS1 substrates and provide a strategy to functionally examine the most promising ones.

Introduction

Correct regulation of reversible protein phosphorylation is required to successfully divide duplicated chromosomes to two newly formed daughter cells. To ensure equal distribution of sister chromatids during anaphase the cell relies on two evolutionary conserved mechanisms. While the error correction machinery ensures that each chromatid pair is correctly attached to spindle microtubules, the spindle assembly checkpoint (SAC) arrests cell in mitosis as long as unattached kinetochores remain (reviewed in [75]). These and other mitotic processes depend on a tight balance between phosphorylation and dephosphorylation. In human cells the mitotic kinases MPS1, BUB1, Aurora B and PLK1 (reviewed in [201]) regulate SAC activation and kinetochore-microtubule attachment. Their activity initiates numerous events required for correct chromosome segregation. For example, BUB1 is known to phosphorylate Histone2A on T120 to establish inner-centromere localization of the chromosomal passenger complex (CPC) [191,192], and Aurora B facilitates error correction by phosphorylating multiple subunits of the main microtubule binding site of kinetochores, the KMN network, as well as various other mitotic proteins [14,211].

MPS1 regulates error correction by direct phosphorylation of the CPC member Borealin [164] and more indirectly by controlling Sgo1 localization [153]. Simultaneously, it is involved in the regulation of the SAC by recruiting checkpoint proteins to unattached kinetochores [76], by facilitating MAD2 dimerization [90] and by ensuring stability of the SAC effector complex MCC [91]. KNL1 is currently the only *bona fide* substrate of MPS1 in SAC regulation in human cells. MPS1 phosphorylates repetitive MELT motifs within KNL1 that are required to recruit BUB1 to kinetochores [118-120]. Given MPS1 many functions in regulating error-correction and the SAC, it is unlikely that Borealin and KNL1 are its only relevant substrates in human cells.

The recent developments in quantitative mass spectrometry (MS)-based proteomics have led to global quantitative phosphoproteomics screens that have allowed the identification of a large number of *in vivo* phosphorylation sites from complex samples [249,250]. These screens have proven a successful method for the identification of PLK1, Aurora B and CDK1 substrates [75,235,251-253]. The use of quantitative MS-based methods to monitor changes in phosphorylation *in vivo* provides an interesting tool to study the role of MPS1 in mitosis. To accomplish this, we used quantitative phosphoproteomics in multiple experimental set-ups to identify phospho-residues regulated by MPS1. In one approach, we used loss-of-function to find down-regulated phosphorylations after MPS1 inhibition. We compared the phosphoproteome of mitotic cells with full MPS1 kinase activity to that of cells treated with two small molecule MPS1 inhibitors. To maximize our chances of identifying relevant substrates, we analyzed both whole-cell phosphoproteomes as well as chromatin-enriched fractions. In a second approach, we used gain-of-function to find upregulated phosphorylations after artificial activation of MPS1. To this end, we investigated the chromatin phosphoproteome of cells in which MPS1 activity was artificially maintained at a high level on bioriented chromosomes to that of cells in which MPS1 was naturally removed from such chromosomes.

Results

Experimental strategies and methods to compare phosphoproteomes of mitotic cells with or without MPS1 kinase activity

Experimental strategies

To investigate the MPS1-dependent phosphoproteome of human mitotic cells, we employed two different strategies: Selective inhibition of MPS1 kinase activity by small molecules in conditions where MPS1 is normally maximally active (see chapters 2, [90,91,132,133,201]), and maintenance of MPS1 activity by artificial tethering of MPS1 to kinetochores in conditions where MPS1 is normally inactivated (see chapter 3 [142,146,149,191,192]).

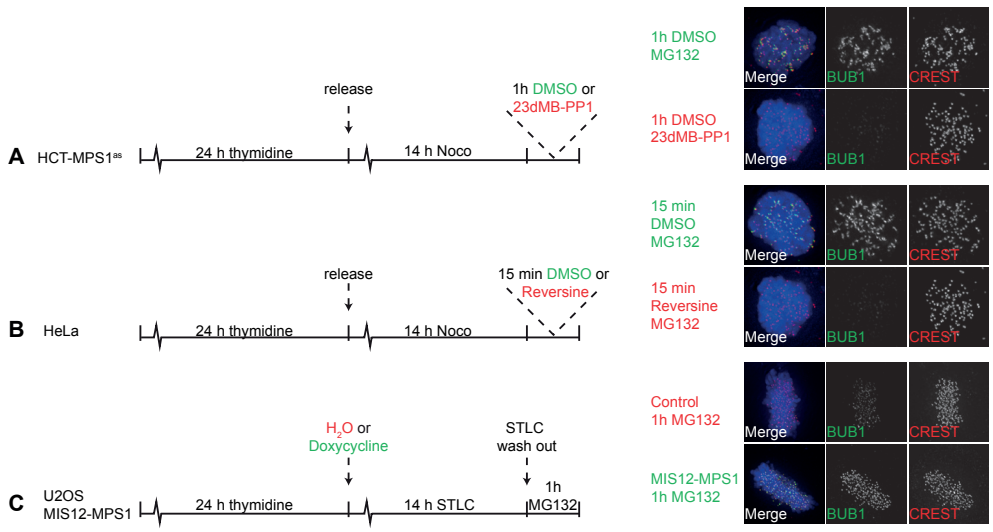

Figure 1 Experimental strategies to study MPS1 phosphoproteome in mitotic cells.

Schematic of the design of the three independent methods employed (left panels). In all strategies, cells were synchronized in S phase by a single, 24 hour thymidine block, followed by a release into medium containing nocodazole **(A, B)** or STLC **(C)** to activate the SAC and synchronize cells in mitosis. 14 hours after release, mitotic cells were harvested and treated either for one hour **(A)** or 15 minutes **(B)** with DMSO (indicated in green) or small molecule MPS1 inhibitors (indicated in red) in combination with MG132. U2OS-MIS12-MPS1 cells were treated with either H_2O (indicated in red) or doxycycline (indicated in green) upon release into STLC containing medium **(C)** after 14 hours they were additionally released from the STLC block into medium containing solely MG132 before being harvested after 1 hour. **(A-C** right panels) Immunolocalization of BUB1 and centromeres (CREST) in cells treated with nocodazole, MG132 and indicated inhibitors **(A, B)**, or released from STLC into MG132 for 1 hour **(C)**, Representative images are shown. Color coding: green: MPS1 active, red: MPS1 inactive.

Selective inhibition of MPS1 was achieved by two independent methods. In the first, we created cell lines in which MPS1 kinase activity can be specifically and reversibly inhibited. For this, we engineered the ATP-binding pocket of MPS1 to create a kinase with unique preference for bulky ATP-like small molecules, and stably replaced endogenous MPS1 of HCT116 cells with this analog sensitive (as) mutant using constitutive shRNA reconstitution (see chapter 2). MPS1^{as} was fully inhibited within 5 minutes after addition of the bulky PP1 analog 23dMB-PP1 to mitotic HCT-MPS1^{as} cells (Chapter 2, Figure 2.1C). In the second method, we used the recently described ATP-competitive MPS1 inhibitor Reversine (Rev)

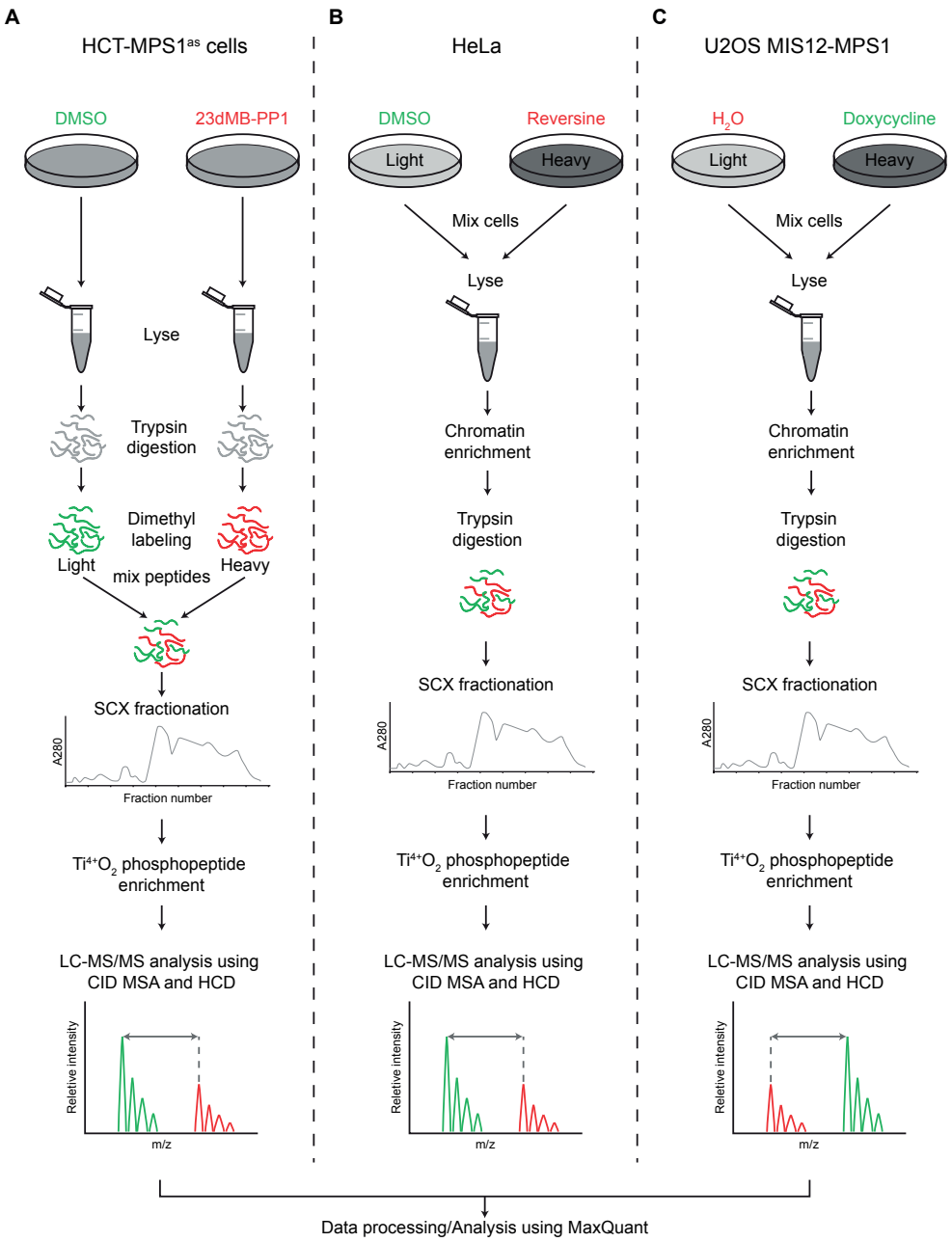

Figure 2. Overview of the experimental workflow

The phosphoproteome of the three independent experiments were probed in duplicate. **(A)** In the 'Forward' experiment (which is displayed here) cells are lysed and proteins are digested using trypsin, control (DMSO, displayed in green) peptides were labeled with light dimethyl labels and peptides from MPS1-inhibited cells (23dMB-PP1, displayed in red) with heavy dimethyl labels. In the 'Reverse' experiment labels were swapped. Subsequently, differently labeled peptides were mixed in a 1:1 ratio, the mixture was subjected to SCX fractionation, and relevant SCX fractions were subjected to titanium (IV) ($Ti^{4+}O_2$) phosphopeptide enrichment then analyzed by liquid chromatography-mass

spectrometry/mass spectrometry (LC-MS/MS) using collision-induced dissociation-multistage activation (CID-MSA) or higher-energy collisional dissociation (HCD). **(B, C)** In the 'Forward' experiments (which are displayed here) cells were grown in the presence of light ((**B)** control: DMSO, displayed in green or **(C)** control: H_2O, displayed in red) or heavy isotope-labeled arginine and lysine ((**B)** reversine, displayed in red or **(C)** MIS12-MPS1 displayed in green). After lysis, chromatin enrichment and tryptic digestion, peptides were fractionated by SCX and relevant SCX fractions were subjected to titanium (IV) ($Ti^{4+}O_2$) phosphopeptide enrichment. Finally, all fractions were analyzed by LC-MS/MS using CID-MSA or HCD. Color coding: green: MPS1 active, red: MPS1 inactive

[133]. In both strategies, cells were synchronized in S phase by a single, 24 hour thymidine block, followed by release into nocodazole-containing medium. As a result, cells cycling through S-phase into mitosis are blocked there due to persistent activation of the SAC. 14 hours after release, mitotic cells were harvested and treated either for one hour (HCT-MPS1^{as} cells) or 15 minutes (HeLa cells) with DMSO (control (green)) or MPS1 inhibitors (red). Treatments were always combined with addition of the proteasome inhibitor MG132 to prevent premature mitotic exit due to MPS1 inactivation (Figure 1A, B). Following these treatments, cells were processed as indicated in Figure 2A and B. In the schemes depicted in Figure 2, phosphorylation events that depend on the kinase activity of MPS1 are expected to have a reduced H/L ratio (H=inhibition, L=control), but both forward (H/L) and reverse (L/H) labelings were done in all cases.

In a parallel approach, conditional activation of MPS1 was achieved using a cell line with inducible expression of the kinetochore-tethered MIS12-MPS1$^{\Delta 200}$ fusion protein (introduced in Chapter 3 and [142,146,149]). In this approach, cells were synchronized in S phase by a single, 24h thymidine block, followed by release into STLC-containing medium complemented with H_2O (control) or doxycycline to induce expression of MIS12-MPS1. STLC is and Eg5 inhibitor that causes monopolar mitotic spindles with many unattached kinetochores [153,254]. Like nocodazole, STLC thus causes synchronization in mitosis by persistent SAC activation. 14 hours after release from thymidine, mitotic cells were harvested and allowed to restore spindle bipolarity and chromosome biorientation for 1 hour by removing STLC (Figure 1C). Again, MG132 was always added in these treatments to prevent premature mitotic exit due to MPS1 inactivation. One hour after washout of STLC, cells were processed as indicated in Figure 2C.

Methods of quantification

We relied on two different approaches for quantitation of the changes of phosphopeptide abundance by MS. Stable isotope labeling by amino acids in cell culture (SILAC) [76,255] was applied to both HeLa and U2OS cells. To this end cells were metabolically labeled by growing them in medium containing either normal (referred to as 'light') arginine and lysine (Arg0/Lys0) or the heavy isotopic variants (referred to as 'heavy') of [$^{13}C_6$,$^{15}N_4$] arginine and [$^{13}C_6$,$^{15}N_2$] lysine (Arg10/Lys8) (Figure 2B, C). Since adaptation to SILAC medium posed limitations to the proliferation rate of HCT-MPS1^{as} cells (not shown), we employed chemical labeling of peptides by the dimethylation of primary amine groups by light (normal isotope: ^{12}C,^{1}H) or heavy (stable isotope: ^{13}C, ^{2}H) isotopologues of formaldehyde [90,256] (Figure 2A). Each experiment was performed in duplicate, in which labels are swapped between treatments, designated as forward and reverse.

Approaches for cellular fractionation and phospho-peptide enrichment

Substrates of MPS1 are likely not very abundant and are likely concentrated on

kinetochores. To maximize identification of regulated phospho-sites, we chose to enrich the cellular sample of the HeLa and U2OS cells for kinetochore-containing chromatin using a chromatin enrichment step in which the cytoplasmic fraction is separated from chromatin fraction through the use of isotonic buffers and sequential purification steps by centrifugation (Fig. 5.2B, C). Validation of our reasons for using the procedure is shown in supplemental Table 1, which indicates significant coverage of outer-kinetochore proteins after chromatin enrichment. In addition, chromatographic fractionation of the tryptic digest of the proteome by strong cation exchange (SCX) provided separation of phosphorylated peptides from non-phosphorylated ones in all experimental conditions. In all experiments SCX fractionation was followed by Titanium Dioxide enrichment for phospho-peptides prior to measurement.

The MPS1-dependent phosphoproteome

After identification and quantification using MaxQuant software version 1.3.0.5 and the andromeda search engine [91,257], we processed all results according to the following acceptance criteria. (1) A false discovery rate (FDR) of less than 1% at the peptide level, (2) a protein FDR of less then 1% (3) and a site FDR of less then 1%. (4) Peptide length was restricted to at least 7. Combining forward and reverse experiments for each individual approach, we identified 8577 unique phosphosites in the experiments with the HCT-MPS1^{as} cells, 5677 unique phosphosites in the experiments with the HeLa cells, and 12726 unique phosphosites in experiments with the U2OS cells (Table 1). When imposing an arbitrary cut-off for regulated phosphosites at a H/L or L/H ratio of ≥ 1.5 fold (up or down) compared to control treatment, and selecting for proteins with known functions in mitosis, the list of candidate MPS1 target sites identified in any of the three strategies was reduced to 154 (Supplemental Table 2). Of these, 45 were found in the HCT-MPS1^{as} experiments, and 66 and 43 were found in the HeLa and U2OS-MIS12-MPS1 experiments, respectively. The top 27 of regulated phospho-peptides belonging to 21 proteins, based on fold change, is listed in Table 2. These include three previously reported MPS1 autophosphorylation sites that appear in all three experimental set-ups, which validated our approaches [118-120,131,147,148]. The list further includes the kinesin-8 motor protein KIF18A which is involved in chromosome congression [249,250,258], the APC/C subunit CDC27, a centromere-binding protein MIS18BP1, the outer-kinetochore protein CENP-F, and a kinetochore-localized dynein receptor, NDE1 [95].

Table 1. Numbers of identified phosphosites from all experiments with the three independent approaches. Percentage overlap indicates overlap of identified phosphosites between forward and reverse experiments.

	HCT-MPS1^{as}	HeLa	MIS12-MPS1
	phospho-sites	phospho-sites	phospho-sites
Forward	6482	4817	11354
Reverse	7470	5309	9126
Total	8577	5677	12726
Overlap	63%	78%	61%

Refinement of list of candidates using kinase motif analysis

It was recently shown by in vitro studies that the preferred motif for phosphorylation by MPS1 is specified by a tendency for phosphorylation of threonines, preceded by acidic amino acids in position -2 and/or -3 relative to the threonine [238,239] (Figure 3A). A slight but significant preference for hydrophobic amino acids at position +3 position was also observed. This motif ([ED]-[ED]-x-T-x-x-[IVL]) resembles the sequence surrounding the MPS1 targets in KNL1

Table 2. Top most regulated sites. Forward and Reverse experiments are indicated by F and R respectively. The phosphorylated residue is in bold and underlined.

Experimental set up	Protein name	Position	Modified sequence	Corrected Ratio
HeLa R	TAOK1	417	TRA**S**DPQSPPQVSR	29.50
HeLa R	SASS6	510	SGI**S**PNLNVVDGR	25.16
HeLa F	ERCC6L	1069	NDI**S**PPGR	24.90
HeLa F	CDC27	220	LNLES**S**NSK	20.15
HCT-MPS1^{as} F	NEK4	661	RL**S**SDCSVTQER	10.01
HCT-MPS1^{as} F	SF1	227	SITNT**T**VCTK	9.75
U2OS M12-MPS1 F	MAP1B	1853	DLS**T**PGLEK	9.47
HCT-MPS1^{as} R	MPS1	33	NEDL**T**DELSLNK	9.22
HeLa R	MDC1	1814	**S**LATM(ox)DSPPHQK	9.11
HeLa F	LSM11	15	SAGAG**S**PARPPSPR	9.10
U2OS M12-MPS1 R	KIF18A	684	**S**PPSQSVQLNDSLSK	9.08
HeLa R	MPS1	33	NEDL**T**DELSLNK	8.06
HeLa F	MIS18BP1	1087	LVETDFS**T**PTPR	7.79
U2OS M12-MPS1 F	RANBP2	21	YIASVQGSTP**S**PR	7.39
HCT-MPS1^{as} F	TICRR	820	**S**PLLSVPFLSSAR	7.30
HeLa R	ANLN	233	EICLQ**S**QSK	7.10
HCT-MPS1^{as} R	RIF1	2172	CVW**S**PLASPSTSILK	7.01
U2OS M12-MPS1 F	MPS1	321	DLVVPGSKPSGND**S**CELR	6.68
HCT-MPS1^{as} F	MPS1	33	NEDL**T**DELSLNK	6.37
U2OS M12-MPS1 R	MPS1	321	DLVVPGSKPSGND**S**CELR	6.32
HeLa R	MPS1	363	NKTE**S**SLLAK	6.29
HeLa F	CHAMP1	184	PASVS**S**PEPPK	6.21
HeLa R	KIF4A	1167	LEDPTEVTPGLSFFNPVCATPN**S**K	6.00
HeLa F	CHAF1B	473	TLQPS**S**QNTK	5.36
U2OS MIS12-MPS1	CENPF	1748	LQLQGLDLS**S**RSLLGIDTEDAIQGR	4.96
HCT-MPS1^{as} F	NDE1	243	GLDDSTGG**T**PLTPAAR	4.78
HeLa F	MPS1	363	NKTE**S**SLLAK	4.71

[67,118-120], and one site in Borealin [164], as well as several auto-phosphorylation sites [131,147,148]. This so-called MPS1 consensus phosphorylation motif thus provides a tool to identify potential direct MPS1 substrates in the list of regulated phospho-peptides (Supplemental Table 2). In order to gain insight if the significantly regulated phosphosites are indeed enriched for sites phosphorylated by MPS1, we used the freeware program IceLogo to reveal any statistically significant over- or underrepresentation in the frequency with which a particular amino acid is present at a certain position [259]. Surprisingly, we identified a kinase consensus motif which resembles the CDK1 consensus motif, which is quite distinct from the MPS1 consensus motif [260,261] (Figure 3B) Indeed, a large amount of the significantly regulated phosphopeptides displayed in Table 2 contained proline-directed phosphosites, a hallmark of CDK1 substrates. We are uncertain about what this means, but one option is that MPS1 regulates kinetochore-localized CDK1 activity, and that the altered phosphorylation of proline-directed sites upon MPS1 inhibition/activation represent indirect effects of this regulation. In support of this, our lab has recently found that Cyclin B1 levels at kinetochore depend on MPS1 activity (not shown).

Computational and experimental attempts to identify direct MPS1-dependent phosphorylation events

Mitotic events are regulated by complex signaling networks involving multiple kinases and phosphatases. Consequently, alterations in MPS1 activity affect the activity and localization

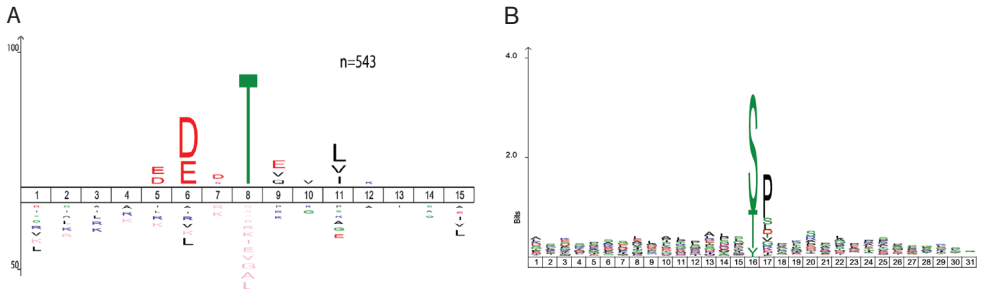

Figure 3. Kinase motif analysis

(A) IceLogo representation of the consensus motif for phosphorylation by MPS1, as defined by[238]. The graph displays statistically over- (top) and under- (bottom) represented amino acids relative to the average. MPS1 has a preference for phosphorylating threonines (considered as position 0) preceded by acidic amino acids at position -2 and/or -3 and followed by hydrophobic amino acids at the +3 position. Picture adapted from [238] **(B)** The IceLogo motif of the sequences surrounding the phospho-residues in the list of 154 regulated peptides from our three screens. Statistically over- (top) represented amino acids are displayed, as in A. A high tendency for serines (considered as position 0) is detected with a strong preference for proline in position +1.

of other mitotic regulators. As such, the pool of regulated phosphorylation sites is also expected to include indirect secondary targets of MPS1, the CDK1 sites being a possible case-in-point. Only 5.5% of the regulated sites that we identified conformed to the 'flexible' previously described MPS1 motif [238,239], a motif which closely resembles the PLK1 consensus motif (D/E-x-pS/T) [234,235].

As a first attempt to mine the list of 154 total sites for potential direct MPS1 targets, we applied 2 additional selection criteria. First, a phosphosite could not be located in a CDK1 motif (i.e. pS/T-P). Second, the phosphosite must be located within a flexible MPS1 motif which dictates

Table 3. Potential MPS1-regulated sites, as determined by selection criteria described in main text. Forward and Reverse experiments are indicated by F and R respectively. The phosphorylated residue is in bold and underlined.

Experimental set up	Protein name	Position	Modified sequence	Corrected Ratio
HeLa F	CDC27	220	LNLES**S**NSK	20.15
HCT-MPS1^{as} R	MPS1	33	NEDL**T**DELSLNK	9.22
HeLa R	MPS1	33	NEDL**T**DELSLNK	8.06
HCT-MPS1^{as} F	MPS1	33	NEDL**T**DELSLNK	6.37
HeLa R	MPS1	363	NKTES**S**LLAK	6.29
U2OS M12-MPS1 F	CENP-F	1748	LQLQGLDL**S**SRSLLGIDTEDAIQGR	4.96
HeLa F	MPS1	363	NKTES**S**LLAK	4.71
HeLa R	RACGAP1	274	TETD**S**VGTPQSNGGM(ox)R	4.69
HCT-MPS1^{as} F	MPS1	33	NEDL**T**DELSLNK	4.17
U2OS M12-MPS1 F	SPC24	129/130	EVDED**TT**VTIPSAVYVAQLYHQVS	2.64
U2OS M12-MPS1 F	BUB1	307	LHQVVET**S**HEDLPASQER	2.09
U2OS M12-MPS1 R	SKA3	34	ALDGEE**S**DFEDYPMR	1.75
U2OS M12-MPS1 R	BUB1	307	LHQVVET**S**HEDLPASQER	1.71
U2OS M12-MPS1 R	BUB1	601	TLAPSPKSPGDF**T**SAAQLASTPFHK	1.70
HCT-MPS1^{as} R	NASP	490	ENDK**T**EEM(ox)PNDSVLENK	1.65
HeLa F	MCM6	762	EIESEID**S**EEELINK	1.55
HeLa F	MAD1L1	428	AILGSYDSELTPAEY**S**PQLTR	3.17
U2OS M12-MPS1 R	MAD1L1	428	AILGSYDSELTPAEY**S**PQLTR	1.57

only the acidic amino acids in position -2 and/or -3 and allows phosphorylation of serine (i.e. D/E-D/E-x-pS/T). Applying these two criteria, we find again the MPS1 autophosphorylation sites [131,147,148], as well as CDC27 and CENP-F. Additional interesting candidates that appear after this analysis further include kinetochore proteins, like BUB1, SPC24 and SKA3, which are known to be involved in SAC signaling and kinetochore-microtubule attachment (Table 3).

In a second attempt to distinguish direct from indirect substrates, various putative MPS1 substrates were tested as substrate for recombinant MPS1 in an in *in vitro* kinase assay. We selected the SAC protein kinase BUB1 and the NDC80 complex member SPC24 for further analysis. The SAC protein MAD1 was also included because although the identified pS428 contains a proline at +1, it is also within a D-x-S-x-x-L MPS1 consensus motif, and because MAD1 is phosphorylated by MPS1 in budding yeast [137]. All three candidate substrates, BUB1 (data not shown), SPC24 (Figure 4A) and MAD1 (Figure 4B), were efficiently phosphorylated by kinase active (WT) but not kinase-dead (KD) MPS1 *in vitro*. Importantly, subsequent analysis of the *in vitro* phosphorylated proteins by mass spectrometry confirmed phosphorylation of the same sites that were found regulated in cells in our screens (Figure 4C).

Discussion

Towards identification of novel MPS1 substrates

Although the three independent experiments are collectively presented, they are the result of sequential experiments, in which each successive experiment was subjected to modifications. Alterations in the experimental set up were based on the results provided from prior experiments. At the onset of this study the development of the HCT-MPS1^{as} cell lines (Chapter 2) allowed for the first time selective, penetrant inhibition of MPS1 and provided us with a tool to investigate the MPS1 phosphoproteome. Results from these initial experiments indicated that inhibition of MPS1 for one-hour results in the identification of a large amount of indirect secondary downstream targets, in particular CDK1 targeted substrates (50%

A

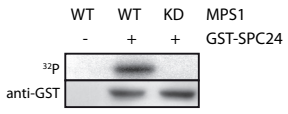

B

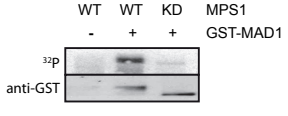

C

Protein	Position	Modified sequence	*In vivo*	*In vitro*
MAD1	323	LDQ**T**MGLSIR	-	yes
MAD1	428	AILGSYDSELTPAY**S**PQLTR	yes	yes
MAD1	551	VLHMSLNPT**S**VAR	-	yes
SPC24	129	EVDED**T**TTIPSAVYAQLYHQVS	yes	yes
SPC24	130	EVDEDT**T**TIPSAVYAQLYHQVS	yes	yes
BUB1	34	ALDGEE**S**DFEDYPMR	yes	-
BUB1	158/159	**TS**EPIHNVQVINQMITSK	-	yes
BUB1	247	GESEF**S**FEELR	-	yes
BUB1	307	LHQVVET**S**HEDLPASQER	yes	-
BUB1	331	MGPSVG**S**QQELR	-	yes
BUB1	563	SVSRLP**S**K	-	yes
BUB1	579	KEEVPHAEEFLDDS**T**VWGIR	yes	yes

Figure 4. Experimental validation of direct MPS1 substrates

In vitro kinase assays using recombinant MPS1. GST-tagged SPC24 **(A)** and MAD1 **(B)** were used as substrates and analyzed for ^{32}P incorporation (top panels) and protein levels (bottom panels). The phosphorylation sites identified by mass spectrometry on *in vitro* phosphorylated GST-SPC24, -MAD1 and -BUB1 are shown in **(C).** Identified phosphorylation sites are underlined and marked in bold.

of total regulated sites). This prompted us to significantly decrease the time of inhibition, and thereby possibly secondary effects of MPS1 inhibition. With the development of small molecule MPS1 inhibitors [90,132,133], we were able to inhibit endogenous MPS1, circumventing possible side effects of overexpression of the MPS1 analog sensitive mutants. In addition, given the relatively low abundance of proteins associated with the kinetochore and SAC in the original screen, we opted for an enrichment strategy to maximize the coverage of relevant proteins. A recent search for PLK1 substrates was aided by the isolation of the mitotic spindle [235]. In line with this, we employed an additional chromatin enrichment step after cell lysis in order to increase kinetochore and SAC associated proteins (supplemental Table 1). Unfortunately, decreasing the duration of inhibition and enrichment of chromatin did not result in less indirect secondary targets, as the amount of CDK1-regulated sites remained relatively high (48% of total regulated sites). In a final attempt to decrease secondary off target phosphorylations, we employed a gain-of-function strategy. In this strategy, cells were allowed to reach metaphase, thereby eliminating most of the phosphorylation events involved in SAC signaling and error-correction. Under these conditions, we artificially maintained MPS1 signaling at kinetochores, using the previously introduced fusion protein of MIS12-MPS1 (Chapter 3). Unexpectedly this approach resulted in increases in CDK1 regulated sites (64%), possibly representing gain-of-function of CDK1 at metaphase kinetochores. Nevertheless, a small increase in MPS1-regulated sites (containing the flexible MPS1 motif) could be observed and several of these have previously reported to be involved in the SAC and kinetochore - microtubule attachment.

Putative MPS1 substrates at mitotic kinetochores

Our efforts to identify novel MPS1 substrates led to the identification of multiple putative substrates, which contain phosphosites regulated *in vivo* upon MPS1 inhibition, which contain a flexible MPS1 motif and which could be confirmed by *in vitro* phosphorylation.

SPC24, a member of the NDC80 complex, is important for kinetochore microtubule attachment [26,262], and phosphorylation of SPC24 might regulate kinetochore microtubule attachments. Future investigations to elucidate if SPC24 phosphorylation is required for kinetochore microtubule attachment will require functional studies with RNAi complementation of SPC24. Interestingly, phosphorylation of Ndc80 by Mps1 in budding yeast modulates SAC activity [263]. While we suspect that NDC80 phosphorylation by MPS1 is not conserved in humans, it is possible that SPC24 phosphorylation might instead serve as MPS1's effector for the SAC within the NDC80 complex.

The protein kinase BUB1 was found to be phosphorylated by MPS1 both *in vivo* and *in vitro*. BUB1 is essential for both SAC activity as well as chromosome alignment ([77,78], and chapter 3). Recently it was shown that MPS1 controls BUB1 kinetochore localization by phosphorylation of conserved MELT-like motifs within KNL1 that bind BUB1 [118,119,192]. It is possible that MPS1 additionally regulates BUB1 activity by direct phosphorylation, especially since some of the *in vitro* identified sites reside within functional motifs/domains. Mutational analysis of some of the BUB1 phosphorylation sites did not, however, uncover any defects in SAC activity or chromosome alignment, but these analyses may have been hampered by insufficient BUB1 depletion (not shown). In addition to SPC24 and BUB1, we identified multiple MAD1 phosphorylation sites which depend on MPS1 activity. MAD1 is also essential for the SAC [137,203,264], and chapter 3), and has previously been reported to be phosphorylated by MPS1 [137] in yeast. Like with the BUB1 mutants, however, MAD1 phosphorylation site mutants were still proficient in SAC signaling (not shown), but again like BUB1, analysis of

MAD1 phosphomutants is hampered by inefficient depletion by RNAi. Investigations into a role of the uncovered phosphorylations in BUB1 and/or MAD1 function may be aided by the sensitized SAC assay described in chapter 4. Lastly, several interesting candidates that are essential for correct execution of mitosis (CENP-F, SKA-3 and CDC27) remain to be investigated.

Lessons learned and future directions

Our search for novel MPS1 targets through the use of quantitative phosphoproteomics was limited by two major issues: A relatively high number of indirect secondary regulated sites, and low coverage of kinetochore and SAC associated proteins. MPS1 is known to regulate the localization of multiple kinases involved in SAC signaling and kinetochore-microtubule attachment. For instance, inhibition of MPS1 causes reduced kinetochore localization of BUB1, PLK1 and Aurora B [91,118-120,151,153]. MPS1 also impacts on MAD1 kinetochore localization ([76] Chapter 3) which is the kinetochore recruiter of Cyclin B-CDK1 complexes (GJLPK & Adrian Saurin, unpublished data). Long term MPS1 inhibition (1 hour) therefore can be expected to have an effect on global phosphorylation events at kinetochores. Conversely, maintaining MPS1 activity at bioriented kinetochores can have similar, opposite effects on the phosphoproteome. Since short-term inhibition (15 minutes) of MPS1 did not significantly alter the appearance of secondary regulated sites, the question remains what the appropriate approach is. The recent development of phospho-specific antibodies can be used to better determine the duration of inhibitor addition. Monitoring direct MPS1 phosphorylation events (MPS1-pT676 and KNL1-pT875 [120,131]) versus phosphorylation events of downstream targets of MPS1 (e.g. Histone 2A-pT120 (BUB1) [191,192], DSN1-pS100 and KNL1-pS24 (Aurora B) [14], BUBR1-pT680 (PLK1) [41] and CENPT-pS47 (CDK1) [27]) can help to determine the appropriate time of inhibition at which direct MPS1 substrates are dephosphorylated but more downstream secondary substrates are not affected.

The coverage of kinetochore and SAC associated proteins was an additional limiting factor in our search for novel MPS1 substrates. Although our efforts to increase kinetochore and SAC associated proteins by enriching for chromatin was successful (see supplemental table 1), this did not lead to additional identifications of MPS1-regulated phosphosites. Either MPS1 regulates both the SAC and kinetochore-microtubule attachment by a truly small number of substrates, or we failed to reach sufficient coverage to identify the phospopeptides which are regulated by MPS1. Since both the previously reported Borealin and KNL1 phosphosites [118-120,164] were not identified in any of our screens, we suspect that the latter holds true. We propose a more directed approach, using selective enrichment of protein complexes in combination with quantitative phosphoproteomics. The recent identification of KNL1 as a MPS1 substrate was aided by selective enrichment of the KMN network. In addition to the KMN network, the APC/C, MCC, the RZZ complex and SKA complex might also be subjected to such an approach.

Materials and Methods

Tissue Culture

HeLa cells were grown in DMEM supplemented with 8% FBS, 50 µg/ml penicillin/streptomycin, and 2 mM L-glutamine, U2OS-MIS12$^{\Delta 200\ 146}$, were cultured in the same medium but containing 8% tetracycline-approved FBS (Clontech) supplemented with zeocin. HCT-MPS1$^{as\ 151}$ were cultured in the same medium but containing 8% tetracycline-approved FBS

(Clontech) supplemented doxycycline (1 μg/ml).
For SILAC experiments, HeLa and U2OS cells were grown in arginine- and lysine-free DMEM with 8% dialyzed FBS (PAA laboratories) supplemented with 50 μg/ml penicillin/streptomycin, and 2 mM L-glutamine and either [$^{13}C_6$,$^{15}N_2$]lysine (100 mg/liter) or [$^{13}C_6$,$^{15}N_4$] arginine (100 mg/liter) (Sigma.) (heavy) or identical concentrations of isotopically normal lysine and arginine (light) for at least six cell doublings. HCT-MPS1^{as} [151] were cultured in the same medium but containing 8% tetracycline-approved FBS (Clontech) supplemented doxycycline (1 μg/ml)

Immunofluorescence, antibodies and reagents
Cells were plated on 12-mm coverslips and treated as described in figure legends, cells were pre-extracted with PEM/TX (100 mM PIPES [pH 6.8], 1 mM $MgCl^2$, 5 mM EGTA, 0.2% Triton X-100) for 1 min. before a 5 min. fixation in 3.7% formaldehyde in PEM/TX-100. Coverslips were blocked with 3% BSA in PBS for 1 hr., incubated with primary antibody for 16 hr. at 4 C °, washed with PBS/0.1% TX-100 and incubated with secondary antibodies for an additional 1 hr. at room temperature. Coverslips were washed and submerged in PBS containing DAPI and mounted using ProLong Gold antifade (Molecular Probes). Image acquisition and quantification were done as described [146], using a DeltaVision RT system (Applied Precision) with a 1003/1.40 numerical aperture (NA) UPlanSApo objective (Olympus) for acquiring images, ImageJ software for quantification and Photoshop CS5 (Adobe) for image processing.
The following primary antibodies were used for immunofluorescence imaging: CREST (Cortex Biochem, CS1058 1:2000), BUB1 (Bethyl, A300-373A, 1:1000), GST (2622 Cell Signaling) Secondary antibodies were high-crossed goat anti–human Alexa Fluor 647 and goat anti–rabbit and anti–mouse Alexa Fluor 488 and Alexa Fluor 568 (Molecular Probes) for immunofluorescence experiments, Thymidine (2.5 mM), nocodazole (830 nM), MG132 (5 μM), reversine (various doses), doxycycline, G-418 (1 mg/ml) and puromycin (1 μg/ml) were all obtained from Sigma. Zeocin (100 μg/ml) was obtained from Invitrogen 23dMB-PP1 (1mM) (gift from Kevan Shokat).

In vitro recombinant kinase assay
Wild-type GST-MPS1, GST-MAD1, GST-SPC24 were expressed and purified from High-Five insect cells using the Life Technologies Bac-to-Bac system. Recombinant active MPS1 was incubated in kinase buffer (50 mM Tris pH 7.4, 10 mM MgCl2, 0.5 mM DTT, 40 mM ATP) at 30°C for 30 minutes. Phosphorylated residues were identified using mass-spectrometry as described [164]

Sample preparation
Cells were treated as described in Figure 1A, B, and C subsequently cells were harvested and lysed in lysis buffer (50 mM ammonium bicarbonate, 8M urea, 2M thiourea (8M Urea only), 1 tablet/10 ml Complete Mini EDTA-free Protease Inhibitor Cocktail (Roche), 1 tablet/10 ml PhosSTOP Phosphatase Inhibitor Cocktail (Roche)) and subjecting them to ultrasonication. Cell debris was removed by centrifugation at 20,000 x g for 15 min at 4 °C after which the supernatant was transferred to a new reaction tube. Protein concentrations were determined using a Bradford assay (Bio-Rad). For each condition 2 mg of protein was reduced using 2 mM dithiothreitol and incubation for 30 min at 56°C and subsequently alkylated using 4 mM iodoacetamide and incubation for 30 min at room temperature in the dark. Next, the initial

digestion was performed by adding Lys-C (WAKO) at an enzyme/protein ratio of 1:75 and incubation for 4 h at 37 °C. The sample was diluted 4-fold to a final urea concentration of 2 M using 50 mM ammonium bicarbonate buffer. The final digestion was performed by adding Trypsin Gold, Mass Spectrometry Grade (Promega), at an enzyme/protein ratio of 1:100 and incubation overnight at 37°C. Formic acid (FA) was added to a final concentration of 10% after which the peptide mixtures were desalted using Sep-Pak Vac C18 cartridges (3 cc/200 mg, Waters). Subsequently, where required, on-column stable isotope dimethyl labeling was performed. Finally, the eluates corresponding to either the 'Forward' or 'Reverse' experiment were mixed in a 1:1 ratio, dried in vacuo and stored at -20 °C. Label incorporation and mixing accuracy were assessed by LC-MS/MS. SILAC samples were prepared as previously described by [255]

Chromatin enrichment

Harvested mitotic cells were washed twice in PBS before treatment with swelling buffer for 10 min on ice. After addition of complete protease inhibitors (Roche) and 5% NP40 cells were lysed by dounce homogenization and subjected to 15 min centrifugation at 3400 x g at 4 °C. Resulting supernatant is collected and stored and pellet is washed with ice cold PBS for 10 min before subjecting to centrifugation at 3400 x g at 4 °C. Pellet is resuspended in 4%SDS, 100mM Tris pH 7.6 and 100 mM DTT followed by sonication, and incubation at 95°C for 3 min followed by 5 min centrifugation at 16000 x g at room temperature. Supernatant is subsequently prepared as described before [255,265].

SCX chromatography for peptide fractionation

The mixture of dimethyl labeled peptides with a 1:1 ratio were reconstituted in 10% FA and loaded onto a C18 cartridge (Aqua, Phenomenex) using an Agilent 1100 HPLC system. The flow rate applied was 100 µL/min using 0.05% FA (pH 2.7) as solvent. Peptides were eluted from the C18 cartridge with 80% acetonitrile (ACN) containing 0.05% FA (pH 2.7) onto a Polysulfoethyl A column (200 x 2.1 mm) (PolyLC) for 10 min at the same flow rate. Separation of peptides was performed using a nonlinear 65 min gradient: from 0 to 10 min, 100% solvent A (5 mM KH2PO4, 0.05% FA, 30% ACN, pH 2.7); from 10 min to 15 min, to 26% solvent B (5 mM KH2 PO4, 0.05% FA, 30% ACN, 350 mM KCl, pH 2.7); from 15 min to 40 min, to 35% solvent B; and from 40 to 45 min, to 60% solvent B. At 49 min, the concentration of solvent B was 100%. The column was subsequently washed for 6 min with 100% solvent B and finally equilibrated with 100% solvent A for 9 min. The flow rate applied during the SCX gradient was 300 µL/min. Fractions were collected every minute for 40 min. After combing a few neighbor 'blank' fractions based on the recorded UV graph, a total of 33 fractions were desalted using Sep-Pak Vac C18 cartridges (3 cc/200 mg, Waters). Finally, the eluted peptides were equally divided over two tubes, dried in vacuo and stored at -20 °C for $Ti^{4+}O_2$ phosphopeptide enrichment and protein analysis.

Mass spectrometry

Mass spectrometry analysis was preformed as previously described by [265]. All data sets were analyzed in the same way, using Perseus 1.4.0.17. Data was filtered for contaminants, reverse hits and "only identified by site", followed by Log2 transformation of ratio values and statistical analysis using significance A. Significant outliers were filtered using Gene Onthology for various mitotic and cell cycle related entries. Subsequent data analysis was preformed as previously described by [266]

Supplemental table 1 Kinetochore associated protein coverage (in % of total protein) in proteome and phosphoproteomes of chromatin fractions of HCT-MPS1^{as} and HeLa reversine experiments

Protein	HCT-MPS1^{as} coverage%	HeLa coverage%
NDC80	7.5	25
NUF2	5.4	17.5
SPC24	0	4.9
SPC25	24.9	53.8
MAD1	5.3	15.7
MAD2	7.8	15.6
MPS1	10.3	8.3
BUB1	6.3	17.6
BUBR1	6.3	14.3
BUB3	4.9	30
Borealin	28.6	56.4
MIS12	12.2	16.1

Supplemental Table 2 All regulated sites identified from all three independent phosphoproteome experiments, as determined by selection criteria described in main text

Experimental set-up	Position	Protein names	Modified sequence	Corrected Ratio
HeLa	417	TAOK1	TRA**S**DPQSPPQVSR	29.59
HeLa	510	SASS6	SGI**S**PNLNVVDGR	25.16
HeLa	1069	ERCC6L	NDI**S**PPGR	24.90
HeLa	220	CDC27	LNLES**S**NSK	20.15
HCT-MPS as	661	NEK4	RL**S**SDCSVTQER	10.01
HCT-MPS as	277	SF1	SITNT**T**VCTK	9.75
U2OS MIS12-MPS1	1853	MAP1B	DLS**T**PGLEK	9.47
HCT-MPS as	33	TTK	NEDL**T**DELSLNK	9.22
HeLa	1814	MDC1	**S**LATM(ox)DSPPHQK	9.11
HeLa	15	LSM11	SAGAG**S**PARPPSPR	9.10
U2OS MIS12-MPS1	684	KIF18A	**S**PPSQSVQLNDSLSK	9.08
HeLa	33	TTK	NEDL**T**DELSLNK	8.06
HeLa	1087	MIS18BP1	LVETDFS**T**PTPR	7.79
U2OS MIS12-MPS1	21	RANBP2	YIASVQGSTP**S**PR	7.39
HCT-MPS as	820	TICRR	**S**PLLSVPFLSSAR	7.30
HeLa	233	ANLN	EICLQ**S**QSK	7.10
HCT-MPS as	2172	RIF1	CVW**S**PLASPSTSILK	7.01
U2OS MIS12-MPS1	321	TTK	DLVVPGSKPSGND**S**CELR	6.68
HCT-MPS as	33	TTK	NEDL**T**DELSLNK	6.37
U2OS MIS12-MPS1	321	TTK	DLVVPGSKPSGND**S**CELR	6.32
HeLa	363	TTK	NKTES**S**LLAK	6.29
HeLa	184	CHAMP1	PASVS**S**PEPPK	6.21
HeLa	1167	KIF4A	LEDPTEVTPGLSFFNPVCATPN**S**K	6.00
HeLa	473	CHAF1B	TLQPS**S**QNTK	5.36
U2OS MIS12-MPS1	1748	CENPF	LQLQGLDLS**S**RSLLGIDTEDAIQGR	4.96
HCT-MPS as	243	NDE1	GLDDSTGG**T**PLTPAAR	4.78
HeLa	363	TTK	NKTES**S**LLAK	4.71
HeLa	274	RACGAP	TETD**S**VGTPQSNGGM(ox)R	4.69
HeLa	141	ANLN	LEATAAS**S**VK	4.29
HeLa	759	MAP1S	AVPMAPAPA**S**PGSSNDSSAR	4.28
HCT-MPS as	37	TTK	NEDLTDEL**S**LNK	4.17
U2OS MIS12-MPS1	12	SMC5	TS**T**P**S**PQPSKR	3.99
U2OS MIS12-MPS1	421	DYNC1LI1	SVSSNVASV**S**PIPAGSK	3.80
HCT-MPS as	806	DLGAP5	SLTTECHLLD**S**PGLNCSNPFTQLER	3.74
HCT-MPS as	812	DLGAP5	SLTTECHLLDSPGLNC**S**NPFTQLER	3.74
HeLa	1016	DICER1	ALPLS**S**AEK	3.59
U2OS MIS12-MPS1	288	GSG2	LVVGNGPEGPGLS**ST**GKR	3.56
U2OS MIS12-MPS1	656	KIF23	AG**S**QLGPGYQHHAQPK	3.40
U2OS MIS12-MPS1	38	STMN1	SKESVPEFPL**S**PPK	3.27
HCT-MPS as	1588	RANBP2	FG**T**SETSKAPK	3.25
HCT-MPS as	428	MAD1L1	AILGSYDSELTPAEY**S**PQLTR	3.17
HCT-MPS as	140	KIF13A	ISLEQNE**S**QTFK	3.15
HCT-MPS as	142	KIF13A	ISLEQNE**S**QTFK	3.15
HCT-MPS as	816	CKAP5	MQGQ**S**PPAPTR	3.13
HCT-MPS as	595	CDK11	AY**T**PVVVTLWYR	3.13
HCT-MPS as	75	CDCA5	VAHAVEVPAVQ**S**PR	3.03
U2OS MIS12-MPS1	1579	RIF1	SNE**S**VDIQDQEEK	3.03
HCT-MPS as	976	ARHGEF2	QELG**S**PEER	2.98
HCT-MPS as	263	INCENP	IAQV**S**PGPRD**S**PAFPD**S**PWRER	2.93
HCT-MPS as	269	INCENP	IAQV**S**PGPRD**S**PAFPD**S**PWRER	2.93
HCT-MPS as	275	INCENP	IAQV**S**PGPRD**S**PAFPD**S**PWRER	2.93
HeLa	684	KIF18A	**S**PPSQSVQLNDSLSK	2.92
U2OS MIS12-MPS1	1042	MIS18BP1	TPQCQHV**S**PGMLG**S**INR	2.87
U2OS MIS12-MPS1	32	PBK	SVLCS**T**PTINIPA**S**PFMQK	2.75
U2OS MIS12-MPS1	656	KIF23	AG**S**QLGPGYQHHAQPK	2.75
HeLa	368	RFC1	KE**S**V**S**PEDSEK	2.71
HCT-MPS as	428	CEP55	**S**P**T**AALNE**S**LVECPK	2.71
U2OS MIS12-MPS1	129	SPC24	EVDED**T**TVTIPSAVYVAQLYHQVSK	2.64
U2OS MIS12-MPS1	130	SPC24	EVDEDT**T**VTIPSAVYVAQLYHQVSK	2.64
HCT-MPS as	1859	NUMA1	ATS**S**TQSLAR	2.63
HCT-MPS as	338	NUSAP1	TITGNSAAVI**T**PFK	2.63
HeLa	48	SLAIN2	SGAVQGAGSLGPG**S**PVR	2.61
HeLa	1883	ZNF318	SLLNPQD**T**PVK	2.32
HeLa	351	CSNK1E	SAAEPVAS**T**PASR	2.29
HeLa	822	HAUS6	Q**T**TPESDFNLQALR	2.23
HeLa	823	HAUS6	Q**T**TPESDFNLQALR	2.23
U2OS MIS12-MPS1	1809	SON	SAA**S**PVVSSM(ox)PER	2.22
HeLa	3426	ASPM	NS**S**ISIPFIPETPVR	2.18

Experimental set-up	Position	Protein names	Modified sequence	Corrected Ratio
U2OS MIS12-MPS1	146	GTSE1	LLA**S**SPALPSSGAQAR	2.18
HCT-MPS as	52	LIN52	SPI**TS**SPPK	2.17
HCT-MPS as	53	LIN52	SPI**TS**SPPK	2.17
HeLa	527	KIF1B	EDGGTLGVF**S**PK	2.17
U2OS MIS12-MPS1	655	BUB1	DGKF**S**PIQEK**S**PK	2.17
HeLa	39	SMC4	**T**ESPATAAETASEELDNR	2.16
HeLa	417	HDAC1	ISIC**S**SDK	2.12
U2OS MIS12-MPS1	510	TTK	YVLGQLVGLN**S**PNSILK	2.12
U2OS MIS12-MPS1	1069	CLASP1	SR**S**DIDVNAAASAK	2.12
HeLa	220	EZH2	LPNNS**S**RP**S**TPTINVLESK	2.10
HeLa	661	RANBP2	IESFG**S**PK	2.10
U2OS MIS12-MPS1	277	BUB1	LHQVVET**S**HEDLPASQER	2.09
HeLa	1853	SKA3	**S**PQLSDFGLER	2.06
HCT-MPS as	33	HJURP	L**S**EPQGSGR	2.05
U2OS MIS12-MPS1	1814	ANLN	TQ**S**LPVTEK	2.04
HeLa	16	MKI67	ELFQTPC**T**DNPTTDEK	2.03
HeLa	618	KIF20A	LQGQV**S**AK	2.03
U2OS MIS12-MPS1	1269	CDCA3	TSSGDPP**S**PLVK	1.99
HCT-MPS as	1088	CDK1	VY**T**HEVVTLWYR	1.99
HeLa	21	PDS5B	TP**S**PSQPK	1.98
U2OS MIS12-MPS1	820	PSRC1	LAAQLEQCALQDRE**S**AGEGLGPR	1.96
U2OS MIS12-MPS1	233	NCAPH	VFDLQFS**T**DSPR	1.95
HeLa	2172	PAK4	**S**LVGTPYWMAPELISR	1.95
HCT-MPS as	321	AURKB	**S**NVQPTAAPGQK	1.92
U2OS MIS12-MPS1	33	BUB1	VQP**S**PTVHTK	1.92
HeLa	321	HCFC1	**S**PAFVQLAPLSSK	1.90
U2OS MIS12-MPS1	363	TTK	HTTFEQPVFSVSKQ**S**PPISTSK	1.90
HeLa	185	ESCO2	LPSANQG**S**PFK	1.88
HeLa	221	INCENP	**S**KTPS**S**PCPASK	1.83
U2OS MIS12-MPS1	915	BUB1	DGKF**S**PIQEK**S**PK	1.82
HeLa	1749	CEP55	SP**T**AALNESLVECPK	1.82
HeLa	243	TOP2B	SQDFGNLFSFP**S**YSQK	1.80
HeLa	363	TOP2B	**S**QDFGNLFSFPSYSQK	1.76
HCT-MPS as	274	CYTSA	KGSSGNA**S**EVSVACLTER	1.76
HeLa	141	NOLC1	**S**LGTQPPK	1.75
HCT-MPS as	759	KIF1C	YPPYT**T**PPR	1.75
U2OS MIS12-MPS1	37	SKA3	ALDGEE**S**DFEDYPMR	1.75
U2OS MIS12-MPS1	12	TTK	VPVNLLN**S**PDCDVK	1.75
HCT-MPS as	421	STMN1	RA**S**GQAFELILSPR	1.75
U2OS MIS12-MPS1	806	BUB1	TLAP**S**PK	1.73
HeLa	812	GTSE1	ETYYLSD**S**PLLGPPVGEPR	1.73
HeLa	1016	TUBB	IMNTFSVVP**S**PK	1.73
HeLa	288	KIF4A	LEDPTEVTPGLSFFNPVCA**T**PNSK	1.72
HCT-MPS as	656	MPHOSPH8	LMPVSAQ**T**PK	1.72
HeLa	38	RACGAP1	TDESLDWDS**S**LVK	1.71
U2OS MIS12-MPS1	1589	BUB1	LHQVVET**S**HEDLPASQER	1.71
U2OS MIS12-MPS1	428	BUB1	TLAPSPKSPGDF**T**SAAQLASTPFHK	1.70
HeLa	140	KRT18	STFSTN**Y**R	1.70
HCT-MPS as	142	HCTP4	SVAEGLSG**S**LVQEPFQLATEK	1.68
U2OS MIS12-MPS1	816	PDS5B	AE**S**PESSAIESTQSTPQK	1.67
HeLa	595	NUSAP1	**S**CGPASQSTLGLK	1.66
HCT-MPS as	75	NASP	ENDK**T**EEM(ox)PNDSVLENK	1.65
HeLa	1579	SKA3	EEPVIV**T**PPTK	1.64
HeLa	976	NCOR1	**SKS**PIPGQGYLGTER	1.64
HeLa	263	NCOR1	**SKS**PIPGQGYLGTER	1.64
HCT-MPS as	269	KIF21A	APYFSGSS**T**FSPTILSSDK	1.63
HeLa	275	SLAIN2	FR**S**PAAP**S**PLALR	1.63
U2OS MIS12-MPS1	684	SMC4	RREEGPPPP**S**PDGA**SS**DAEPEPPSGR	1.62
U2OS MIS12-MPS1	1043	HCFC1	S**S**VGAGEPR	1.62
HeLa	32	CYTSA	R**SS**TSSEPTPTVK	1.62
HeLa	656	CYTSA	R**SS**TSSEPTPTVK	1.62
HeLa	368	CLASP2	DYNPYNYSDSI**S**PFNK	1.61
U2OS MIS12-MPS1	428	TTK	YVLGQLVGLN**S**PNSILK	1.60
HCT-MPS as	129	ANAPC1	AH**S**PALGVH**S**FSGVQR	1.60
HCT-MPS as	130	KIF2C	GS**S**SANPVNSVR	1.60
HeLa	1859	ASPM	NEV**T**PSSTTASVAR	1.59
HCT-MPS as	338	CTDP1	LVL**S**PDAPDR	1.59
HeLa	3718	NCAPD2	NPRE**S**TGNMVTGQTVCK	1.59

Experimental set-up	Position	Protein names	Modified sequence	Corrected Ratio
HeLa	5553	LMNA	**S**NEDQSM(ox)GNWQIK	1.59
U2OS MIS12-MPS1	351	BUB1B	NK**S**PPADPPR	1.58
HeLa	822	CDCA8	ANTV**T**PAVGR	1.58
HeLa	823	KIF18B	RG**S**LPDTQPSQGPS**T**PK	1.58
HeLa	1809	MKI67	**S**GGSGHAVAEPA**S**PEQELDQNK	1.58
HeLa	3426	RB1	INQMVCN**S**DR	1.58
U2OS MIS12-MPS1	146	KNTC1	HKPGS**T**PEPIAAEVR	1.57
U2OS MIS12-MPS1	52	MAD1L1	AILGSYDSELTPAEY**S**PQLTR	1.57
HeLa	53	SIN3A	LDDQE**S**PVYAAQQR	1.56
U2OS MIS12-MPS1	527	BUB1	**S**PGDFTSAAQLASTPFHK	1.55
HeLa	655	MCM6;MCM6	EIESEID**S**EEELINK	1.55
HeLa	39	CASC5	QDQSNVQIAAAP**T**PEK	1.55
HCT-MPS as	417	SKA3	TNS**S**SNDLEVEDR	1.52
HCT-MPS as	510	BUB1	LHQVVET**S**HEDLPASQER	1.52
HCT-MPS as	1069	CCP110	FHGVAIL**S**PLLNIEK	1.51
HCT-MPS as	220	ANLN	S**T**TPGGTGIK	1.50
HCT-MPS as	661	NUMA1	SQAPLES**S**LDSLGDVFLD**S**GRK	1.50
U2OS MIS12-MPS1	277	CASC5	LAEPLRK**S**L**S**NPTPDYCHDK	1.50

5

Chapter 6

Summary & Discussion

Summary

The importance of MPS1 in mitosis has been established for several years. Even though recent years have seen quite some development in the elucidation of the molecular pathways concerning MPS1 signaling, many aspects remained to be uncovered at the onset of the research presented in this thesis. In **Chapter 2** we report the development of mutant cell lines that allow specific, highly penetrant and reversible inhibition of MPS1, providing us with the opportunity to study the role of MPS1 in mitosis. One of these functions - the recruitment of MAD1 to unattached kinetochores - is studied in more detail in **Chapter 3**. We provide evidence that feedback control between MPS1, BUB1 and ZW10 regulates MAD1 kinetochore recruitment and subsequent SAC activity. In this chapter, we furthermore show that the predominant function for RZZ and BUB1 in SAC signaling is ensuring MAD1 localization. **Chapter 4** describes the identification of PLK1 as an auxiliary factor in the establishment and maintenance of the SAC. Under conditions of maximal SAC activity, PLK1 is dispensable, but when SAC signaling is suboptimal, PLK1 becomes essential to maintain SAC signaling. Our data suggest that under these conditions PLK1 activity promotes MCC stability. The work presented in **Chapter 5** describes the efforts put into identification of direct MPS1 targets and provides useful lessons for future investigation in the search for novel MPS1 targets.

Discussion

The role of MPS1 in the SAC

MPS1 has long been known to be involved in maintenance of the SAC [129,135]. In **chapter 2** we used chemical genetics to investigate the role of MPS1 in mitosis. In accordance with previous studies we found MPS1 kinase activity to be essential for SAC activity, the recruitment of checkpoint proteins to kinetochores and MCC formation. In **Chapter 3** we investigated in particular the role of MPS1 in the recruitment of MAD1. We reveal that MPS1-dependent recruitment of MAD1 is mediated by BUB1 and ZW10. BUB1 was recently shown to be recruited to KNL1 by MPS1-dependent phosphorylation of conserved MELT-like motifs [118-120]. BUB1 therefore may be the crucial and perhaps even the only effector for MPS1 in regulating MAD1 kinetochore recruitment. We were unable to prove this, however, since a kinetochore-tethered BUB1 could not rescue MAD1 kinetochore levels in MPS1-inhibited cells (not shown). This may mean that MPS1 has additional impact on kinetochore MAD1 or, alternatively, that tethered BUB1 cannot recapitulate BUB1's role in MAD1 localization. With regards to the first option, MPS1 has been shown to phosphorylate MAD1 in yeast [137] but to date a specific phosphosite or functional role for this phosphorylation in the SAC has not been reported. Interestingly in **Chapter 5** we identify multiple MAD1 sites that are regulated upon MPS1 inhibition. Mutation of these sites did not, however, influence MAD1 kinetochore localization (data not shown), although this does not exclude the possibility of additional, unidentified MPS1-dependent MAD1 phosphoresidues that impact its localization. Alternatively, the sites we identified might contribute to the recently identified role of MPS1 kinase activity in regulating MAD2 dimerization [90]. The recent development of antibodies specifically recognizing O-MAD2 [90,237] and C-MAD2 [267] might be helpful in investigating this. MAD2 itself is also an interesting candidate for direct regulation by MPS1, since both the MAD2 conformational change and MCC stability require MPS1 activity [90,91]. Fission yeast Mad2 is phosphorylated by Mps1 in vitro and a Mad2 mutant lacking all five sites was SAC deficient [150]. Contrary to intuition, phosphorylation of Ser187 of Fission yeast Mad2 was suggested to reduce Mad2-Mad1 binding in fission yeast, suggesting that Mps1 kinase activity inhibits aspects of SAC signaling. In line with this, phosphorylation of the C-terminal region of human MAD2 has also been shown to negatively regulate checkpoint activity by inhibiting the conformational transition of MAD2 [268,269]. Thus, there is currently no evidence that the MPS1-dependent regulation of MAD2 structural conversion to activate the SAC occurs via direct phosphorylation. Rather, it seems more likely that MPS1 promotes the MAD2 conformational change indirectly, for instance by activating/recruiting a protein phosphatase that counteracts inhibitory phosphorylations. Any of these mechanisms could also account for the observed impact of MPS1 activity on MCC stability. In addition, the other MCC subunits BUBR1 and CDC20 are also subjected to phosphorylation and other post translation modifications [41,85,233,270,271]. MPS1-mediated MCC stability might thus also be promoted via CDC20 or BUBR1. Another intriguing option is that MPS1 does not actively promote MCC stability but rather counters its disassembly. There are several, possibly related, mechanisms described that promote MCC disassembly. These include p31^{comet}-mediated extraction of MAD2 from the MCC, aided by CDK1-dependent phosphorylation of CDC20 and possibly by CUEDC2 [110,112,270,272], and auto-ubiquitination of CDC20, aided by APC15 and perhaps even by p31^{comet} [102-105,111,112]. Any of these events could be impacted by MPS1 activity. Due to the complexity of the pathways, I propose that the best way to identify the mechanisms by which MPS1 regulates the various aspects of SAC signaling is

quantitative proteomics studies of protein complexes. For a more elaborate discussion, see below.

Budding yeast NDC80 can be phosphorylated by MPS1 *in vitro*, and some evidence in budding yeast supports the idea that MPS1-dependent phosphorylation of NDC80 contributes to SAC activity [263]. Although both human and budding yeast MPS1 require HEC1/NDC80 for its recruitment to kinetochores [142,145,146,263,273], there is no evidence that the phosphoregulation of HEC1/NDC80 by MPS1 is conserved in humans. Indeed, despite extensive phosphoproteomic examinations of the KMN network ([8,14,202], and our data in chapter 5), no MPS1-like sites in the tail of HEC1/NDC80 have been found. We furthermore showed previously that the sole function of HEC1/NDC80 in SAC signaling in human cells is recruitment of MPS1 to kinetochores [146], so it seems unlikely that MPS1 itself could initiate that event. It is of interest to note that the mitotic kinase NEK2 was reported to phosphorylate HEC1 in its CH domain on Ser165, a phosphorylation that was shown to modulate SAC activity in human cell [12,264]. Although the fact that NEK2 is degraded in early mitosis [274] argues against a prominent role for this kinase in the SAC, these findings could indicate that SAC-modulating phosphorylation of HEC1 is present in human cells as it is in yeast, even if the kinase may not be conserved. Interestingly, in **Chapter 5** we found phosphorylation of SPC24, a member of the NDC80 complex, to be regulated. Future experiments need to elucidate if SPC24 phosphorylation in humans serves a similar purpose as NDC80 phosphorylation in yeast. Relatively straightforward RNAi rescue experiments of SPC24 phosphosite mutants should give an initial clue as to whether the SAC, weakened or not, depends to some extent on SPC24 phosphorylation. More sophisticated subsequent analysis will be needed to determine the mechanism by which such phosphoresidues might act.

Identification of novel MPS1 targets

Despite the multiple critical functions of MPS1 in mitosis, only a limited number of targets proteins have been identified and studied in detail [118-120,164]. It has proven to be quite difficult to identify *bona fide* MPS1 substrates, which might stem from low abundance of MPS1 substrates, low phosphorylation site occupancy, lack of a well-defined consensus motif and lack of stringent binding between MPS1 and its substrates. The latter finds support in the above-mentioned studies that, although successful at identifying KNL1 and Borealin as direct MPS1 substrates, fail to identify a direct interaction between MPS1 and its substrates. The recent developments in quantitative MS-based proteomics have allowed the identification of a large number of in vivo phosphorylation sites from complex samples and has proven a successful method for the identification of PLK1, Aurora B and CDK1 substrates [235,251-253]. **Chapter 5** describes the experimental optimization of quantitative phosphoproteomics methods aimed at identifying new MPS1 substrates. Although our search has yielded several interesting candidates which will be subjected to future research, we conclude that the different experimental set-ups used were not ideal for the identification of MPS1 substrates. Although we have been successful in identifying large quantities of phosphopeptides, the relative abundance of kinetochore- and spindle-associated proteins was low. Furthermore, the amount of significantly regulated, MPS1-dependent phosphopeptides also seems relatively low compared to, for instance, studies that used similar approaches to identify PLK1 substrates [235,251]. The latter might imply that MPS1 regulates the SAC and error-correction through only a small number of target proteins. However, since we also failed to identify the presumably heavily phosphorylated *bona-fide* MPS1 substrate KNL1 [67,118-120],

we suspect that poor recovery of kinetochore and spindle proteins has limited successful identification of novel MPS1 targets. Several recent studies have circumvented this by selective enrichment of phosphorylated substrates of a kinase of interest using chemical genetics [275-277]. Using the analog-sensitive MPS1 mutants described in **Chapter 2**, we attempted similar approaches. Unfortunately, poor activity of recombinant gatekeeper MPS1 mutants prevented us from using such analyses to identify MSP1 substrates. Since I feel that defining the MPS1 substrates and pinpointing the relevant phosphoresidues is key in understanding the mechanisms of SAC control, this begs the question how future research towards the identification of novel MPS1 substrates should be directed? Although quantitative phosphoproteomics provides us with the opportunity to identify phosphorylation sites that occur at least in cell culture conditions, future research might benefit from selective enrichment of kinetochore and spindle-associated proteins and protein complexes. It was recently shown that native kinetochore particles can be isolated from budding yeast by affinity capture of the MIS12 complex component Dsn1 [278]. A quantitative MS-based approach combined with selective enrichment of kinetochore particles or subcomplexes of the more elaborate human kinetochore might aid in the identification of novel MPS1 substrates, as was previously shown for KNL1 in budding yeast [118]. Similar strategies can be envisioned for the APC/C and MCC complex as well as the KMN network, CCAN proteins and, for instance, the SKA-complex. Elucidating which of the undoubtedly many candidate phosphorylations identified in this way are truly done by MPS1 will be greatly aided by the recent identifications of the MPS1 consensus phosphorylation motif [239,279] that closely resembles the sequence surrounding the MPS1 targets in the bona fide substrate KNL1 [67,118-120].

Auxiliary checkpoint proteins

In **Chapter 4** we investigated if the activity of the SAC depends on the presence or activity of so called auxiliary, or modulating, proteins. We previously identified Aurora B as such a modulating protein. The role of Aurora B in SAC regulation is not an essential one since SAC maintenance is not significantly affected by depletion or inactivation of Aurora B. Aurora B is only required for timely establishment of the SAC by promoting efficient recruitment of MPS1 to unattached kinetochores at the onset of mitosis. [146,153,212]. The role of Aurora B in the SAC is therefore auxiliary and only revealed in a sensitized SAC assay [146,212]. Like Aurora B, PLK1 activity is not essential for SAC maintenance when it is fully activated, but becomes essential to maintain a mitotic arrest when SAC activity is low. A role for PLK1 in the SAC has been tentatively proposed [226] but has remained unclear. This is perhaps due to the fact that PLK1 acts as an auxiliary factor combined with its essential role in a multitude of other mitotic processes, inhibition of which prominently activate the SAC [224,225,227,228]. In contrast to Aurora B, PLK1 does not influence MPS1 kinetochore localization in human cells, as was recently suggested in *Drosophila* cells [228]. Instead, we show that PLK1 regulates checkpoint activity downstream of MAD1 and serves to promote MCC stability when SAC activity is low. Although future experiments need to elucidate the exact mechanism by which PLK1 promotes MCC stability, our data suggests that phosphorylation within the BUBR1 GLEBS motif might be an important factor, by promoting the BUBR1-BUB3 interaction. If so, BUBR1 is a focal point for PLK1 signaling at the kinetochore: It was recently shown that PLK1 phosphorylates BUBR1 in another motif termed the KARD, promoting a BUBR1-PP2A interaction that is required for stabilizing kinetochore-microtubule interactions [41,42].

Our sensitized SAC assay is a powerful tool to examine SAC modulating factors, as shown

by our identification of Aurora B and PLK1 as auxiliary components of the SAC. Besides allowing functional analysis of these two kinases in the SAC, we show in **Chapter 3** that the sensitized SAC assay enhances the checkpoint phenotypes of ZW10 and BUB1 RNAi, proteins that are difficult to deplete efficiently. This may also hold true for NDC80 depletion, and the sensitized SAC assay has been instrumental in determining its contribution and that of its CH domain to SAC signaling [142]. Future investigations using this sensitized set up might yield more auxiliary SAC regulators and might aid the study of essential regulators that have proven difficult to functionally inactivate. For instance, depletion of MAD1 has proven difficult and has obstructed the investigation of MAD1 phosphorylations that we identified in **Chapter 5.** Combining the described MAD1 phosphomutants with the sensitized SAC assay might allow functional studies, and this will be a subject of future studies.

Feedback in the SAC

Correct regulation of many cellular processes is controlled by feedback networks that enable cellular mechanism to rapidly respond to changing stimuli. The decision to enter mitosis for instance, is mediated by a network of several feedbacks loops that correctly regulate the activation of the Cyclin B-CDK1 complex to ensure that once the commitment to cell division is made, it is executed rapidly and robustly [3]. A snowballing amount of evidence suggests that SAC regulation also depends on multiple feedback mechanisms. We previously showed that timely establishment of MPS1 kinetochore localization depends on Aurora B [146]. Activity and localization of Aurora B in turn is regulated by MPS1 through direct phosphorylation of Borealin and promoting BUB1-dependent histone H2A phosphorylation respectively [132,151,153,164,191,192]. MPS1 and Aurora B are thus engaged in a positive feedback loop ensuring rapid establishment of both the SAC and the error correction mechanisms as cells enter mitosis (Figure 1).

In **Chapter 3** we identify feedback control in the regulation of MAD1 kinetochore binding. MPS1 recruitment of MAD1 is mediated by BUB1 and ZW10. BUB1 regulates ZW10 localization, and ZW10 in turn recruits MAD1 while simultaneously facilitating KMN network stability consequently regulating MPS1 localization. Feedback regulation thus ensures rapid activation and subsequent maintenance of the SAC by promoting MPS1-dependent MAD1 kinetochore binding (Figure 6.1). Although not fully recognized, other feedback mechanisms involving MPS1 are easily envisioned. By promoting MCC formation and stability [90,91,151], MPS1 guarantees high Cyclin B-CDK1 activity, which in turn promotes MPS1 activity by direct phosphorylation [280]. The involvement of MPS1 in MCC stability might also be subjected to feedback regulation, for instance by regulation of a phosphatase, p31^{comet} or the APC/C as mentioned above. Lastly, it has been shown that MPS1 promotes PLK1 kinetochore binding [91]. Since in **chapter 4** we show that MCC stability requires PLK1 activity, it might thus be possible that an additional feedback loop regulates MCC stability. We suspect that the multitude of feedback loops in SAC regulation provides timely establishment of SAC signaling as cells enter mitosis, while also enabling the SAC to rapidly respond to kinetochore attachment status and ensuring rapid inactivation of the SAC once all kinetochores have attached. Although technically challenging, it will therefore be interesting to address whether feedback loops, like the Aurora B - MPS1 feedback, is essential to maintain SAC signaling when only few unattached kinetochores remain, while the same feedback might simultaneously function in the rapid extinguishing of SAC signaling once the last kinetochore has attached. Since MPS1 plays a central role in various SAC feedbacks, small alterations in its activity or expression might have drastic effects on genome stability and result in aneuploidy. Future

studies investigating the consequence of minor alterations in MPS1 activity or expression on genome stability in cells and mouse models can provide more insight in the contribution of the SAC to chromosomal instability and cancer.

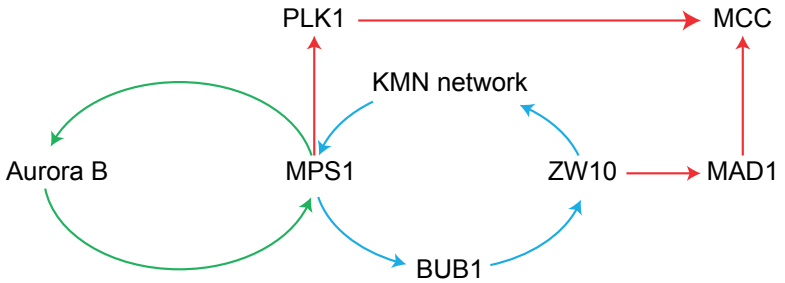

Figure 6.1. MPS1-centered feedback loops control the SAC

Schematic representation of various feedbacks that regulate SAC signaling and error correction. The first feedback loop between Aurora B and MPS1 (green) ensures timely establishment of both SAC signaling and error correction. The second feedback control between MPS1, BUB1 and ZW10 (blue) promotes MAD1 localization. The third, and more elaborate, feedback regulates MCC production and stability (red). In this feedback, MPS1 activity is required for MCC production through MAD1 localization while simultaneously ensuring PLK1 kinetochore localization, which is required for MCC stability when SAC signaling is low.

Addendum

References

1. Hochegger, H., Takeda, S. & Hunt, T. Cyclin-dependent kinases and cell-cycle transitions: does one fit all? *Nat Rev Mol Cell Biol* **9,** 910–916 (2008).
2. Morgan, D. O. Cyclin-dependent kinases: engines, clocks, and microprocessors. *Annu. Rev. Cell Dev. Biol.* **13,** 261–291 (1997).
3. Lindqvist, A., Rodriguez-Bravo, V. & Medema, R. H. The decision to enter mitosis: feedback and redundancy in the mitotic entry network. *The Journal of Cell Biology* **185,** 193–202 (2009).
4. Pines, J. & Rieder, C. L. Re-staging mitosis: a contemporary view of mitotic progression. *Nature cell Biology* **3,** E3–6 (2001).
5. Fukagawa, T. Assembly of kinetochores in vertebrate cells. *Experimental Cell Research* **296,** 21–27 (2004).
6. Mendiburo, M. J., Padeken, J., Fulop, S., Schepers, A. & Heun, P. Drosophila CENH3 Is Sufficient for Centromere Formation. *Science* **334,** 686–690 (2011).
7. Allshire, R. C. & Karpen, G. H. Epigenetic regulation of centromeric chromatin: old dogs, new tricks? *Nat Rev Genet* **9,** 923–937 (2008).
8. Cheeseman, I. M. *et al.* A conserved protein network controls assembly of the outer kinetochore and its ability to sustain tension. *Genes & Development* **18,** 2255–2268 (2004).
9. Cheeseman, I. M., Chappie, J. S., Wilson-Kubalek, E. M. & Desai, A. The Conserved KMN Network Constitutes the Core Microtubule-Binding Site of the Kinetochore. *CELL* **127,** 983–997 (2006).
10. DeLuca, J. G. *et al.* Kinetochore Microtubule Dynamics and Attachment Stability Are Regulated by Hec1. *CELL* **127,** 969–982 (2006).
11. McCleland, M. L. *et al.* The Vertebrate Ndc80 Complex Contains Spc24 and Spc25 Homologs, which Are Required to Establish and Maintain Kinetochore-Microtubule Attachment. *Current Biology* **14,** 131–137 (2004).
12. Wei, R., Ngo, B., Wu, G. & Lee, W.-H. Phosphorylation of the Ndc80 complex protein, HEC1, by Nek2 kinase modulates chromosome alignment and signaling of the spindle assembly checkpoint. *molecular biology of the cell* **22,** 3584–3594 (2011).
13. Ciferri, C. *et al.* Implications for Kinetochore-Microtubule Attachment from the Structure of an Engineered Ndc80 Complex. *CELL* **133,** 427–439 (2008).
14. Welburn, J. P. I. *et al.* Aurora B Phosphorylates Spatially Distinct Targets to Differentially Regulate the Kinetochore-Microtubule Interface. *Mol Cell* **38,** 383–392 (2010).
15. DeLuca, J. G. & Musacchio, A. Structural organization of the kinetochore–microtubule interface. *Current Opinion in Cell Biology* **24,** 48–56 (2012).
16. Gaitanos, T. N. *et al.* emboj200996a. *EMBO J* **28,** 1442–1452 (2009).
17. Schmidt, J. C. *et al.* The Kinetochore-Bound Ska1 Complex Tracks Depolymerizing Microtubules and Binds to Curved Protofilaments. *Developmental Cell* **23,** 968–980 (2012).
18. Schaar, B. T., Chan, G. K., Maddox, P., Salmon, E. D. & Yen, T. J. CENP-E function at kinetochores is essential for chromosome alignment. *The Journal of Cell Biology* **139,** 1373–1382 (1997).
19. Yao, X., Abrieu, A., Zheng, Y., Sullivan, K. F. & Cleveland, D. W. CENP-E forms a link between attachment of spindle microtubules to kinetochores and the mitotic checkpoint. *Nature cell Biology* **2,** 484–491 (2000).

20. Kim, Y., Heuser, J. E., Waterman, C. M. & Cleveland, D. W. CENP-E combines a slow, processive motor and a flexible coiled coil to produce an essential motile kinetochore tether. *The Journal of Cell Biology* **181,** 411–419 (2008).
21. Tanenbaum, M. E., Galjart, N., van Vugt, M. A. T. M. & Medema, R. H. CLIP-170 facilitates the formation of kinetochore-microtubule attachments. *EMBO J* **25,** 45–57 (2006).
22. Lansbergen, G. *et al.* Conformational changes in CLIP-170 regulate its binding to microtubules and dynactin localization. *The Journal of Cell Biology* **166,** 1003–1014 (2004).
23. Cheeseman, I. M. & Desai, A. Molecular architecture of the kinetochore–microtubule interface. *Nat Rev Mol Cell Biol* **9,** 33–46 (2008).
24. Gascoigne, K. E. & Cheeseman, I. M. Kinetochore assembly: if you build it, they will come. *Current Opinion in Cell Biology* **23,** 102–108 (2011).
25. Nishino, T. *et al.* CENP-T-W-S-X Forms a Unique Centromeric Chromatin Structure with a Histone-like Fold. *CELL* **148,** 487–501 (2012).
26. Malvezzi, F. *et al.* A structural basis for kinetochore recruitment of the Ndc80 complex via two distinct centromere receptors. *EMBO J* **32,** 409–423 (2013).
27. Gascoigne, K. E. *et al.* Induced ectopic kinetochore assembly bypasses the requirement for CENP-A nucleosomes. *CELL* **145,** 410–422 (2011).
28. Kitajima, T. S., Ohsugi, M. & Ellenberg, J. Complete Kinetochore Tracking Reveals Error-Prone Homologous Chromosome Biorientation in Mammalian Oocytes. *CELL* **146,** 568–581 (2011).
29. Kops, G. J. P. L., Saurin, A. T. & Meraldi, P. Finding the middle ground: how kinetochores power chromosome congression. *Cell. Mol. Life Sci.* **67,** 2145–2161 (2010).
30. Ault, J. G. & Rieder, C. L. Chromosome mal-orientation and reorientation during mitosis. *Cell Motil. Cytoskeleton* **22,** 155–159 (1992).
31. Cimini, D. *et al.* Merotelic kinetochore orientation is a major mechanism of aneuploidy in mitotic mammalian tissue cells. *The Journal of Cell Biology* **153,** 517–527 (2001).
32. Hauf, S. *et al.* The small molecule Hesperadin reveals a role for Aurora B in correcting kinetochore-microtubule attachment and in maintaining the spindle assembly checkpoint. *The Journal of Cell Biology* **161,** 281–294 (2003).
33. Ditchfield, C. *et al.* Aurora B couples chromosome alignment with anaphase by targeting BubR1, Mad2, and Cenp-E to kinetochores. *The Journal of Cell Biology* **161,** 267–280 (2003).
34. Lampson, M. A., Renduchitala, K., Khodjakov, A. & Kapoor, T. M. Correcting improper chromosome–spindle attachments during cell division. *Nature cell Biology* **6,** 6–237 (2004).
35. Guimaraes, G. J., Dong, Y., McEwen, B. F. & DeLuca, J. G. Kinetochore-Microtubule Attachment Relies on the Disordered N-Terminal Tail Domain of Hec1. *Current Biology* **18,** 1778–1784 (2008).
36. Chan, Y. W., Jeyaprakash, A. A., nigg, E. A. & Santamaria, A. Aurora B controls kinetochore-microtubule attachments by inhibiting Ska complex-KMN network interaction. *The Journal of Cell Biology* **196,** 563–571 (2012).
37. Liu, D., Vader, G., Vromans, M. J. M., Lampson, M. A. & Lens, S. M. A. Sensing chromosome bi-orientation by spatial separation of aurora B kinase from kinetochore substrates. *Science* **323,** 1350–1353 (2009).
38. Campbell, C. S. & Desai, A. nature12057. *Nature* **497,** 118–121 (2013).
39. Liu, D. *et al.* Regulated targeting of protein phosphatase 1 to the outer kinetochore

by KNL1 opposes Aurora B kinase. *The Journal of Cell Biology* **188,** 809–820 (2010).
40. Kim, Y., Holland, A. J., Lan, W. & Cleveland, D. W. Aurora Kinases and Protein Phosphatase 1 Mediate Chromosome Congression through Regulation of CENP-E. *CELL* **142,** 444–455 (2010).
41. Suijkerbuijk, S. J. E., Vleugel, M., Teixeira, A. & Kops, G. J. P. L. Integration of Kinase and Phosphatase Activities by BUBR1 Ensures Formation of Stable Kinetochore-Microtubule Attachments. *Developmental Cell* **23,** 745–755 (2012).
42. Kruse, T. *et al.* Direct binding between BubR1 and B56-PP2A phosphatase complexes regulate mitotic progression. *Journal of Cell Science* **126,** 1086–1092 (2013).
43. Li, X. & Nicklas, R. B. Mitotic forces control a cell-cycle checkpoint. *Nature* **373,** 630–632 (1995).
44. Rieder, C. L., Cole, R. W., Khodjakov, A. & Sluder, G. The checkpoint delaying anaphase in response to chromosome monoorientation is mediated by an inhibitory signal produced by unattached kinetochores. *The Journal of Cell Biology* **130,** 941–948 (1995).
45. Rieder, C. L., Schultz, A., Cole, R. & Sluder, G. Anaphase onset in vertebrate somatic cells is controlled by a checkpoint that monitors sister kinetochore attachment to the spindle. *The Journal of Cell Biology* **127,** 1301–1310 (1994).
46. Pines, J. Cubism and the cell cycle: the many faces of the APC/C. *Nat Rev Mol Cell Biol* **12,** 427–438 (2011).
47. Barford, D. Structure, function and mechanism of the anaphase promoting complex (APC/C). *Quart. Rev. Biophys.* **44,** 153–190 (2010).
48. Yu, H., King, R. W., Peters, J.-M. & Kirschner, M. W. Identification of a novel ubiquitin-conjugating enzyme involved in mitotic cyclin degradation. *Current Biology* **6,** 455–466 (1996).
49. Aristarkhov, A. *et al.* E2-C, a cyclin-selective ubiquitin carrier protein required for the destruction of mitotic cyclins. *Proc Natl Acad Sci USA* **93,** 4294–4299 (1996).
50. Garnett, M. J. *et al.* ncb1983. *Nature cell Biology* **11,** 1363–1369 (2009).
51. Wu, T. *et al.* UBE2S drives elongation of K11-linked ubiquitin chains by the Anaphase-Promoting Complex. *Proceedings of the National Academy of Sciences* **107,** 1355–1360 (2010).
52. Williamson, A. *et al.* Identification of a physiological E2 module for the human anaphase-promoting complex. *Proceedings of the National Academy of Sciences* **106,** 18213–18218 (2009).
53. Glotzer, M., Murray, A. W. & Kirschner, M. W. Cyclin is degraded by the ubiquitin pathway. *Nature* **349,** 132–138 (1991).
54. Pfleger, C. M. & Kirschner, M. W. The KEN box: an APC recognition signal distinct from the D box targeted by Cdh1. *Genes & Development* **14,** 655–665 (2000).
55. Carroll, C. W., Enquist-Newman, M. & Morgan, D. O. The APC Subunit Doc1 Promotes Recognition of the Substrate Destruction Box. *Current Biology* **15,** 11–18 (2005).
56. Buschhorn, B. A. *et al.* nsmb.1979. *Nat Struct Mol Biol* **18,** 6–13 (2010).
57. da Fonseca, P. C. A. *et al.* nature09625(1). *Nature* **470,** 274–278 (2011).
58. Elzen, den, N. & Pines, J. Cyclin A is destroyed in prometaphase and can delay chromosome alignment and anaphase. *The Journal of Cell Biology* **153,** 121–136 (2001).
59. Geley, S. *et al.* Anaphase-promoting complex/cyclosome-dependent proteolysis of human cyclin A starts at the beginning of mitosis and is not subject to the spindle

assembly checkpoint. *The Journal of Cell Biology* **153,** 137–148 (2001).
60. Hagting, A. *et al.* Human securin proteolysis is controlled by the spindle checkpoint and reveals when the APC/C switches from activation by Cdc20 to Cdh1. *The Journal of Cell Biology* **157,** 1125–1137 (2002).
61. Sigrist, S., Jacobs, H., Stratmann, R. & Lehner, C. F. Exit from mitosis is regulated by Drosophila fizzy and the sequential destruction of cyclins A, B and B3. *EMBO J* **14,** 4827–4838 (1995).
62. Fang, G., Yu, H. & Kirschner, M. W. Direct binding of CDC20 protein family members activates the anaphase-promoting complex in mitosis and G1. *Mol Cell* **2,** 163–171 (1998).
63. Kramer, E. R., Scheuringer, N., Podtelejnikov, A. V., Mann, M. & Peters, J.-M. Mitotic regulation of the APC activator proteins CDC20 and CDH1. *molecular biology of the cell* **11,** 1555–1569 (2000).
64. Lindon, C. & Pines, J. Ordered proteolysis in anaphase inactivates Plk1 to contribute to proper mitotic exit in human cells. *The Journal of Cell Biology* **164,** 233–241 (2004).
65. Stewart, S. & fang, G. Destruction Box-Dependent Degradation of Aurora B Is Mediated by the Anaphase-Promoting Complex/Cyclosome and Cdh1. *Cancer Research* **65,** 8730–8735 (2005).
66. Kraft, C. *et al.* Mitotic regulation of the human anaphase-promoting complex by phosphorylation. *EMBO J* **22,** 6598–6609 (2003).
67. Vleugel, M., Hoogendoorn, E., Snel, B. & Kops, G. J. P. L. Evolution and function of the mitotic checkpoint. *Developmental Cell* **23,** 239–250 (2012).
68. Hoyt, M. A., Totis, L. & Roberts, B. T. S. cerevisiae genes required for cell cycle arrest in response to loss of microtubule function. *CELL* **66,** 507–517 (1991).
69. Li, R. & Murray, A. W. Feedback control of mitosis in budding yeast. *CELL* **66,** 519–531 (1991).
70. Herzog, F. *et al.* Structure of the anaphase-promoting complex/cyclosome interacting with a mitotic checkpoint complex. *Science* **323,** 1477–1481 (2009).
71. Sudakin, V., Chan, G. K. & Yen, T. J. Checkpoint inhibition of the APC/C in HeLa cells is mediated by a complex of BUBR1, BUB3, CDC20, and MAD2. *The Journal of Cell Biology* **154,** 925–936 (2001).
72. Chao, W. C. H., Kulkarni, K., Zhang, Z., Kong, E. H. & Barford, D. nature10896. *Nature* **484,** 208–213 (2012).
73. Lara-Gonzalez, P., Scott, M. I. F., Diez, M., Sen, O. & Taylor, S. S. BubR1 blocks substrate recruitment to the APC/C in a KEN-box-dependent manner. *Journal of Cell Science* **124,** 4332–4345 (2012).
74. Burton, J. L. & Solomon, M. J. Mad3p, a pseudosubstrate inhibitor of APCCdc20 in the spindle assembly checkpoint. *Genes & Development* **21,** 655–667 (2007).
75. Musacchio, A. & Salmon, E. D. The spindle-assembly checkpoint in space and time. *Nat Rev Mol Cell Biol* **8,** 379–393 (2007).
76. Lan, W. & Cleveland, D. W. A chemical tool box defines mitotic and interphase roles for Mps1 kinase. *The Journal of Cell Biology* **190,** 21–24 (2010).
77. Klebig, C., Korinth, D. & Meraldi, P. Bub1 regulates chromosome segregation in a kinetochore-independent manner. *The Journal of Cell Biology* **185,** 841–858 (2009).
78. Meraldi, P., Draviam, V. M. & Sorger, P. K. Timing and checkpoints in the regulation of mitotic progression. *Developmental Cell* **7,** 45–60 (2004).
79. Kops, G. J. P. L. *et al.* ZW10 links mitotic checkpoint signaling to the structural kinetochore. *The Journal of Cell Biology* **169,** 49–60 (2005).

80. Basto, R., Gomes, R. & Karess, R. E. Rough deal and Zw10 are required for the metaphase checkpoint in Drosophila. *Nature cell Biology* **2,** 939–943 (2000).
81. Sironi, L. *et al.* Crystal structure of the tetrameric Mad1-Mad2 core complex: implications of a 'safety belt' binding mechanism for the spindle checkpoint. *EMBO J* **21,** 2496–2506 (2002).
82. Mapelli, M. & Musacchio, A. MAD contortions: conformational dimerization boosts spindle checkpoint signaling. *Current Opinion in Structural Biology* **17,** 716–725 (2007).
83. Kulukian, A., Han, J. S. & Cleveland, D. W. Unattached Kinetochores Catalyze Production of an Anaphase Inhibitor that Requires a Mad2 Template to Prime Cdc20 for BubR1 Binding. *Developmental Cell* **16,** 105–117 (2009).
84. Han, J. S. *et al.* Catalytic Assembly of the Mitotic Checkpoint Inhibitor BubR1-Cdc20 by a Mad2-Induced Functional Switch in Cdc20. *Mol Cell* 1–13 (2013). doi:10.1016/j.molcel.2013.05.019
85. Tang, Z., Bharadwaj, R., Li, B. & Yu, H. Mad2-Independent inhibition of APCCdc20 by the mitotic checkpoint protein BubR1. *Developmental Cell* **1,** 227–237 (2001).
86. Nilsson, J., Yekezare, M., Minshull, J. & Pines, J. The APC/C maintains the spindle assembly checkpoint by targeting Cdc20 for destruction. *Nature cell Biology* **10,** 1411–1420 (2008).
87. Davenport, J., Harris, L. D. & Goorha, R. Spindle checkpoint function requires Mad2-dependent Cdc20 binding to the Mad3 homology domain of BubR1. *Experimental Cell Research* **312,** 1831–1842 (2006).
88. Pan, J. Spindle checkpoint regulates Cdc20p stability in Saccharomyces cerevisiae. *Genes & Development* **18,** 1439–1451 (2004).
89. Tang, Z., Shu, H., Oncel, D., Chen, S. & Yu, H. Phosphorylation of Cdc20 by Bub1 provides a catalytic mechanism for APC/C inhibition by the spindle checkpoint. *Mol Cell* **16,** 387–397 (2004).
90. Hewitt, L. *et al.* Sustained Mps1 activity is required in mitosis to recruit O-Mad2 to the Mad1-C-Mad2 core complex. *The Journal of Cell Biology* **190,** 25–34 (2010).
91. Maciejowski, J. *et al.* Mps1 directs the assembly of Cdc20 inhibitory complexes during interphase and mitosis to control M phase timing and spindle checkpoint signaling. *The Journal of Cell Biology* **190,** 89–100 (2010).
92. Maldonado, M. & Kapoor, T. M. Constitutive Mad1 targeting to kinetochores uncouples checkpoint signalling from chromosome biorientation. *Nature cell Biology* **13,** 475–482 (2011).
93. Howell, B. J. *et al.* Cytoplasmic dynein/dynactin drives kinetochore protein transport to the spindle poles and has a role in mitotic spindle checkpoint inactivation. *The Journal of Cell Biology* **155,** 1159–1172 (2001).
94. Famulski, J. K., Vos, L. J., Rattner, J. B. & Chan, G. K. Dynein/Dynactin-mediated transport of kinetochore components off kinetochores and onto spindle poles induced by nordihydroguaiaretic acid. *PLoS ONE* **6,** e16494 (2011).
95. Bader, J. R. & Vaughan, K. T. Dynein at the kinetochore: Timing, Interactions and Functions. *Semin Cell Dev Biol* **21,** 269–275 (2010).
96. Pfarr, C. M. *et al.* Cytoplasmic dynein is localized to kinetochores during mitosis. *Nature* **345,** 263–265 (1990).
97. Steuer, E. R., Wordeman, L., Schroer, T. A. & Sheetz, M. P. Localization of cytoplasmic dynein to mitotic spindles and kinetochores. *Nature* **345,** 266–268 (1990).
98. Sharp, D. J., Rogers, G. C. & Scholey, J. M. Cytoplasmic dynein is required for poleward chromosome movement during mitosis in Drosophila embryos. *Nature*

cell Biology **2,** 922–930 (2000).
99. Yang, Z., Tulu, U. S., Wadsworth, P. & Rieder, C. L. Kinetochore Dynein Is Required for Chromosome Motion and Congression Independent of the Spindle Checkpoint. *Current Biology* **17,** 973–980 (2007).
100. Gassmann, R. *et al.* A new mechanism controlling kinetochore–microtubule interactions revealed by comparison of two dynein-targeting components: SPDL-1 and the Rod/Zwilch/Zw10 complex. *Genes & Development* **22,** 2302–2307 (2008).
101. Barisic, M. *et al.* Spindly/CCDC99 is required for efficient chromosome congression and mitotic checkpoint regulation. *molecular biology of the cell* **21,** 1968–1981 (2010).
102. Reddy, S. K., Rape, M., Margansky, W. A. & Kirschner, M. W. Ubiquitination by the anaphase-promoting complex drives spindle checkpoint inactivation. *Nature* **446,** 921–925 (2007).
103. Mansfeld, J., Collin, P., Collins, M. O., Choudhary, J. S. & Pines, J. ncb2347. *Nature cell Biology* **13,** 1234–1243 (2011).
104. Uzunova, K. *et al.* APC15 mediates CDC20 autoubiquitylation by APC/CMCC and disassembly of the mitotic checkpoint complex. *Nat Struct Mol Biol* **19,** 1116–1123 (2012).
105. Foster, S. A. & Morgan, D. O. The APC/C Subunit Mnd2/Apc15 Promotes Cdc20 Autoubiquitination and Spindle Assembly Checkpoint Inactivation. *Mol Cell* **47,** 921–932 (2012).
106. Habu, T., Kim, S. H., Weinstein, J. & Matsumoto, T. Identification of a MAD2-binding protein, CMT2, and its role in mitosis. *EMBO J* **21,** 6419–6428 (2002).
107. Xia, G. *et al.* Conformation-specific binding of p31(comet) antagonizes the function of Mad2 in the spindle checkpoint. *EMBO J* **23,** 3133–3143 (2004).
108. Yang, M. *et al.* p31comet blocks Mad2 activation through structural mimicry. *CELL* **131,** 744–755 (2007).
109. Mapelli, M. *et al.* Determinants of conformational dimerization of Mad2 and its inhibition by p31comet. *EMBO J* **25,** 1273–1284 (2006).
110. Westhorpe, F. G., Tighe, A., Lara-Gonzalez, P. & Taylor, S. S. p31comet-mediated extraction of Mad2 from the MCC promotes efficient mitotic exit. *Journal of Cell Science* **124,** 3905–3916 (2011).
111. Varetti, G., Guida, C., Santaguida, S., Chiroli, E. & Musacchio, A. Homeostatic Control of Mitotic Arrest. *Mol Cell* **44,** 710–720 (2011).
112. Jia, L. *et al.* Defining pathways of spindle checkpoint silencing: functional redundancy between Cdc20 ubiquitination and p31comet. *molecular biology of the cell* **22,** 4227–4235 (2011).
113. Xu, P., Raetz, E. A., Kitagawa, M., Virshup, D. M. & Lee, S. H. BUBR1 recruits PP2A via the B56 family of targeting subunits to promote chromosome congression. *Biology Open* **2,** 479–486 (2013).
114. Foley, E. A., Maldonado, M. & Kapoor, T. M. ncb2327. *Nature cell Biology* **13,** 1265–1271 (2011).
115. Vanoosthuyse, V. & Hardwick, K. G. A Novel Protein Phosphatase 1-Dependent Spindle Checkpoint Silencing Mechanism. *Current Biology* **19,** 1176–1181 (2009).
116. Pinsky, B. A., Nelson, C. R. & Biggins, S. Protein Phosphatase 1 Regulates Exit from the Spindle Checkpoint in Budding Yeast. *Current Biology* **19,** 1182–1187 (2009).
117. Rosenberg, J. S., Cross, F. R. & Funabiki, H. KNL1/Spc105 Recruits PP1 to Silence the Spindle Assembly Checkpoint. *Current Biology* **21,** 942–947 (2011).
118. London, N., Ceto, S., Ranish, J. A. & Biggins, S. Phosphoregulation of Spc105 by

Mps1 and PP1 Regulates Bub1 Localization to Kinetochores. *Current Biology* **22,** 900–906 (2012).
119. Shepperd, L. A. *et al.* Phosphodependent recruitment of Bub1 and Bub3 to Spc7/KNL1 by Mph1 kinase maintains the spindle checkpoint. *Current Biology* **22,** 891–899 (2012).
120. Yamagishi, Y., Yang, C.-H., Tanno, Y. & Watanabe, Y. MPS1/Mph1 phosphorylates the kinetochore protein KNL1/Spc7 to recruit SAC components. *Nature cell Biology* **14,** 746–752 (2012).
121. Liu, S.-T. *et al.* Human MPS1 kinase is required for mitotic arrest induced by the loss of CENP-E from kinetochores. *molecular biology of the cell* **14,** 1638–1651 (2003).
122. Meadows, J. C. *et al.* Spindle Checkpoint Silencing Requires Association of PP1 to Both Spc7 and Kinesin-8 Motors. *Developmental Cell* **20,** 739–750 (2011).
123. Espeut, J., Cheerambathur, D. K., Krenning, L., Oegema, K. & Desai, A. Microtubule binding by KNL-1 contributes to spindle checkpoint silencing at the kinetochore. *The Journal of Cell Biology* **196,** 469–482 (2012).
124. Whyte, J. *et al.* Phosphorylation regulates targeting of cytoplasmic dynein to kinetochores during mitosis. *The Journal of Cell Biology* **183,** 819–834 (2008).
125. Winey, M., Goetsch, L., Baum, P. & Byers, B. MPS1 and MPS2: novel yeast genes defining distinct steps of spindle pole body duplication. *The Journal of Cell Biology* **114,** 745–754 (1991).
126. Schutz, A. R. & Winey, M. New alleles of the yeast MPS1 gene reveal multiple requirements in spindle pole body duplication. *molecular biology of the cell* **9,** 759–774 (1998).
127. Fisk, H. A. & Winey, M. The mouse Mps1p-like kinase regulates centrosome duplication. *CELL* **106,** 95–104 (2001).
128. Fisk, H. A., Mattison, C. P. & Winey, M. Human Mps1 protein kinase is required for centrosome duplication and normal mitotic progression. *Proc Natl Acad Sci USA* **100,** 14875–14880 (2003).
129. Stucke, V. M., Silljé, H. H. W., Arnaud, L. & Nigg, E. A. Human Mps1 kinase is required for the spindle assembly checkpoint but not for centrosome duplication. *EMBO J* **21,** 1723–1732 (2002).
130. Stucke, V. M., Baumann, C. & Nigg, E. A. Kinetochore localization and microtubule interaction of the human spindle checkpoint kinase Mps1. *Chromosoma* **113,** (2004).
131. Jelluma, N. *et al.* Chromosomal Instability by Inefficient Mps1 Auto-Activation Due to a Weakened Mitotic Checkpoint and Lagging Chromosomes. *PLoS ONE* **3,** e2415 (2008).
132. Kwiatkowski, N. *et al.* Small-molecule kinase inhibitors provide insight into Mps1 cell cycle function. *Nature Methods* **6,** 359–368 (2010).
133. Santaguida, S., Tighe, A., D'Alise, A. M., Taylor, S. S. & Musacchio, A. Dissecting the role of MPS1 in chromosome biorientation and the spindle checkpoint through the small molecule inhibitor reversine. *The Journal of Cell Biology* **190,** 73–87 (2010).
134. Schmidt, M., Budirahardja, Y., Klompmaker, R. & Medema, R. H. Ablation of the spindle assembly checkpoint by a compound targeting Mps1. *EMBO Rep.* **6,** 866–872 (2005).
135. Abrieu, A. *et al.* Mps1 is a kinetochore-associated kinase essential for the vertebrate mitotic checkpoint. *CELL* **106,** 83–93 (2001).
136. Weiss, E. & Winey, M. The Saccharomyces cerevisiae spindle pole body duplication

gene MPS1 is part of a mitotic checkpoint. *The Journal of Cell Biology* **132,** 111–123 (1996).
137. Hardwick, K. G., Weiss, E., Luca, F. C., Winey, M. & Murray, A. W. Activation of the budding yeast spindle assembly checkpoint without mitotic spindle disruption. *Science* **273,** 953–956 (1996).
138. Maure, J.-F., Kitamura, E. & Tanaka, T. U. Mps1 Kinase Promotes Sister-Kinetochore Bi-orientation by a Tension-Dependent Mechanism. *Current Biology* **17,** 2175–2182 (2007).
139. Liu, C. *et al.* Ubiquitin Ligase Ufd2 Is Required for Efficient Degradation of Mps1 Kinase. *Journal of Biological Chemistry* **286,** 43660–43667 (2011).
140. Cui, Y. *et al.* Degradation of the Human Mitotic Checkpoint Kinase Mps1 Is Cell Cycle-regulated by APC-cCdc20 and APC-cCdh1 Ubiquitin Ligases. *Journal of Biological Chemistry* **285,** 32988–32998 (2010).
141. Howell, B. J. *et al.* Spindle checkpoint protein dynamics at kinetochores in living cells. *Current Biology* **14,** 953–964 (2004).
142. Nijenhuis, W. *et al.* A TPR domain-containing N-terminal module of MPS1 is required for its kinetochore localization by Aurora B. *The Journal of Cell Biology* (2013). doi:10.1083/jcb.201210033
143. Lee, S. *et al.* Characterization of the Spindle Checkpoint Kinase Mps1 Reveals a Domain with Functional and Structural Similarities to the Tetratricopeptide Repeat Motifs of the Bub1 and BubR1 Checkpoint Kinases. *Journal of Biological Chemistry* 1–22 (2011). doi:10.1074/jbc.M111.307355
144. Montembault, E., Dutertre, S., Prigent, C. & Giet, R. PRP4 is a spindle assembly checkpoint protein required for MPS1, MAD1, and MAD2 localization to the kinetochores. *The Journal of Cell Biology* **179,** 601–609 (2007).
145. Martin-Lluesma, S., Stucke, V. M. & Nigg, E. A. Role of Hec1 in Spindle Checkpoint Signaling and Kinetochore Recruitment of Mad1/Mad2. *Science* **297,** 2267–2270 (2002).
146. Saurin, A. T., van der Waal, M. S., Medema, R. H., Lens, S. M. A. & Kops, G. J. P. L. Aurora B potentiates Mps1 activation to ensure rapid checkpoint establishment at the onset of mitosis. *Nature Communications* **2,** 316 (2011).
147. Kang, J., Chen, Y., Zhao, Y. & Yu, H. Autophosphorylation-dependent activation of human Mps1 is required for the spindle checkpoint. *Proceedings of the National Academy of Sciences* **104,** 20232–20237 (2007).
148. Mattison, C. P. *et al.* Mps1 Activation Loop Autophosphorylation Enhances Kinase Activity. *Journal of Biological Chemistry* **282,** 30553–30561 (2007).
149. Jelluma, N., Dansen, T. B., Sliedrecht, T., Kwiatkowski, N. P. & Kops, G. J. P. L. Release of Mps1 from kinetochores is crucial for timely anaphase onset. *The Journal of Cell Biology* **191,** 281–290 (2010).
150. Zich, J. *et al.* Kinase Activity of Fission Yeast Mph1 Is Required for Mad2 and Mad3 to Stably Bind the Anaphase Promoting Complex. *Current Biology* **22,** 296–301 (2012).
151. Sliedrecht, T., Zhang, C., Shokat, K. M. & Kops, G. J. P. L. Chemical genetic inhibition of Mps1 in stable human cell lines reveals novel aspects of Mps1 function in mitosis. *PLoS ONE* **5,** e10251 (2010).
152. Bourhis, E., Lingel, A., Phung, Q., Fairbrother, W. J. & Cochran, A. G. Phosphorylation of a Borealin Dimerization Domain Is Required for Proper Chromosome Segregation. *Biochemistry* **48,** 6783–6793 (2009).
153. van der Waal, M. S. *et al.* Mps1 promotes rapid centromere accumulation of Aurora B. *EMBO Rep.* **13,** 847–854 (2012).

154. Shimogawa, M. M. *et al.* Mps1 Phosphorylation of Dam1 Couples Kinetochores to Microtubule Plus Ends at Metaphase. *Current Biology* **16,** 1489–1501 (2006).
155. Espeut, J. *et al.* Phosphorylation Relieves Autoinhibition of the Kinetochore Motor Cenp-E. *Mol Cell* **29,** 637–643 (2008).
156. Wei, J. H. TTK/hMps1 Participates in the Regulation of DNA Damage Checkpoint Response by Phosphorylating CHK2 on Threonine 68. *Journal of Biological Chemistry* **280,** 7748–7757 (2004).
157. Leng, M. *et al.* MPS1-dependent mitotic BLM phosphorylation is important for chromosome stability. *Proc Natl Acad Sci USA* **103,** 11485–11490 (2006).
158. Huang, Y. F., Chang, M. D. T. & Shieh, S. Y. TTK/hMps1 Mediates the p53-Dependent Postmitotic Checkpoint by Phosphorylating p53 at Thr18. *Molecular and Cellular Biology* **29,** 2935–2944 (2009).
159. Ruchaud, S., Carmena, M. & Earnshaw, W. C. Chromosomal passengers: conducting cell division. *Nat Rev Mol Cell Biol* **8,** 798–812 (2007).
160. Jones, M. H. *et al.* Chemical Genetics Reveals a Role for Mps1 Kinase in Kinetochore Attachment during Mitosis. *Current Biology* **15,** 160–165 (2005).
161. He, X., Jones, M. H., Winey, M. & Sazer, S. Mph1, a member of the Mps1-like family of dual specificity protein kinases, is required for the spindle checkpoint in S. pombe. *Journal of Cell Science* **111 (Pt 12),** 1635–1647 (1998).
162. Fischer, M. G., Heeger, S., Häcker, U. & Lehner, C. F. The Mitotic Arrest in Response to Hypoxia and of Polar Bodies during Early Embryogenesis Requires Drosophila Mps1. *Current Biology* **14,** 2019–2024 (2004).
163. Liu, S. T., Rattner, J. B., Jablonski, S. A. & Yen, T. J. Mapping the assembly pathways that specify formation of the trilaminar kinetochore plates in human cells. *The Journal of Cell Biology* **175,** 41–53 (2006).
164. Jelluma, N. *et al.* Mps1 Phosphorylates Borealin to Control Aurora B Activity and Chromosome Alignment. *CELL* **132,** 233–246 (2008).
165. Jallepalli, P. V. & Lengauer, C. Chromosome segregation and cancer: cutting through the mystery. *Nat Rev Cancer* **1,** 109–117 (2001).
166. Janssen, A., Kops, G. J. P. L. & Medema, R. H. Elevating the frequency of chromosome mis-segregation as a strategy to kill tumor cells. *Proceedings of the National Academy of Sciences* **106,** 19108–19113 (2009).
167. Dorer, R. K. *et al.* A Small-Molecule Inhibitor of Mps1 Blocks the Spindle-Checkpoint Response to a Lack of Tension on Mitotic Chromosomes. *Current Biology* **15,** 1070–1076 (2005).
168. Bishop, A. C., Buzko, O. & Shokat, K. M. Magic bullets for protein kinases. *Trends in Cell Biology* **11,** 167–172 (2001).
169. Tighe, A., Staples, O. & Taylor, S. Mps1 kinase activity restrains anaphase during an unperturbed mitosis and targets Mad2 to kinetochores. *The Journal of Cell Biology* **181,** 893–901 (2008).
170. Vigneron, S. *et al.* Kinetochore localization of spindle checkpoint proteins: who controls whom? *molecular biology of the cell* **15,** 4584–4596 (2004).
171. De Antoni, A. *et al.* The Mad1/Mad2 Complex as a Template for Mad2 Activation in the Spindle Assembly Checkpoint. *Current Biology* **15,** 214–225 (2005).
172. Kapoor, T. M., Mayer, T. U., Coughlin, M. L. & Mitchison, T. J. Probing spindle assembly mechanisms with monastrol, a small molecule inhibitor of the mitotic kinesin, Eg5. *The Journal of Cell Biology* **150,** 975–988 (2000).
173. Khodjakov, A., La Terra, S. & Chang, F. Laser Microsurgery in Fission Yeast. *Current Biology* **14,** 1330–1340 (2004).
174. Tanaka, T. U. *et al.* Evidence that the Ipl1-Sli15 (Aurora kinase-INCENP) complex

promotes chromosome bi-orientation by altering kinetochore-spindle pole connections. *CELL* **108,** 317–329 (2002).
175. Pinsky, B. A. & Biggins, S. The spindle checkpoint: tension versus attachment. *Trends in Cell Biology* **15,** 486–493 (2005).
176. Kinoshita, E. Phosphate-binding Tag, a New Tool to Visualize Phosphorylated Proteins. *Molecular & Cellular Proteomics* **5,** 749–757 (2005).
177. Kops, G. J. P. L., Weaver, B. A. A. & Cleveland, D. W. On the road to cancer: aneuploidy and the mitotic checkpoint. *Nat Rev Cancer* **5,** 773–785 (2005).
178. Chen, R. H., Shevchenko, A., Mann, M. & Murray, A. W. Spindle checkpoint protein Xmad1 recruits Xmad2 to unattached kinetochores. *The Journal of Cell Biology* **143,** 283–295 (1998).
179. Luo, X., Tang, Z., Rizo, J. & Yu, H. The Mad2 spindle checkpoint protein undergoes similar major conformational changes upon binding to either Mad1 or Cdc20. *Mol Cell* **9,** 59–71 (2002).
180. Sironi, L. *et al.* Mad2 binding to Mad1 and Cdc20, rather than oligomerization, is required for the spindle checkpoint. *EMBO J* **20,** 6371–6382 (2001).
181. King, E. M. J., van der Sar, S. J. A. & Hardwick, K. G. Mad3 KEN Boxes Mediate both Cdc20 and Mad3 Turnover, and Are Critical for the Spindle Checkpoint. *PLoS ONE* **2,** e342 (2007).
182. Suijkerbuijk, S. J. E. *et al.* The vertebrate mitotic checkpoint protein BUBR1 is an unusual pseudokinase. *Developmental Cell* **22,** 1321–1329 (2012).
183. Chan, G. K., Jablonski, S. A., Starr, D. A., Goldberg, M. L. & Yen, T. J. Human Zw10 and ROD are mitotic checkpoint proteins that bind to kinetochores. *Nature cell Biology* **2,** 944–947 (2000).
184. Kim, S., Sun, H., Tomchick, D. R., Yu, H. & Luo, X. Structure of human Mad1 C-terminal domain reveals its involvement in kinetochore targeting. *Proceedings of the National Academy of Sciences* **109,** 6549–6554 (2012).
185. Civril, F. *et al.* Structural Analysis of the RZZ Complex Reveals Common Ancestry with Multisubunit Vesicle Tethering Machinery. *Structure* **18,** 616–626 (2010).
186. Karess, R. Rod–Zw10–Zwilch: a key player in the spindle checkpoint. *Trends in Cell Biology* **15,** 386–392 (2005).
187. Starr, D. A., Williams, B. C., Hays, T. S. & Goldberg, M. L. ZW10 helps recruit dynactin and dynein to the kinetochore. *The Journal of Cell Biology* **142,** 763–774 (1998).
188. Gassmann, R. *et al.* Removal of Spindly from microtubule-attached kinetochores controls spindle checkpoint silencing in human cells. *Genes & Development* **24,** 957–971 (2010).
189. Wojcik, E. *et al.* Kinetochore dynein: its dynamics and role in the transport of the Rough deal checkpoint protein. *Nature cell Biology* **3,** 1001–1007 (2001).
190. Kang, J. & Yu, H. Kinase Signaling in the Spindle Checkpoint. *Journal of Biological Chemistry* **284,** 15359–15363 (2009).
191. Kawashima, S. A., Yamagishi, Y., Honda, T., Ishiguro, K. I. & Watanabe, Y. Phosphorylation of H2A by Bub1 Prevents Chromosomal Instability Through Localizing Shugoshin. *Science* **327,** 172–177 (2010).
192. Yamagishi, Y., Honda, T., Tanno, Y. & Watanabe, Y. Two histone marks establish the inner centromere and chromosome bi-orientation. *Science* **330,** 239–243 (2010).
193. Sharp-Baker, H. & Chen, R. H. Spindle checkpoint protein Bub1 is required for kinetochore localization of Mad1, Mad2, Bub3, and CENP-E, independently of its kinase activity. *The Journal of Cell Biology* **153,** 1239–1250 (2001).

194. Krenn, V., Wehenkel, A., Li, X., Santaguida, S. & Musacchio, A. Structural analysis reveals features of the spindle checkpoint kinase Bub1-kinetochore subunit Knl1 interaction. *The Journal of Cell Biology* **196,** 451–467 (2012).
195. Bolanos-Garcia, V. M. *et al.* Structure of a Blinkin-BUBR1 Complex Reveals an Interaction Crucial for Kinetochore-Mitotic Checkpoint Regulation via an Unanticipated Binding Site. *Structure* **19,** 1691–1700 (2011).
196. Kiyomitsu, T., Obuse, C. & Yanagida, M. Human Blinkin/AF15q14 Is Required for Chromosome Alignment and the Mitotic Checkpoint through Direct Interaction with Bub1 and BubR1. *Developmental Cell* **13,** 663–676 (2007).
197. Warren, C. D. *et al.* Distinct chromosome segregation roles for spindle checkpoint proteins. *molecular biology of the cell* **13,** 3029–3041 (2002).
198. Janicki, S. M. & Spector, D. L. Nuclear choreography: interpretations from living cells. *Current Opinion in Cell Biology* **15,** 149–157 (2003).
199. Paulmurugan, R. & Gambhir, S. S. Monitoring Protein−Protein Interactions Using Split Synthetic Renilla Luciferase Protein-Fragment-Assisted Complementation. *Anal. Chem.* **75,** 1584–1589 (2003).
200. Malureanu, L. A. *et al.* BubR1 N terminus acts as a soluble inhibitor of cyclin B degradation by APC/C(Cdc20) in interphase. *Developmental Cell* **16,** 118–131 (2009).
201. Foley, E. A. & Kapoor, T. M. Microtubule attachment and spindle assembly checkpoint signalling at the kinetochore. *Nat Rev Mol Cell Biol* **14,** 25–37 (2013).
202. Obuse, C. *et al.* A conserved Mis12 centromere complex is linked to heterochromatic HP1 and outer kinetochore protein Zwint-1. *Nature cell Biology* **6,** 1135–1141 (2004).
203. Brady, D. M. & Hardwick, K. G. Complex formation between Mad1p, Bub1p and Bub3p is crucial for spindle checkpoint function. *Current Biology* **10,** 675–678 (2000).
204. Famulski, J. K., Vos, L. J., Sun, X. & Chan, G. K. Stable hZW10 kinetochore residency, mediated by hZwint-1 interaction, is essential for the mitotic checkpoint. *The Journal of Cell Biology* **180,** 507–520 (2008).
205. Shah, J. V. *et al.* Dynamics of centromere and kinetochore proteins; implications for checkpoint signaling and silencing. *Current Biology* **14,** 942–952 (2004).
206. Yamamoto, T. G., Watanabe, S., Essex, A. & Kitagawa, R. SPDL-1 functions as a kinetochore receptor for MDF-1 in Caenorhabditis elegans. *The Journal of Cell Biology* **183,** 187–194 (2008).
207. Chung, E. & Chen, R.-H. Spindle checkpoint requires Mad1-bound and Mad1-free Mad2. *molecular biology of the cell* **13,** 1501–1511 (2002).
208. Kiyomitsu, T., Murakami, H. & Yanagida, M. Protein Interaction Domain Mapping of Human Kinetochore Protein Blinkin Reveals a Consensus Motif for Binding of Spindle Assembly Checkpoint Proteins Bub1 and BubR1. *Molecular and Cellular Biology* **31,** 998–1011 (2011).
209. Vos, L. J., Famulski, J. K. & Chan, G. K. T. hZwint-1 bridges the inner and outer kinetochore: identification of the kinetochore localization domain and the hZw10-interaction domain. *Biochem. J.* **436,** 157–168 (2011).
210. Ciliberto, A. & Shah, J. V. A quantitative systems view of the spindle assembly checkpoint. *EMBO J* **28,** 2162–2173 (2009).
211. Carmena, M., Wheelock, M., Funabiki, H. & Earnshaw, W. C. nrm3474. *Nat Rev Mol Cell Biol* **13,** 789–803 (2012).
212. Santaguida, S., Vernieri, C., Villa, F., Ciliberto, A. & Musacchio, A. Evidence that Aurora B is implicated in spindle checkpoint signalling independently of error

correction. *EMBO J* **30,** 1508–1519 (2011).
213. van Vugt, M. A. T. M. Polo-like Kinase-1 Is Required for Bipolar Spindle Formation but Is Dispensable for Anaphase Promoting Complex/Cdc20 Activation and Initiation of Cytokinesis. *Journal of Biological Chemistry* **279,** 36841–36854 (2004).
214. Sumara, I. *et al.* Roles of polo-like kinase 1 in the assembly of functional mitotic spindles. *Current Biology* **14,** 1712–1722 (2004).
215. Sunkel, C. E. & Glover, D. M. polo, a mitotic mutant of Drosophila displaying abnormal spindle poles. *Journal of Cell Science* **89,** 25–38 (1988).
216. Lane, H. A. & nigg, E. A. Antibody microinjection reveals an essential role for human polo-like kinase 1 (Plk1) in the functional maturation of mitotic centrosomes. *The Journal of Cell Biology* **135,** 1701–1713 (1996).
217. Elowe, S., Hummer, S., Uldschmid, A., Li, X. & nigg, E. A. Tension-sensitive Plk1 phosphorylation on BubR1 regulates the stability of kinetochore microtubule interactions. *Genes & Development* **21,** 2205–2219 (2007).
218. Elowe, S. *et al.* Uncoupling of the spindle-checkpoint and chromosome-congression functions of BubR1. *Journal of Cell Science* **123,** 84–94 (2010).
219. Matsumura, S., Toyoshima, F. & Nishida, E. Polo-like Kinase 1 Facilitates Chromosome Alignment during Prometaphase through BubR1. *Journal of Biological Chemistry* **282,** 15217–15227 (2007).
220. Petronczki, M., Lénárt, P. & Peters, J.-M. Polo on the Rise-from Mitotic Entry to Cytokinesis with Plk1. *Developmental Cell* **14,** 646–659 (2008).
221. Elia, A. E. H., Cantley, L. C. & Yaffe, M. B. Proteomic screen finds pSer/pThr-binding domain localizing Plk1 to mitotic substrates. *Science* **299,** 1228–1231 (2003).
222. Elia, A. E. H. *et al.* The molecular basis for phosphodependent substrate targeting and regulation of Plks by the Polo-box domain. *CELL* **115,** 83–95 (2003).
223. Seong, Y.-S. *et al.* A spindle checkpoint arrest and a cytokinesis failure by the dominant-negative polo-box domain of Plk1 in U-2 OS cells. *J Biol Chem* **277,** 32282–32293 (2002).
224. Lénárt, P. *et al.* The Small-Molecule Inhibitor BI 2536 Reveals Novel Insights into Mitotic Roles of Polo-like Kinase 1. *Current Biology* **17,** 304–315 (2007).
225. Chi, Y.-H. *et al.* Requirements for protein phosphorylation and the kinase activity of polo-like kinase 1 (Plk1) for the kinetochore function of mitotic arrest deficiency protein 1 (Mad1). *J Biol Chem* **283,** 35834–35844 (2008).
226. van de Weerdt, B. C. M. *et al.* Uncoupling Anaphase-Promoting Complex/Cyclosome Activity from Spindle Assembly Checkpoint Control by Deregulating Polo-Like Kinase 1. *Molecular and Cellular Biology* **25,** 2031–2044 (2005).
227. Wong, O. K. & Fang, G. Plx1 is the 3F3/2 kinase responsible for targeting spindle checkpoint proteins to kinetochores. *The Journal of Cell Biology* **170,** 709–719 (2005).
228. Conde, C. *et al.* Drosophila Polo regulates the spindle assembly checkpoint through Mps1-dependent BubR1 phosphorylation. *EMBO J* 1–17 (2013). doi:10.1038/emboj.2013.109
229. Descombes, P. & nigg, E. A. The polo-like kinase Plx1 is required for M phase exit and destruction of mitotic regulators in Xenopus egg extracts. *EMBO J* **17,** 1328–1335 (1998).
230. Golan, A., Yudkovsky, Y. & Hershko, A. The cyclin-ubiquitin ligase activity of cyclosome/APC is jointly activated by protein kinases Cdk1-cyclin B and Plk. *J Biol Chem* **277,** 15552–15557 (2002).
231. Chu, Y. *et al.* Aurora B kinase activation requires survivin priming phosphorylation

by PLK1. *Journal of Molecular Cell Biology* **3,** 260–267 (2011).
232. Salimian, K. J. *et al.* Feedback Control in Sensing Chromosome Biorientation by the Aurora B Kinase. *Current Biology* **21,** 1158–1165 (2011).
233. Huang, H. *et al.* Phosphorylation sites in BubR1 that regulate kinetochore attachment, tension, and mitotic exit. *The Journal of Cell Biology* **183,** 667–680 (2008).
234. Nakajima, H., Toyoshima-Morimoto, F., Taniguchi, E. & Nishida, E. Identification of a consensus motif for Plk (Polo-like kinase) phosphorylation reveals Myt1 as a Plk1 substrate. *J Biol Chem* **278,** 25277–25280 (2003).
235. Santamaria, A. *et al.* The Plk1-dependent Phosphoproteome of the Early Mitotic Spindle. *Molecular & Cellular Proteomics* **10,** M110.004457–M110.004457 (2010).
236. Taylor, S. S., Ha, E. & McKeon, F. The human homologue of Bub3 is required for kinetochore localization of Bub1 and a Mad3/Bub1-related protein kinase. *The Journal of Cell Biology* **142,** 1–11 (1998).
237. Westhorpe, F. G. & Straight, A. F. Functions of the centromere and kinetochore in chromosome segregation. *Current Opinion in Cell Biology* **25,** 334–340 (2013).
238. Heinrich, S., Windecker, H., Hustedt, N. & Hauf, S. Mph1 kinetochore localization is crucial and upstream in the hierarchy of spindle assembly checkpoint protein recruitment to kinetochores. *Journal of Cell Science* **125,** 4720–4727 (2012).
239. Dou, Z. *et al.* Quantitative Mass Spectrometry Analysis Reveals Similar Substrate Consensus Motif for Human Mps1 Kinase and Plk1. *PLoS ONE* **6,** e18793 (2011).
240. Cahill, D. P. *et al.* Mutations of mitotic checkpoint genes in human cancers. *Nature* **392,** 300–303 (1998).
241. Ricke, R. M. & van Deursen, J. M. Aneuploidy in health, disease, and aging. *The Journal of Cell Biology* **201,** 11–21 (2013).
242. Holland, A. J. & Cleveland, D. W. Boveri revisited: chromosomal instability, aneuploidy and tumorigenesis. *Nat Rev Mol Cell Biol* **10,** 478–487 (2009).
243. Thompson, S. L. & Compton, D. A. Chromosomes and cancer cells. *Chromosome Res* **19,** 433–444 (2010).
244. Tanaka, K. *et al.* Mitotic checkpoint protein hsMAD2 as a marker predicting liver metastasis of human gastric cancers. *Japanese journal of cancer research* **92,** 952–958 (2001).
245. Yuan, B. *et al.* Increased expression of mitotic checkpoint genes in breast cancer cells with chromosomal instability. *Clin. Cancer Res.* **12,** 405–410 (2006).
246. Myrie, K. A., Percy, M. J., Azim, J. N., Neeley, C. K. & Petty, E. M. Mutation and expression analysis of human BUB1 and BUB1B in aneuploid breast cancer cell lines. *Cancer Lett.* **152,** 193–199 (2000).
247. Berdougo, E., Terret, M.-E. & Jallepalli, P. V. Functional dissection of mitotic regulators through gene targeting in human somatic cells. *Methods Mol. Biol.* **545,** 21–37 (2009).
248. Oppermann, F. S. *et al.* Combination of Chemical Genetics and Phosphoproteomics for Kinase Signaling Analysis Enables Confident Identification of Cellular Downstream Targets. *Molecular & Cellular Proteomics* **11,** O111.012351–O111.012351 (2012).
249. Dephoure, N. *et al.* A quantitative atlas of mitotic phosphorylation. *Proceedings of the National Academy of Sciences* **105,** 10762–10767 (2008).
250. Olsen, J. V. *et al.* Global, In Vivo, and Site-Specific Phosphorylation Dynamics in Signaling Networks. *CELL* **127,** 635–648 (2006).
251. Kettenbach, A. N. *et al.* Quantitative Phosphoproteomics Identifies Substrates and Functional Modules of Aurora and Polo-Like Kinase Activities in Mitotic Cells.

Science Signaling **4,** rs5–rs5 (2011).
252. Koch, A., Krug, K., Pengelley, S., Macek, B. & Hauf, S. Mitotic Substrates of the Kinase Aurora with Roles in Chromatin Regulation Identified Through Quantitative Phosphoproteomics of Fission Yeast. *Science Signaling* **4,** rs6–rs6 (2011).
253. Ubersax, J. A. *et al.* Targets of the cyclin-dependent kinase Cdk1. *Nature* **425,** 859–864 (2003).
254. Skoufias, D. A., Indorato, R.-L., Lacroix, F., Panopoulos, A. & Margolis, R. L. Mitosis persists in the absence of Cdk1 activity when proteolysis or protein phosphatase activity is suppressed. *The Journal of Cell Biology* **179,** 671–685 (2007).
255. Ong, S.-E. *et al.* Stable isotope labeling by amino acids in cell culture, SILAC, as a simple and accurate approach to expression proteomics. *Molecular & Cellular Proteomics* **1,** 376–386 (2002).
256. Hsu, J.-L., Huang, S.-Y., Chow, N.-H. & Chen, S.-H. Stable-Isotope Dimethyl Labeling for Quantitative Proteomics. *Anal. Chem.* **75,** 6843–6852 (2003).
257. Cox, J. *et al.* Andromeda: A Peptide Search Engine Integrated into the MaxQuant Environment. *J. Proteome Res.* **10,** 1794–1805 (2011).
258. Stumpff, J., Dassow, von, G., Wagenbach, M., Asbury, C. & Wordeman, L. The Kinesin-8 Motor Kif18A Suppresses Kinetochore Movements to Control Mitotic Chromosome Alignment. *Developmental Cell* **14,** 252–262 (2008).
259. Colaert, N., Helsens, K., Martens, L., Vandekerckhove, J. & Gevaert, K. nmeth1109-786. *Nature Methods* **6,** 786–787 (2009).
260. Holt, L. J. *et al.* Global Analysis of Cdk1 Substrate Phosphorylation Sites Provides Insights into Evolution. *Science* **325,** 1682–1686 (2009).
261. Songyang, Z. *et al.* Use of an oriented peptide library to determine the optimal substrates of protein kinases. *Current Biology* **4,** 973–982 (1994).
262. Wei, R. R. *et al.* Structure of a central component of the yeast kinetochore: the Spc24p/Spc25p globular domain. *Structure* **14,** 1003–1009 (2006).
263. Kemmler, S. *et al.* emboj200962a. *EMBO J* 1–12 (2009). doi:10.1038/emboj.2009.62
264. Chen, Y. Phosphorylation of the Mitotic Regulator Protein Hec1 by Nek2 Kinase Is Essential for Faithful Chromosome Segregation. *Journal of Biological Chemistry* **277,** 49408–49416 (2002).
265. Meijer, L. A. T. *et al.* Quantitative global phosphoproteomics of human umbilical vein endothelial cells after activation of the Rap signaling pathway. *Mol. BioSyst.* **9,** 732 (2013).
266. Wiśniewski, J. R. & Mann, M. Consecutive Proteolytic Digestion in an Enzyme Reactor Increases Depth of Proteomic and Phosphoproteomic Analysis. *Anal. Chem.* **84,** 2631–2637 (2012).
267. Fava, L. L., Kaulich, M., Nigg, E. A. & Santamaria, A. Probing the in vivo function of Mad1:C-Mad2 in the spindle assembly checkpoint. *EMBO J* **30,** 3322–3336 (2011).
268. Kim, S. *et al.* Phosphorylation of the spindle checkpoint protein Mad2 regulates its conformational transition. *Proceedings of the National Academy of Sciences* **107,** 19772–19777 (2010).
269. Wassmann, K., Liberal, V. & Benezra, R. Mad2 phosphorylation regulates its association with Mad1 and the APC/C. *EMBO J* **22,** 797–806 (2003).
270. Miniowitz-Shemtov, S. *et al.* Role of phosphorylation of Cdc20 in p31comet-stimulated disassembly of the mitotic checkpoint complex. *Proceedings of the National Academy of Sciences* **109,** 8056–8060 (2012).
271. Choi, E. *et al.* emboj2009123a. *EMBO J* **28,** 2077–2089 (2009).
272. Gao, Y.-F. *et al.* Cdk1-phosphorylated CUEDC2 promotes spindle checkpoint

inactivation and chromosomal instability. *Nature cell Biology* **13,** 924–933 (2011).
273. Meraldi, P. & Sorger, P. K. A dual role for Bub1 in the spindle checkpoint and chromosome congression. *EMBO J* **24,** 1621–1633 (2005).
274. Hames, R. S., Wattam, S. L., Yamano, H., Bacchieri, R. & Fry, A. M. APC/C-mediated destruction of the centrosomal kinase Nek2A occurs in early mitosis and depends upon a cyclin A-type D-box. *EMBO J* **20,** 7117–7127 (2001).
275. Hengeveld, R. C. C. *et al.* Development of a chemical genetic approach for human aurora B kinase identifies novel substrates of the chromosomal passenger complex. *Molecular & Cellular Proteomics* **11,** 47–59 (2012).
276. Blethrow, J. D., Glavy, J. S., Morgan, D. O. & Shokat, K. M. Covalent capture of kinase-specific phosphopeptides reveals Cdk1-cyclin B substrates. *Proceedings of the National Academy of Sciences* **105,** 1442–1447 (2008).
277. Allen, J. J., Lazerwith, S. E. & Shokat, K. M. Bio-orthogonal Affinity Purification of Direct Kinase Substrates. *J. Am. Chem. Soc.* **127,** 5288–5289 (2005).
278. Gonen, S. *et al.* nsmb.2358. *Nat Struct Mol Biol* **19,** 925–929 (2012).
279. Hennrich, M. L. *et al.* Universal Quantitative Kinase Assay Based on Diagonal SCX Chromatography and Stable Isotope Dimethyl Labeling Provides High-definition Kinase Consensus Motifs for PKA and Human Mps1. *J. Proteome Res.* **12,** 2214–2224 (2013).
280. Morin, V. *et al.* CDK-Dependent Potentiation of MPS1 Kinase Activity Is Essential to the Mitotic Checkpoint. *Current Biology* (2012). doi:10.1016/j.cub.2011.12.048

Nederlandse samenvatting voor niet ingewijde

Het menselijk lichaam is opgebouwd uit miljarden cellen, deze cellen vormen de bouwstenen voor alle verschillende weefsels en organen waaruit ons lichaam bestaat. Het is dan ook niet verwonderlijk dat er honderden verschillende soorten cellen zijn met elk een specifieke functie en vorm naargelang hun taak in het lichaam. De slijtgevoelige darmwand bijvoorbeeld, bevat snel reproducerende cellen die zijn gespecialiseerd in het afscheiden van darmsappen voor de spijsvertering. Terwijl de neuronen in de hersenen zijn gespecialiseerd in het ontvangen en doorgeven van signalen.
Ondanks de verschillende taken van de cellen bevatten ze allen het identieke handleidingenboek “het DNA” dat ligt opgeslagen in de celkern. In dit handleidingenboek staan de instructies die nodig zijn voor een cel om goed te functioneren. Afhankelijk van de variërende functies van cellen zullen de instructies per celtype verschillen. Het handleidingenboek bestaat uit 46 hoofdstukken, ofwel chromosomen. Tijdens de bevruchting heeft u 23 hoofdstukken van uw moeder meegekregen en de andere 23 van uw vader. Vanaf het moment van de bevruchting zijn we begonnen met delen om vervolgens niet meer te stoppen. Het proces van celdeling staat aan de basis van de ontwikkeling van alle organismen en het is dit wonderlijke proces dat ik de afgelopen vijf jaar heb bestudeerd en waarvan de onderzoeksresultaten beschreven staan in dit proefschrift.

Celdeling

De deling van één ‘moedercel’ in twee nieuwe ‘dochtercellen’ wordt mitose genoemd. Eén van de meest essentiële taken van de mitose is het eerlijk verdelen van het erfelijk materiaal op een dusdanige manier dat beide dochtercellen uiteindelijk exact dezelfde kopie van het handleidingenboek bezitten. Voordat een cel dus kan overgaan tot de mitose zal eerst het erfelijk materiaal, het DNA, moeten worden verdubbeld. Nadat alle 46 chromosomen foutloos zijn overgeschreven blijven kopie en origineel - die we nu zusterchromosomen noemen - aan elkaar gebonden. De cel is nu klaar voor de mitose. Mitose is opgedeeld in meerdere opeenvolgende fasen (zie figuur 1), tijdens de eerste fasen, de ‘pro- en prometafase’ genoemd, groeien vanuit twee tegenoverliggende polen dynamische draden, microtubuli, om een spoelfiguur te vormen. In deze fasen moeten de microtubuli van het spoelfiguur de zusterchromosomen zien te binden. Na veel duw- en trekwerk zullen alle zusterchromosomen zich uiteindelijk in het midden van de cel bevinden. Op het moment dat de ene zuster via microtubuli gebonden is aan één pool, en de andere zuster aan de tegenoverliggende pool heeft de cel ‘metafase’ bereikt en is klaar om te delen. De zusterchromosomen worden fysiek van elkaar gescheiden en netjes verdeeld over de twee dochtercellen in ‘anafase’. De uiteindelijke vorming van de twee nieuwe dochtercellen vindt plaats in de laatste fasen; ‘telofase en cytokinese’ van de mitose. In deze fasen begint het celmembraan in het midden in te snoeren tot er een scheiding tussen de twee cellen optreedt. Uit één cel hebben zich aldus twee cellen gevormd met precies hetzelfde erfelijk materiaal.

Het Mitotische Checkpoint

Het is van essentieel belang dat er tijdens de deling geen fouten worden gemaakt in de chromosoomverdeling. Het goed functioneren van de cel wordt door het genetisch materiaal bepaalt en het hebben van een verkeerd aantal chromosomen (aneuploidy) kan desastreuze gevolgen hebben. Aneuploidy is een kenmerk van bijna alle tumoren, het is echter nog

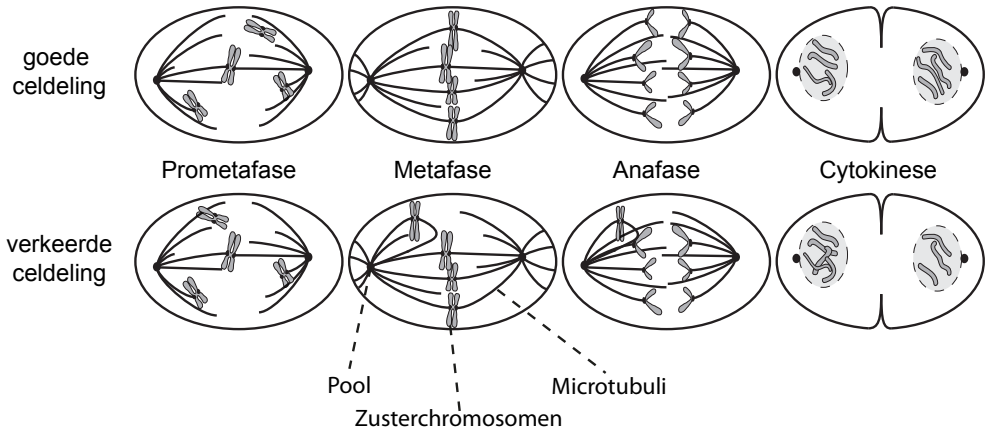

Figuur 1. Schematische weergave van de celdeling
Voor aanvang van de celdeling bevinden de verdubbelde chromosomen zich nog in de celkern, wanneer de celkern aan het begin van de mitose afbreekt vormt zich een spoelfiguur(prometafase). De dynamische draden (microtubuli) van het spoelfiguur binden de zusterchromosomen op gespecialiseerde aanhecht plaatsen (kinetochoren). Na veel duw en trekwerk bevinden de zusterchromosomen zich in het midden van de cel (metafase). De zusters worden van elkaar gescheiden in anafase en elk naar een kant van de cel getrokken. Tijdens de laatste fase van de celdeling zullen de twee dochtercellen zich vormen, beiden met een gelijke hoeveelheid chromosomen. Fouten tijdens de celdeling die mogelijk voortkomen uit een slecht functionerend mitotisch checkpoint leiden tot een ongelijke hoeveelheid chromosomen in de dochtercellen (aneuploidy).

onduidelijk of het maken van fouten tijdens de celdeling bijdraagt aan het ontstaan van kanker. Naast de aanwezigheid van aneuploidy in kanker, heeft de aanwezigheid van een verkeerd aantal chromosomen ook tijdens de humane ontwikkeling grote effecten. Dit wordt bijvoorbeeld geïllustreerd in het syndroom van Down, waarbij de aanwezigheid van een extra chromosoom (nummer 21) grote gevolgen heeft. Om aneuploidy te voorkomen, beschikt de cel over een controlemechanisme, het mitotische checkpoint, welke de voortgang van de deling nauwlettend in de gaten houdt.
Aan de basis van het mitotische checkpoint staat het kinetochoor, een structuur van eiwitten die zich aan weerszijden van de zusterchromosomen bevindt. De kinetochoor vormt de bindingsplaats voor microtubuli. In afwezigheid van stabiel gebonden microtubuli zal het kinetochoor een stopsignaal produceren welke de deling van de cel tegenhoudt. Pas als alle kinetochoren stabiel gebonden zijn in metafase (één zusterschromosoom met de ene pool, en de andere zuster met de tegenoverliggende pool) laat het mitotische checkpoint deling van de zusterchromosomen toe. De microtubuli trekken de dan gescheiden zusters naar de tegenoverliggende kanten van de cel.

Het onderzoek beschreven in dit proefschrift
Ondanks het belang van het mitotische checkpoint, is het nog onduidelijk hoe veel aspecten van het mitotische checkpoint functioneren. Een groep eiwitten genaamd kinasen, vervullen een centrale rol in mitose en het mitotische checkpoint. Eén van deze kinasen, genaamd MPS1, staat centraal in het onderzoek beschreven in dit proefschrift. Alvorens ik het onderzoek omtrent MPS1 bespreek, is het van belang het functioneren van kinasen kort toe te lichten.
Een belangrijk mechanisme dat cellen gebruiken om een signaal door te geven is het

aanbrengen van een modificatie op een ander eiwit. Eén van de bekendste en meest onderzochte modificaties, is het aanbrengen van een fosfaatgroep op een eiwit. Dit mechanisme, fosforylering genaamd, reguleert een breed scala van cellulaire processen. De introductie van een negatief geladen fosfaatgroep kan de structuur en activiteit van een eiwit veranderen of de interacties met andere eiwitten verstoren of stimuleren. Kinasen bezitten de enzymatische activiteit om een fosfaatgroep te koppelen aan andere eiwitten. Een kleine groep kinasen is verantwoordelijk voor de regulatie van het mitotische checkpoint.
Het belang van het MPS1 gen voor het mitotische checkpoint werd in 1996 voor het eerst beschreven in gist. Later bleek dat ook het humane MPS1 essentieel is voor het goed functioneren van het checkpoint. Zonder MPS1 (of MPS1 activiteit) zullen cellen delen terwijl één of meerdere kinetochoren niet aan microtubuli gehecht zijn, met aneuploidy als gevolg. Uit recentelijk onderzoek blijkt dat MPS1 op meerdere manieren het checkpoint beïnvloedt.
In **hoofdstuk 1** behandel ik wat in de literatuur bekend is over mitose, de kinetochoor, het mitotische checkpoint en wat de rol van MPS1 hierin is.
Om een beter beeld te krijgen van alle verschillende functies van MPS1 in mitose wordt in **hoofdstuk 2** beschreven hoe wij door middel van mutaties in het ATP bindingsdomein van MPS1, het kinase gevoelig hebben gemaakt voor chemische remmers. Deze aanpak stelde ons in staat MPS1 activiteit op zeer snelle en specifieke wijze te remmen. Deze remming van MPS1 bleek een handig hulpmiddel om de functie van MPS1 in mitose te bestuderen.
Een belangrijke functie van MPS1 is het rekruteren van andere checkpoint eiwitten naar de kinetochoor.
In **hoofdstuk 3** onderzoeken we hoe MPS1 het checkpoint eiwit MAD1 naar de kinetochoor rekruteert. Kinetochoor lokalisatie van MAD1 is essentieel voor het goed functioneren van het checkpoint. Naast MPS1 heeft ook het checkpoint kinase BUB1 en het MAD1-rekruterende eiwit ZW10 invloed op de lokalisatie van MAD1. Wij hebben ontdekt dat al deze eiwitten samenwerken om de lokalisatie van MAD1 naar de kinetochoor te reguleren.
Hoofdstuk 4 beschrijft de zoektocht naar nieuwe regulatoren van het mitotische checkpoint. Uit recentelijk onderzoek is gebleken dat niet alle regulatoren van het checkpoint essentieel zijn. De functie van deze eiwitten in het checkpoint komt pas aan het licht als het checkpoint verzwakt is en gevoelig is voor kleine veranderingen. Onze data laat zien dat het kinase PLK1 een dergelijke niet-essentiële regulator van het checkpoint is. PLK1 heeft veel verschillende functies in mitose, hierdoor is de door ons beschreven functie in het checkpoint tot nu toe onderbelicht gebleven. Onze data laat zien dat PLK1 activiteit alleen essentieel wordt wanneer het checkpoint verzwakt is. Een situatie die waarschijnlijk gelijk staat aan een cel met nog maar één of twee niet gebonden kinetochoren.
Ondanks het belang van MPS1 in het mitotische checkpoint was er bij aanvang van mijn promotie onderzoek nog geen enkel eiwit bekend dat wordt gefosforyleerd door MPS1 om het checkpoint te reguleren. **Hoofdstuk 5** beschrijft het gebruik van kwantitatieve massaspectrometrie om nieuwe substraten van MPS1 te identificeren. Met behulp van massaspectrometrie kan bepaald worden of een eiwit gefosforyleerd is. Wij beschrijven verschillende experimentele methodes die wij hebben gebruikt om te bepalen welke eiwitten worden gefosforyleerd door MPS1.
Alle experimentele data in dit proefschrift wordt in **hoofdstuk 6** samengevat en bediscussieerd in het licht van relevante literatuur. Het beschreven onderzoek heeft nieuwe inzichten geboden in het mitotische checkpoint en roept nieuwe vragen op. Aan de hand van deze vragen doe ik tevens suggesties voor toekomstig onderzoek.

Dank

Beste Geert, het was me wat de afgelopen vijf jaar. Wat heb ik veel van je geleerd. Jouw kijk op wetenschap is verfrissend en aanstekelijk. Bedankt voor al je geduld tijdens mijn promotie en vooral ook tijdens het schrijfproces (Martine, sorry van je vakantie, ik maak het nog een keer goed). Naast de wetenschap kon je me tevens ook een beetje wijsmaken in het ouderschap en heb je me regelmatig de les gelezen op de squashbaan. Misschien moeten we binnenkort nog eens een potje squashen dan hoef ik je niet meer te laten winnen nu mijn doctoraat binnen is.

Dan de paranimfen. Mathijs, de afgelopen jaren zouden een stuk minder “nice, nice” zijn geweest zonder jou. Onze gedeelde passie voor biertjes, een bakkie, tafeltennis (wie stond er ook alweer voor?) het JSF en zowaar ook nog de wetenschap maakte het elke dag weer een dolle boel op het Stratenum. Andre, wie had kunnen denken dat uitgerekend de persoon die mijn pogingen tot studeren altijd systematisch wist te interrumperen met de vraag biertje.....? of eitje.....? naast mij zou staan tijdens mijn verdediging. Ik ben blij dat we na al die jaren de passie voor biertjes en eitjes niet verloren zijn.

Dan de rest van de “Kops groep”. Dames eerst!, Nannette, Saskia en Aniek, dank jullie wel voor het warme welkom op het lab en voor alle wijze lessen op het lab en daarbuiten. Dan Wilco, de man met duizend namen. De beste is toch wel WIKI Woelmeister, want wat weet jij veel. Ik ga alle woelies missen en het wordt even wennen om je na vijf jaar niet meer elke dag te zien. Vincent, ‘my man in the Heck lab’. We hebben wat af gemass-spect, helaas niet met het gewenste resultaat. Misschien was het dan toch KI-67, bedankt voor alle peptides! Ade, you amazed me with all your models. Your view on science is exceptional and I learned a lot from you, thanks dude. Dan alle nieuwe aanwas Snees, Manja, Richard, Wilma, Carlos, Nina, Ajit, Antoinette, (bedankt voor de PLK1 proeven) Eelco, Bas, Claudia, Roy, Tim en Debby.
Benaf, ik vond het leuk om de laatste maanden met je samen te werken, ik geloof dat het wel goed gaat komen met jou.
Jasmin! Mijn student met een voorkeur voor enzymen met exotische (licht vulgaire) namen. Je onsamenhangende verhalen, het gebruik van het woord giecheltje, de gezelligheid en intresse in het onderzoek maakten de 9 maanden dat je er was erg leuk. Ik hoop dat je wat van me geleerd hebt, bedankt!

Dan alle kansloze AIO’s, waarvan de helft toch helemaal niet zo kansloos is. Rick (dem Book), Andree, Astrid, Maaike, Arne (hoe kwam je nou precies aan die bijnaam van je?), en Pascal, kopjes koffie, biertjes, lekker eten en voornamelijk de rest van het Stratenum door het slijk halen was toch het leukste met jullie.

Niets werkt beter dan je wetenschappelijke frustraties van je afslaan met een goed potje squash! Livio jouw scheldkannonades, overmatig zweten, geboer en overweldigende vorming van sop onder de douche zal ik missen en niet te vergeten je hulp bij de microscopen. Sander, Niels en Peter jullie slappe gelul (Niels), briljante/tragische slechte woordgrappen (Sander) en scheten (Peter) en alle biertjes bij Olympus zal ik missen.
David, Rutger, Maria, Maike, Jonne, Wytze, Lenno, Martijn, Anna, WJ, Anneke, Sarah, bedankt voor alle gezelligheid. En niet te vergeten Lars, de eerste jaren met jou en Wilco op

de mannenkamer waren echt top, hoe gaat het eigenlijk met mijn bosjesman? En natuurlijk de rest van de Timmers, Vermeulen, Burgering, Bos, Lens, Dansen, Holstege, Voest, Rowland en Medema labs bedankt voor alle gezelligheid.
Cristina, de jaarurenkaart bij jou inleveren was altijd weer een groot avontuur en ik mis het eigenlijk best wel.

Daarnaast was mijn onderzoek regelmatig onderhevig aan de kritische blik van vele wetenschappers van de Medema en Lens groepen. Iedereen bedankt voor het meedenken. Susanne, dank dat je in mijn leescommissie zat en succes met het professorschap. René, je kritische blik ontgaat niets, dat in combinatie met je platte humor maakte werken met je heel prettig, bedankt.

De leden van de beoordelings- en OiO commissie: Tobias en Albert heel erg bedankt voor de bijdrage tijdens de jaarlijkse evaluatie en het lezen van dit proefschrift. Judith Klumperman en Frank Holstege bedankt voor het lezen en beoordelen van dit proefschrift.

Abdel, het was fijn om in een wetenschappelijke omgeving iemand als jou tegen te komen. Ik ken weinig mensen die zoveel lachen en zoveel kletsen. Ik ben blij dat ik je heb leren kennen.

Pap en Mam, wat leuk dat jullie een paar keer op het lab zijn geweest. Het is en zal een mysterie blijven wat ik nou eigenlijk heb gedaan de afgelopen vijf jaar, maar ik besef maar al te vaak dat deze dag er niet zou zijn geweest zonder de degelijke basis die jullie hebben gelegd. Bedankt voor de FF-en lijst, Bonnie, remedial teaching, bijles Duits, half 6 naar de Jan Ligthart en alle andere dingen die ik in de loop der jaren ben vergeten.
Eelke bedankt dat je al mijn Nederlandse stukken op fouten hebt gecorrigeerd. De Nederlandse taal blijft ondanks alle bovengenoemde maatregelen niet mijn sterkste kant.

Lieve Tessel. Ik heb de afgelopen anderhalf jaar vaak moeten kiezen tussen nog een western blot inzetten of nog net op tijd thuis zijn om jou op bed te leggen. Jij trok vaak aan het langste eind! Ook al klaag ik vaak (vanochtend werd je om half 6 wakker!!!!!) en zal ik dat waarschijnlijk blijven doen. Je bent en blijft de leukste.

Liefste Mari, al te veel woorden zal ik er niet aan vuil maken. Maar de afgelopen 5 jaar waren een stuk minder leuk geweest zonder jou aan mijn zijde. Je weet de wetenschappelijke sores altijd goed te relativeren (fotosynthese is overated!). Ik ben blij dat je me na een dag werken in elke vorm accepteert; als P de P, Malarie, de Zieligheid, neutraal, of gewoon lekker hangend op de bank. Dank je voor alles, je bent de liefste.

Curriculum Vitae

Tale Sliedrecht werd op 8 september 1980 in Deventer geboren. In juni 1998 behaalde hij zijn HAVO diploma aan het Baudartius College te Zutphen. Na het behalen van de bachelor of Applied Science (BASc) aan de Hogeschool Larenstein, begon Tale in 2006 aan de Master Plant Biology aan de Universiteit Utrecht. Tijdens deze opleiding heeft Tale een onderzoeksstage gedaan binnen de Plant Microbe Interactions groep in het laboratorium van Prof. dr. Corné Pieterse onder begeleiding van dr. Tita Ritsema. Daarna heeft hij voor zijn tweede onderzoeksstage het effect van DNA-schade onderzocht in het laboratorium van dr. Wim Vermeulen onder begeleiding van dr. Hannes Lans. In 2008 studeerde Tale cum laude af. In datzelfde jaar is Tale gestart als Onderzoeker in Opleiding in het laboratorium van Prof. dr. Geert Kops op de afdeling Molecular Cancer Research in het Universitair Medisch Centrum te Utrecht, waar hij heeft gewerkt aan het onderzoek dat is beschreven in dit proefschrift

Publications

Sliedrecht, T., Zhang, C., Shokat, K. M. & Kops, G. J. P. L. Chemical genetic inhibition of Mps1 in stable human cell lines reveals novel aspects of Mps1 function in mitosis. PLoS ONE 5, e10251 (2010).

Jelluma, N., Dansen, T. B., **Sliedrecht, T**., Kwiatkowski, N. P. & Kops, G. J. P. L. Release of Mps1 from kinetochores is crucial for timely anaphase onset. *The Journal of Cell Biology* 191, 281–290 (2010).